NUREG-0678

The Effects of Temperature, Moisture, Concentration, Pressure and Mass Transfer on the Adsorption of Krypton and Xenon on Activated Carbon

Manuscript Completed: July 1980
Date Published: August 1980

*D. W. Underhill, D. W. Moeller

Advisory Committee on Reactor Safeguards
U.S. Nuclear Regulatory Commission
Washington, D.C. 20555

*Currently, Associate Professor, Graduate School of Public Health, University of Pittsburgh

ABSTRACT

This report is a critical review of the published literature on the adsorption of radioactive krypton and xenon on activated charcoal. The report includes a tabulation and evaluation of the adsorption coefficients for these two gases as related to temperature, pressure, moisture, mass transfer effects, and the nature of the carrier gas. Wherever possible, the resulting data have been used to develop simple correlations for quantitatively evaluating the effects of these parameters on noble gas adsorption. Important conclusions of the study include the observations that (a) individual charcoals have a wide range of adsorption coefficients and therefore the performance of a given bed is heavily dependent on the quality of the charcoal it contains; (b) because of the detrimental effects of mass transfer on noble gas adsorption, consideration should be given to including this factor in developing technical specifications for adsorption beds; and (c) additional research is needed on the determination of the inter-relationship of moisture and temperature and their effects on adsorption bed performance.

TABLE OF CONTENTS

LIST OF FIGURES

LIST OF FIGURES

LIST OF FIGURES

LIST OF TABLES

LIST OF TABLES

LIST OF TABLES

LIST OF SYMBOLS

Symbol	Definition
A, B, C	coefficients for the Antoine equation
a,b	coefficients for the Freundlich isotherm
α	pressure coefficient, dimensionless
C_1	concentration of xenon (krypton), ppm
$\overline{C}_1$	Langmuir coefficient for the effect of xenon (krypton) on the adsorption of xenon (krypton)
C_2	concentration of krypton (xenon), ppm
$\overline{C}_2$	Langmuir coefficient for the effect of krypton (xenon) on the adsorption of xenon (krypton)
DF	decontamination factor, dimensionless
D_m	molecular diffusion coefficient for fission gas in carrier gas, $cm^2/sec.$
d_p	mean adsorbent particle size, cm
ϵ	fraction of adsorption bed consisting of interparticle void volume, dimensionless
γ	tortuosity factor for interparticle diffusion, dimensionless
H	height equivalent to one theoretical plate, cm
h	reduced height equivalent to one theoretical plate, dimensionless
k	adsorption coefficient, cc(NTP)/gm
Δk	loss in adsorption coefficient, present
k_a, k_b	adsorption coefficients at temperatures T_a and T_b, respectively, cc(NTP)/gm
k_1	adsorption coefficient of xenon (krypton) at infinitely low xenon and krypton concentrations, cc(NTP)/gm
K_1	adsorption coefficient at 1 atmosphere (abs), cc(NTP)/gm
K_2	adsorption coefficient at pressure, P_2, cc(NTP)/gm

LIST OF SYMBOLS (Continued)

Symbol	Definition
λ_p	coefficient for axial dispersion, dimensionless
m	mass of adsorbent, gms
n	number of data points
N	number of theoretical plates
NTP	normal temperature and pressure [25°C and 1 atmosphere (abs.)]
P	partial pressure of the adsorbed gas, atmospheres
P_o	vapor pressure of the pure liquid at the temperature of the measurement, atmospheres
ppm	concentration, parts per million
q	volume of adsorbed gas per gram of adsorbent, cc(NTP)
ρ	bulk density of the adsorbent, gm/cc
RH	relative humidity
R	ideal gas constant, cal/gm mole-°K
σ	geometric standard deviation, dimensionless
T	absolute temperature, °K
$t_{\frac{1}{2}}$	isotopic half life, sec
$\dot{V}$	flow of carrier gas, cc/sec
v_f	reduced interparticle velocity, dimensionless
V_s	superficial carrier gas velocity, cm/sec
z	$mk/\dot{V}t_{\frac{1}{2}}$, dimensionless

ACKNOWLEDGMENT

The authors gratefully acknowledge the many helpful suggestions and comments offered by their colleagues in the preparation of this report. Particular appreciation is expressed to Clifford A. Burchsted, Engineering Technology Division, Oak Ridge National Laboratory, and to Ronald R. Bellamy, Division of Site Safety & Environmental Analysis, U. S. Nuclear Regulatory Commission, for their detailed reviews of the final manuscript, and to Professor Yves Alarie, Chairman, Department of Industrial and Environmental Health Sciences, Graduate School of Public Health, University of Pittsburgh, for providing time to the senior author to complete this report.

Chapter 1

INTRODUCTION

Of all the components in the safety systems of a nuclear reactor, among the most difficult to quantify in terms of performance are the activated charcoal beds used to remove radioactive noble gases. Knowledge of the basic parameters influencing adsorption behavior has often not been sufficient to permit the calculation of adsorption coefficients under the full range of necessary conditions. Further complicating this situation is that samples of charcoal taken from sequential lots, or even from the same lot, can be significantly different in their adsorption effectiveness.

In spite of this situation, it appears that existing uncertainties in the analyses of the performance of fission gas adsorption systems can be reduced. This can be accomplished through better summarization and interpretation of data relating to the various parameters that affect the performance of such systems. The resulting information should make it possible not only to gain a better understanding of the variabilities associated with the performance of adsorption systems, but also to predict their behavior under conditions that differ substantially from those described in licensing documents for specific nuclear facilities. The purpose of this report is to review the published information on the adsorption of krypton and xenon and to tabulate and present it in a format that accomplishes these goals.

1.1 Correlations With Surface Area

If the adsorption coefficients for krypton and xenon can be correlated successfully with commonly measured physical parameters, such as pore

structure or the surface area of the adsorbent, then these parameters can serve as secondary standards in evaluating charcoals. However, current correlations between surface areas and adsorption coefficients of activated charcoals are not good. This can be shown by specific examples from the literature. As may be noted from the data in Table 1.1, First, et al. (1971b), were unable to observe any apparent correlation between the adsorption coefficients for krypton and the surface areas of several samples of charcoal tested. Table 1.2, from Kitani, et al. (1968), and Table 1.3, from Nakhutin, et al. (1976), also show no apparent relationship between either the pore volume or the surface area and the adsorption coefficient for krypton. In experiments with radon, Strong and Levins (1979) observed a linear relationship between surface area and the adsorption coefficient. Why a similar relationship has not been observed for krypton and xenon is not known.

1.2 Correlations With Density

Nankhutin, et al.(1976), showed that there appears to be a positive correlation between the apparent density of a charcoal sample and its adsorption coefficients for krypton and xenon. This result may be related to the observation of Kovach and Etheridge (1973) that the adsorption coefficient for krypton was a maximum if the charcoal was activated to give a surface area of 900 square meters per gram (Figure 1.1). Schroeter, et al. (1974), obtained a patent for the use of dense charcoals for the adsorption of krypton and xenon. The data developed by these authors (Table 1.4) also show clearly that the

adsorption coefficients for krypton and xenon are not proportional to the surface area of the adsorbent, and that high surface area and/or pore volume are not necessarily indicators of high adsorption capacity for krypton and xenon. This is also shown by the data of Kovach and Etheridge (Figure 1.1). In view of past practice, this is an important point for the U. S. Nuclear Regulatory Commission and other regulatory agencies to recognize.

1.3 Correlations Among Charcoals at Different Temperatures

Correlations between coefficients for the adsorption of different gases on a single sample of charcoal are more easily established. As may be noted from Figure 1.2, charcoals that have good adsorption coefficients for krypton and xenon at one temperature are likely to have correspondingly good adsorption coefficients for these same two gases at another temperature. Similarly, a charcoal that has a high adsorption coefficient for krypton is likely to have a high adsorption coefficient for xenon. Data from the published literature illustrating this latter fact are shown in Figure 1.3.

1.4 Predictions of Adsorbent Performance

Although such a capability would be desirable, it is not possible at this time to predict the adsorption coefficients for krypton and xenon with high accuracy on the basis of the physical properties of a charcoal. Chapters 2 through 6 of this report describe present approaches to the development of other general and, hopefully, more useful correlations. In Chapter 2, the adsorption coefficients for dilute krypton and xenon, at atmospheric pressure and under moisture free conditions, are tabulated and analyzed as a function of temperature.

Chapters 3, 4, and 5 present data and analyses related to the effects on adsorption of moisture, pressure, and concentration, respectively. Chapter 6 then concludes with an analysis of the effects of mass transfer. It is hoped that the provision of all such information in a single document will prove useful both in the design of fission gas adsorption beds and in the evaluation of their performance.

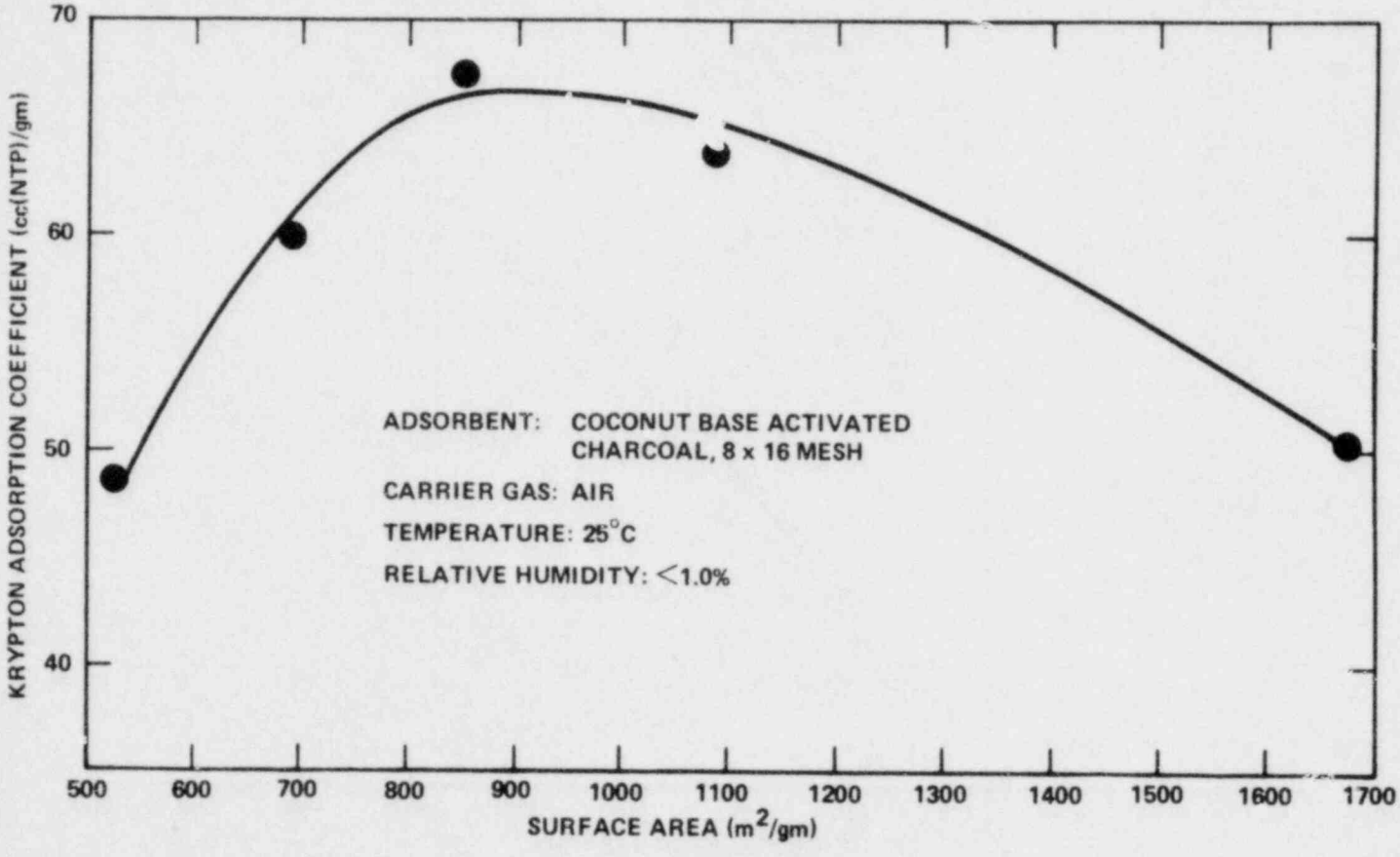

Figure 1.1 Correlation between surface area and krypton adsorption coefficient.

Reference: Kovach and Etheridge (1973)

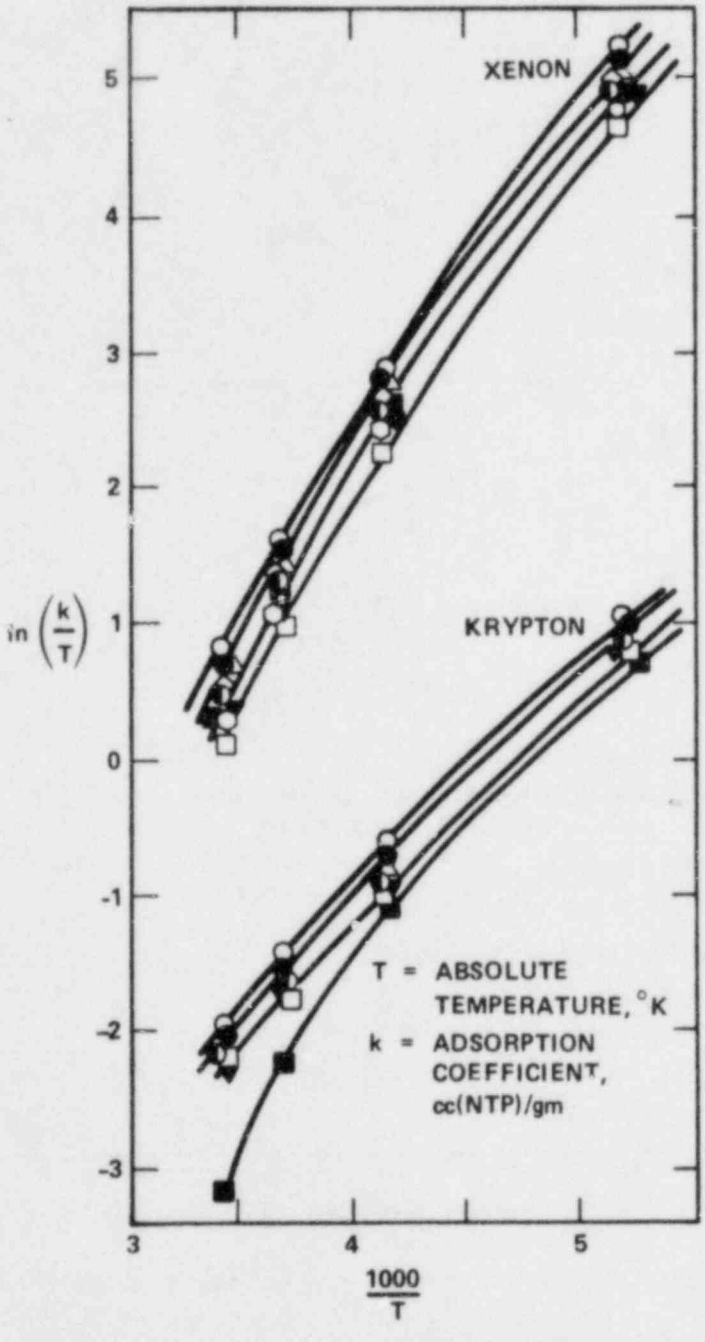

Figure 1.2 Comparison of adsorption coefficients for krypton and xenon on a variety of charcoals at different temperatures.

Reference: Nakhutin et al (1976)

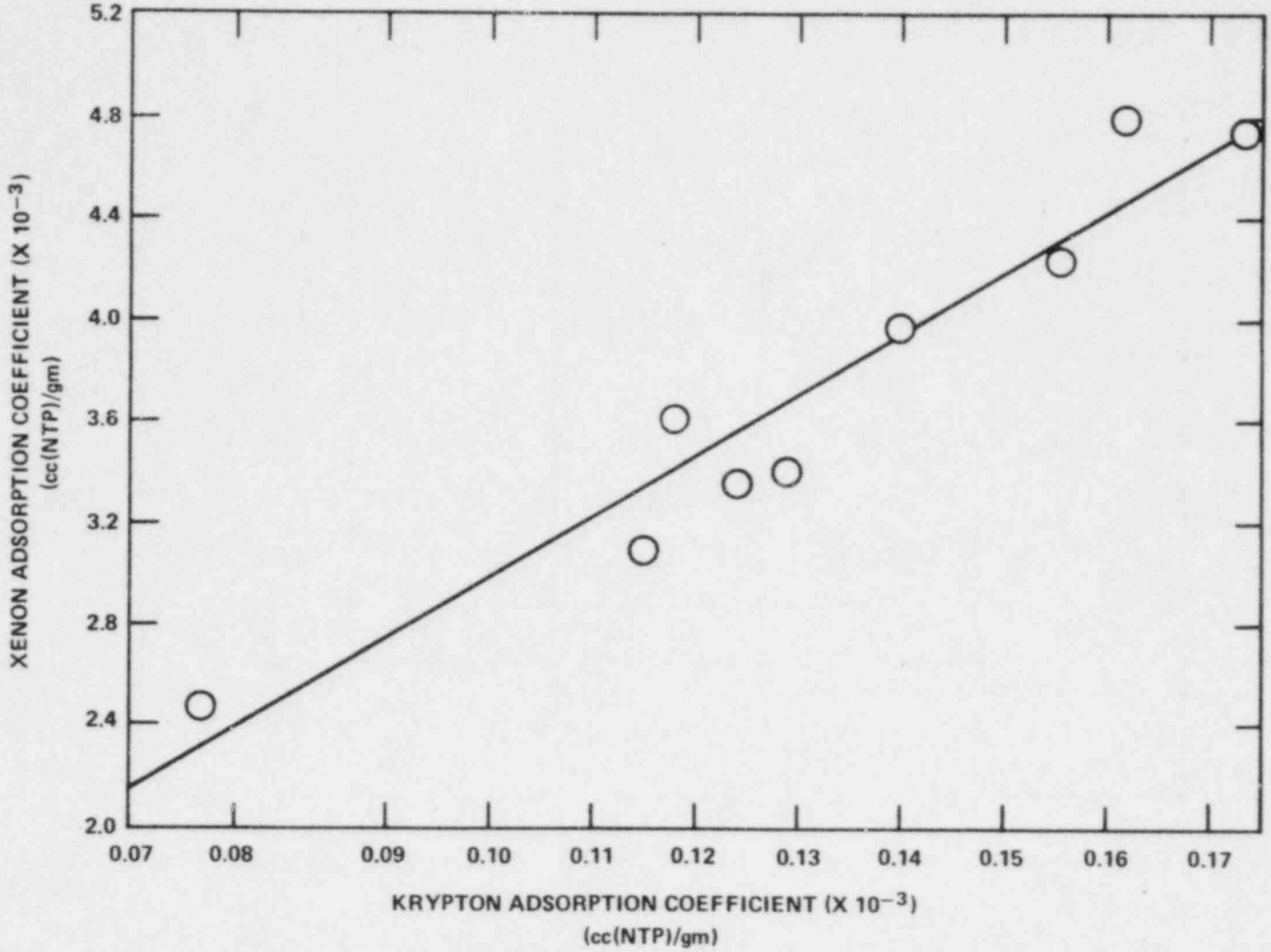

Figure 1.3 Correlation between krypton and xenon adsorption coefficients.

Reference: Underhill (1975)*

*Underhill, D. W. (1975): Unpublished Results.

TABLE 1.1

Surface Areas and Adsorption Coefficients for Krypton, Xenon and Argon on Various Charcoals at One Atmosphere

Charcoal Sample	Surface Area (as Stated by Vendor) (m^2/gm)	Adsorption Coefficients /cc(NTP)/gm/ for Xenon From an Argon Carrier Gas at 37.5°C	Xenon From an Argon Carrier Gas at -78°C	Krypton From an Argon Carrier Gas at 37.5°C	Krypton From an Argon Carrier Gas at -78°C	Argon Carrier Gas at 27°C
National ACC	1100	489		36.3		7.1
NACAR G210	1150	531	100,000	39.1		8.0
NACAR G212	1500	481		36.2	939	7.2
NACAR G352	1275	314		25.2		5.5
Pittsburgh PCB	1200	581	107,000	41.7	1189	8.7
Witco 888	1750	460				7.8
Witco 337	1300	485				6.2

Reference: First, et al. (1971b)

TABLE 1.2

Physical Characteristics and Adsorption Coefficients
for Krypton on Various Charcoals

Adsorbent Type	Surface Area (m^2/gm)	Shape	Mesh	Krypton Adsorption Coefficient at 0°C /cc(NTP)/gm/
Tsurumi GW	1,115	Granule	8/10	124
Tsurumi GLS	1,183	Granule	8/10	121
Tsurumi 2GM	1,188	Pellet	8/10	103
Columbia CXC	1,209	Granule	6/8	121
Columbia HCC	1,279	Granule	6/14	136
Takeda HGK-530	1,279	Granule	8/10	121
Tsurumi 2GR-T	1,302	Pellet	8/10	96
Shirasagi G	1,40C	Granule	8/10	87

Reference: Kitani, et al. (1968)

TABLE 1.3

Correlation of Several Properties of Activated Carbons
With Their Adsorption Coefficients for Xenon

Grade	Apparent Density (gm/cc)	Heat of Adsorption of Xenon from Helium (kcal/mole)	Specific Surface Area* (m^2/gm)	Micropore Volume** (cc/gm)	Ranking of the Adsorption Coefficient for Xenon from Air (at -80°C)***
SKT-2B	0.498	7.4	1,040	0.44	1
SKT-1B	0.458	-	1,050	0.47	4
SKT	0.457	-	1,090	0.47	7
SKT-3	0.472	7.3	1,100	0.47	2
SKT-1A	0.470	-	1,120	0.45	3
ART-2	0.428	-	1,130	0.49	5
SKT-2A	0.441	8.2	1,170	0.49	6
SKT-4A	0.418	-	1,330	0.55	8
SKT-6A	0.388	7.5	1,500	0.66	9

* By BET Method

** By Dubinin Method

*** Based on data in Figure 1.2

Reference: Nakhutin, et al. (1976)

TABLE 1.4

Correlation Between Bulk Density, Surface Area and the Adsorption Coefficients for Krypton and Xenon

Source of Carbon	Bulk Density (gms/cc)	Surface Area (m^2/gm)	Adsorption Coefficient /cc(NTP)/gm/ For Krypton	For Xenon
Mineral Coal	0.380	1,380	39.2	539
	0.490	973	45.9	721
	0.570	600	46.1	721
	0.635	298	44.2	685
	0.680	30	25.7	147
Wood Coal	0.300	649	58.3	626
	0.503	416	49.7	738
Coconut Shell	0.420	1,228	39.1	590
	0.510	869	41.0	668

Reference: Schroeder, et al. (1974)

Chapter 2

THE EFFECTS OF TEMPERATURE ON THE ADSORPTION OF KRYPTON AND XENON

Coefficients for the adsorption of dilute krypton or xenon from a dry carrier gas at one atmosphere are summarized in Tables 2.1.1 through 2.1.14. These data are based on a review of reports obtained through searches of Chemical Abstracts, Nuclear Science Abstracts, Atomindex and the computerized data bank of the Nuclear Safety Information Center. In these Tables, the adsorption coefficients are presented separately for each carrier gas, since the carrier gas can strongly influence the numerical value of the coefficient. Information regarding the nature of each adsorbent and the experimental conditions under which the data were obtained are also included in the Tables.

In order to provide the most useful tabulation of the available data, the authors have taken the liberty of omitting from the summary tables the results of tests which they judged to be misleading or in error. To make such a judgment, two tests of consistency were applied. As will be shown in Chapter 6, the adsorption coefficient should remain independent of carrier gas velocity. Whenever this was not the case, reliance on the data was considered unjustifiable and the results of these particular experiments were omitted. A second requirement was that, in a given test, sufficient charcoal should have been used to negate the effects of dead space. In some experiments, patterned after the methodology of gas chromatography, such small amounts of charcoal were used that it appears doubtful that the results could be either accurate or representative. In these cases, the data were again omitted.

Coefficients for the adsorption of krypton and xenon from oxygen, nitrogen, and air are listed in Tables 2.1.3 to 2.1.5 and 2.1.11 and 2.1.12. The data in all of these Tables, however, may not be equivalent. Kitani, et al. (1968), observed that at $0^{o}C$ differences existed in the adsorption of krypton from oxygen, from nitrogen, and from equal mixtures of these two gases. As may be noted in Figure 2.1, Schumann (1973) found that the coefficients for the adsorption of krypton at $-20^{o}C$ from oxygen-nitrogen mixtures depended on the percent of oxygen present. Examination of these findings indicates that adsorption coefficients obtained with a nitrogen carrier gas are low (conservative) in relation to those obtained with air or oxygen.

2.1 Analysis of Adsorption Data

To calculate the coefficients for the adsorption of krypton and xenon on charcoal, use was made of the Antoine equation (Antoine, 1888) where k, the adsorption coefficient [in units of cc (NTP)/gm], is expressed as follows:

$$k = e^{\left(A + \frac{B}{C + T(^{o}C)}\right)} \qquad (2.1)$$

The geometric standard deviation, σ, is given by:

$$\ln(\sigma) = \sqrt{\frac{\Sigma_n \left[\ln(k_i) - \ln(k_i')\right]^2}{n - 3}} \qquad (2.2)$$

where k_i' is the estimate of the i^{th} data point, k_i. The adsorption coefficient, k_j, corresponding to the j^{th} percentile was calculated from the equation:

$$\frac{100}{\sqrt{2\pi}} \int_{-\infty}^{\frac{\ln k_j - \ln k_{50}}{\ln \sigma}} e^{-x^2/2}\, dx = j \qquad (2.3)$$

To correct for the change in temperature,

$$\frac{k_a}{k_b} = e^{B\left(\frac{1}{C+T_b} - \frac{1}{C+T_a}\right)} \qquad (2.4)$$

where k_a and k_b are the adsorption coefficients at temperatures T_a and T_b(^oC), respectively.

The constants obtained by fitting the adsorption coefficients in Tables 2.1.1 through 2.1.14 to this equation are presented in Table 2.2. Included in these calculations were the standard deviations from the values predicted by the Antoine Equation. From this analysis, it was possible to construct Tables 2.3 through 2.10 and Figures 2.2 through 2.5, which provide the expected values for the adsorption coefficients for krypton and xenon from several common carrier gases over a range of temperatures.

The wide range in the distribution of values for the adsorption coefficients at any one temperature is illustrated in Figures 2.4 and 2.5, which give the distribution of adsorption coefficients for krypton and xenon in air. To be specific, at 25^oC the adsorption coefficient (Table 2.6) for krypton from

air was estimated to be < 22 cc (NTP)/gm for five percent of the charcoals; for 95% of the charcoals tested the corresponding value was 72 cc (NTP)/gm. If two adsorption beds were being operated, one of which contained charcoal represented by the lower of these two extremes, and the second of which contained charcoal represented by the higher of these two extremes, the difference in their adsorptive capacities for krypton would be greater than a factor of three. In this regard, it is worthy to note that a value of 70 cc(NTP)/gm, suggested by Cardile and Bellamy (1979), has been used by the NRC as an estimate for the adsorption coefficient under these same conditions. Although this value could probably be surpassed by a number of commercial charcoals, it is significantly higher than the 40 cc(NTP)/gm mean value found here.

The above example illustrates what should be well known; that is, that there are numerous commercial charcoals that are not suited for the adsorption of krypton and xenon and that it is unwise to assume adsorption coefficients for krypton and xenon without conducting tests to confirm them. In order to obtain adequate information for design purposes, representative samples of the adsorbent must be tested for the holdup of krypton and xenon at the temperature and in the carrier gas to be used in the actual system. If it becomes necessary to estimate the adsorption coefficients at other temperatures, Equation 2.4 can be used.

It is generally accepted that there is no scaleup factor for applying laboratory data to full scale plant design (Kabele and Bohringer, 1975; Foerster, 1971). Care must also be taken in applying laboratory data directly to operational adsorption systems. Littlefield, et al. (1975), for example, showed significant variations in data collected under different conditions. Although the data in Table 2.11 show that intralaboratory reproducibility of adsorption coefficients is quite good, the reproducibility of interlaboratory data (Table 2.12) leaves much to be desired. Further complicating the situation is that other factors create day-to-day variability in the effectiveness of adsorption beds (Table 2.13).

In order to calculate the release of fission gases in the event of the rupture of a pressurized adsorption bed, it is necessary to know the adsorption coefficient of the carrier gas (Underhill, 1972). Data on the adsorption coefficients of argon, nitrogen, and helium have been published by Hotchkiss (1976) and Trofimov and Pankov (1965). Similar information on the adsorption of air on several grades of charcoal have been published by Nakhutin, et al. (1976). Adsorption coefficients for argon at NTP are summarized in Table 1.1. These data can also be used to calculate the holdup of ^{41}Ar in an argon carrier gas.

On the basis of the above information, it is apparent not only that temperature has a strong effect on the adsorption coefficients for krypton and xenon, but also that there is a significant range in the possible values of the adsorption coefficients for these two gases at any one temperature.

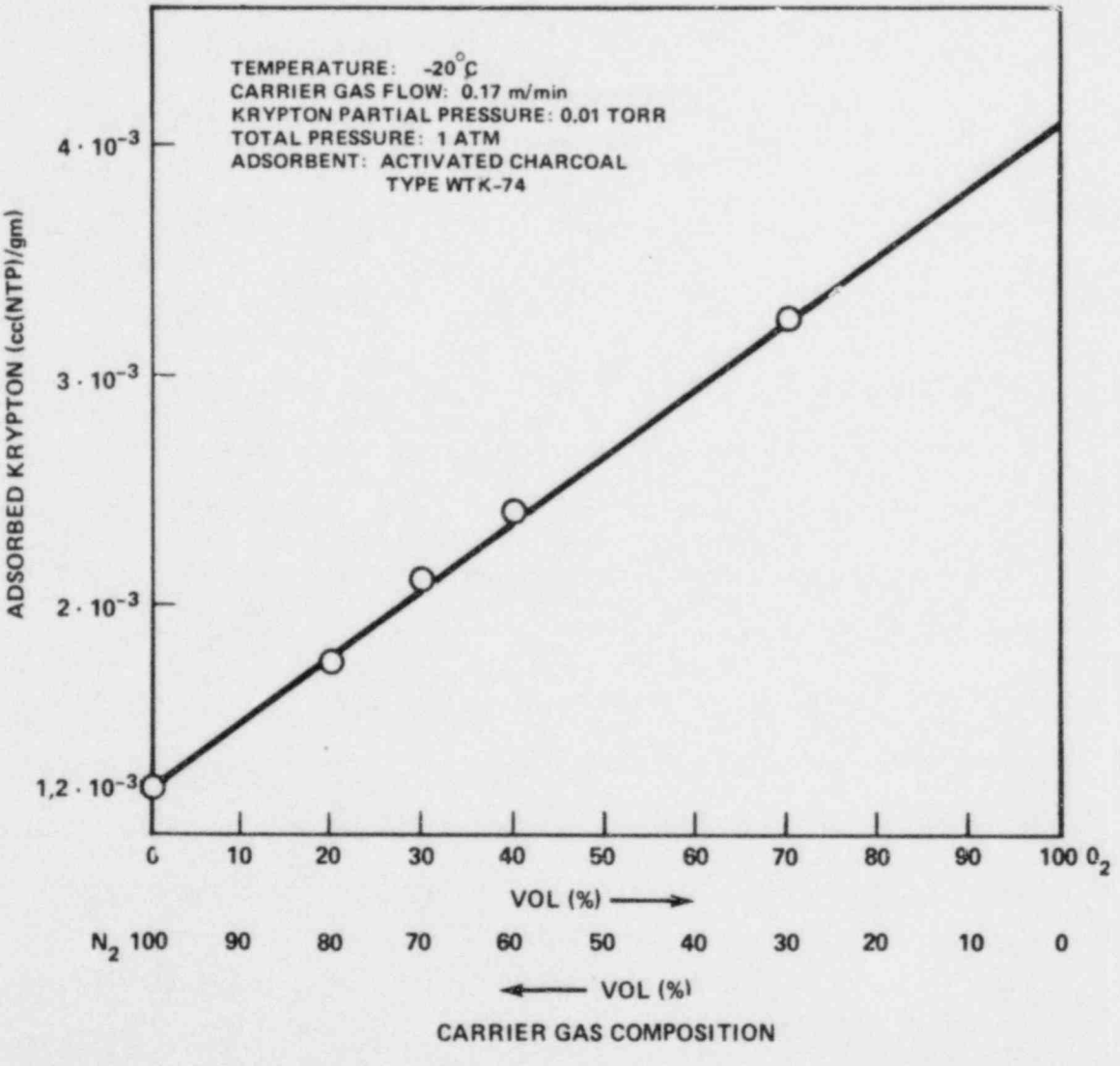

Figure 2.1 Effect of oxygen/nitrogen content of carrier gas on krypton adsorption. Reference: Schumann (1973).

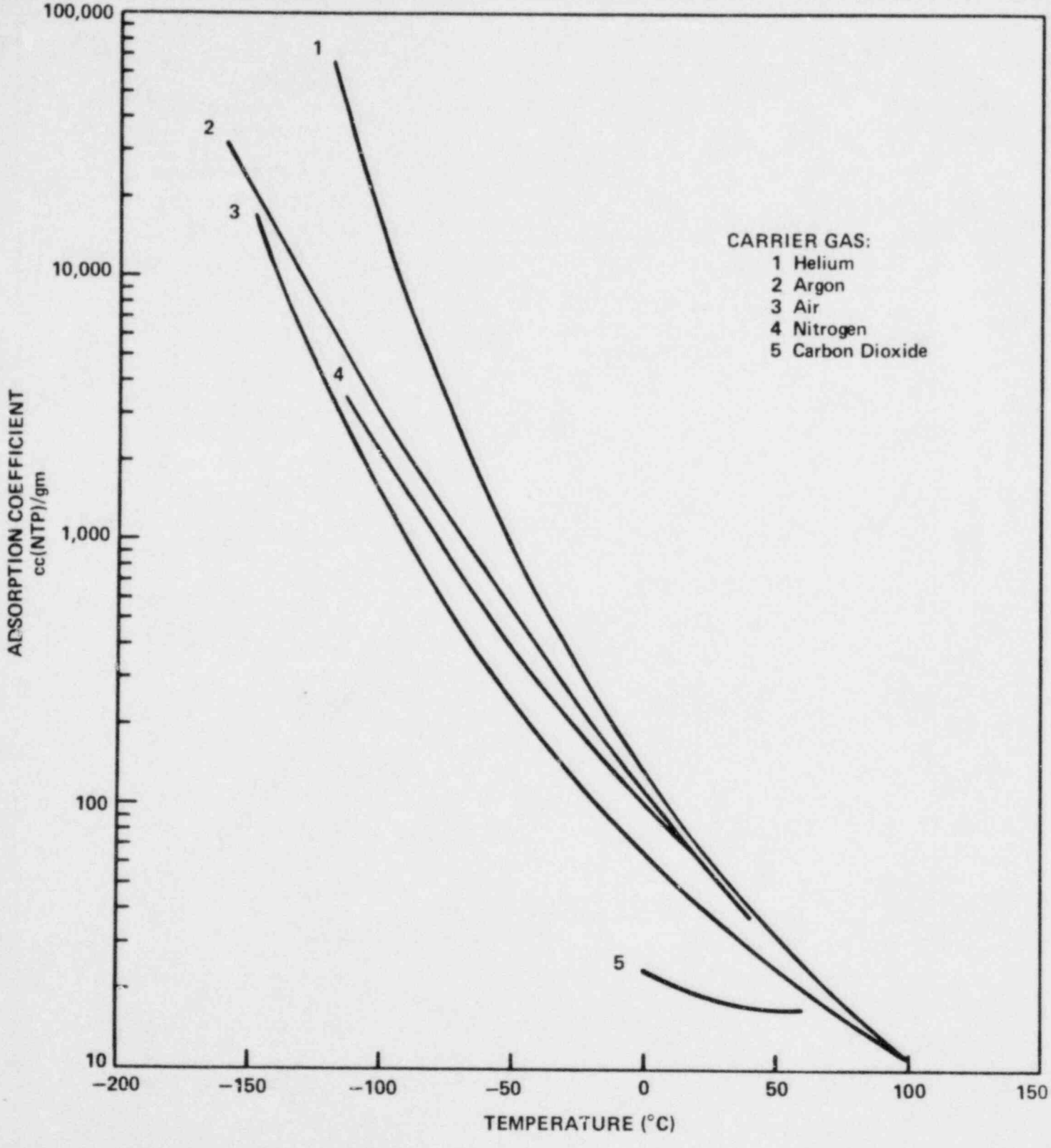

Figure 2.2 Effect of temperature and carrier gas on the adsorption of krypton.

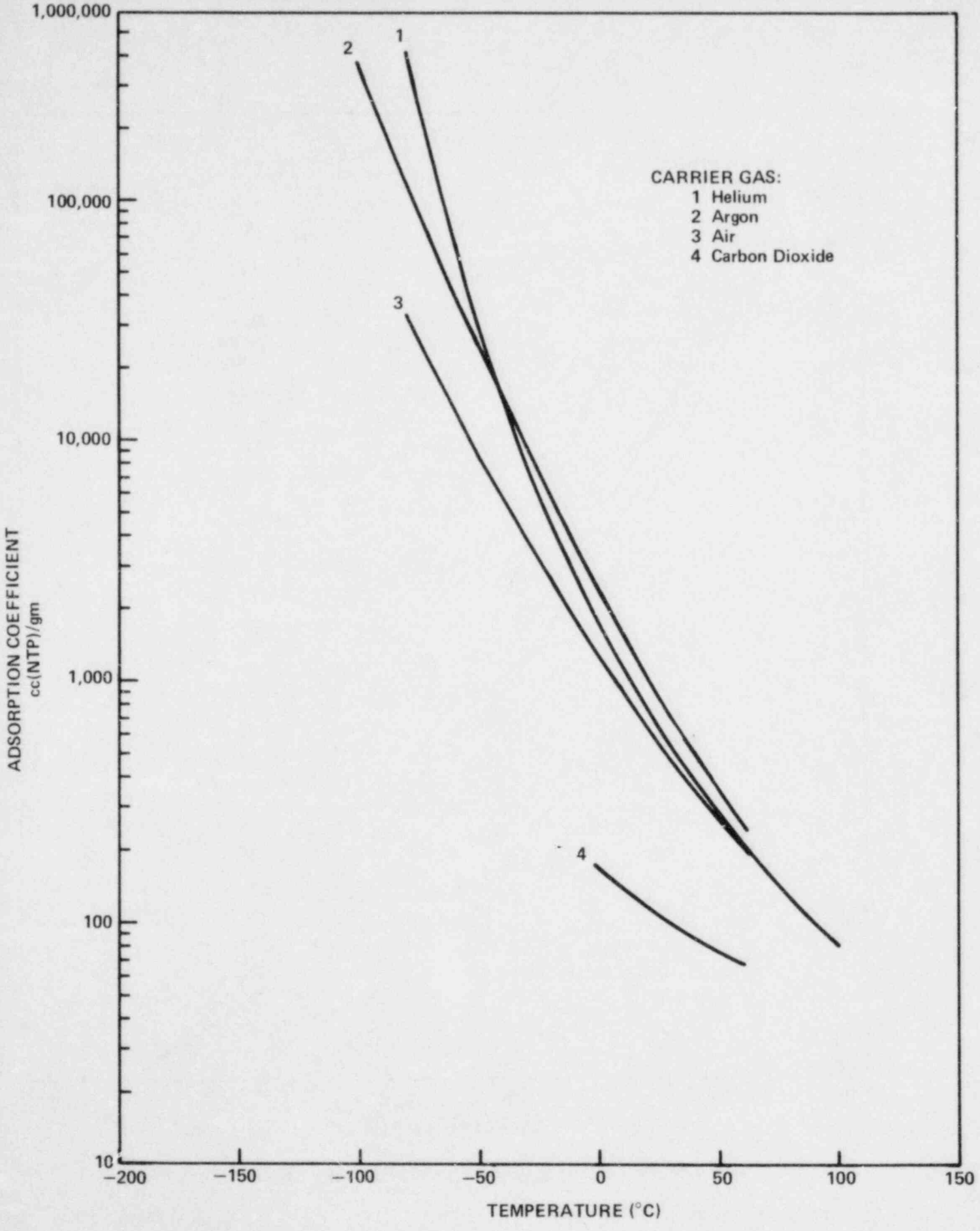

Figure 2.3 Effect of temperature and carrier gas on the adsorption of xenon.

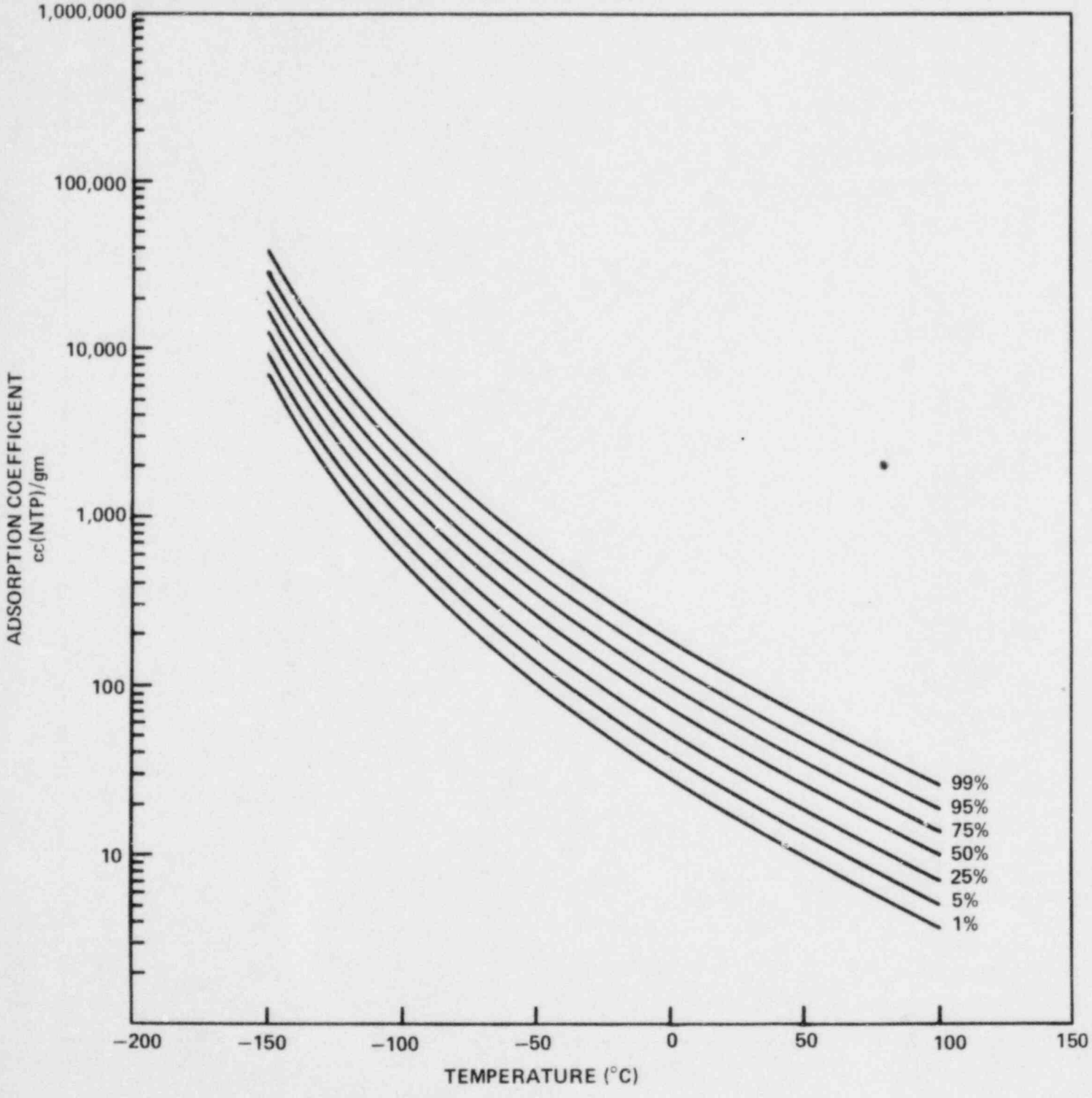

Figure 2-4 Adsorption of krypton from air: percent of adsorption coefficients expected to be less than stated value.

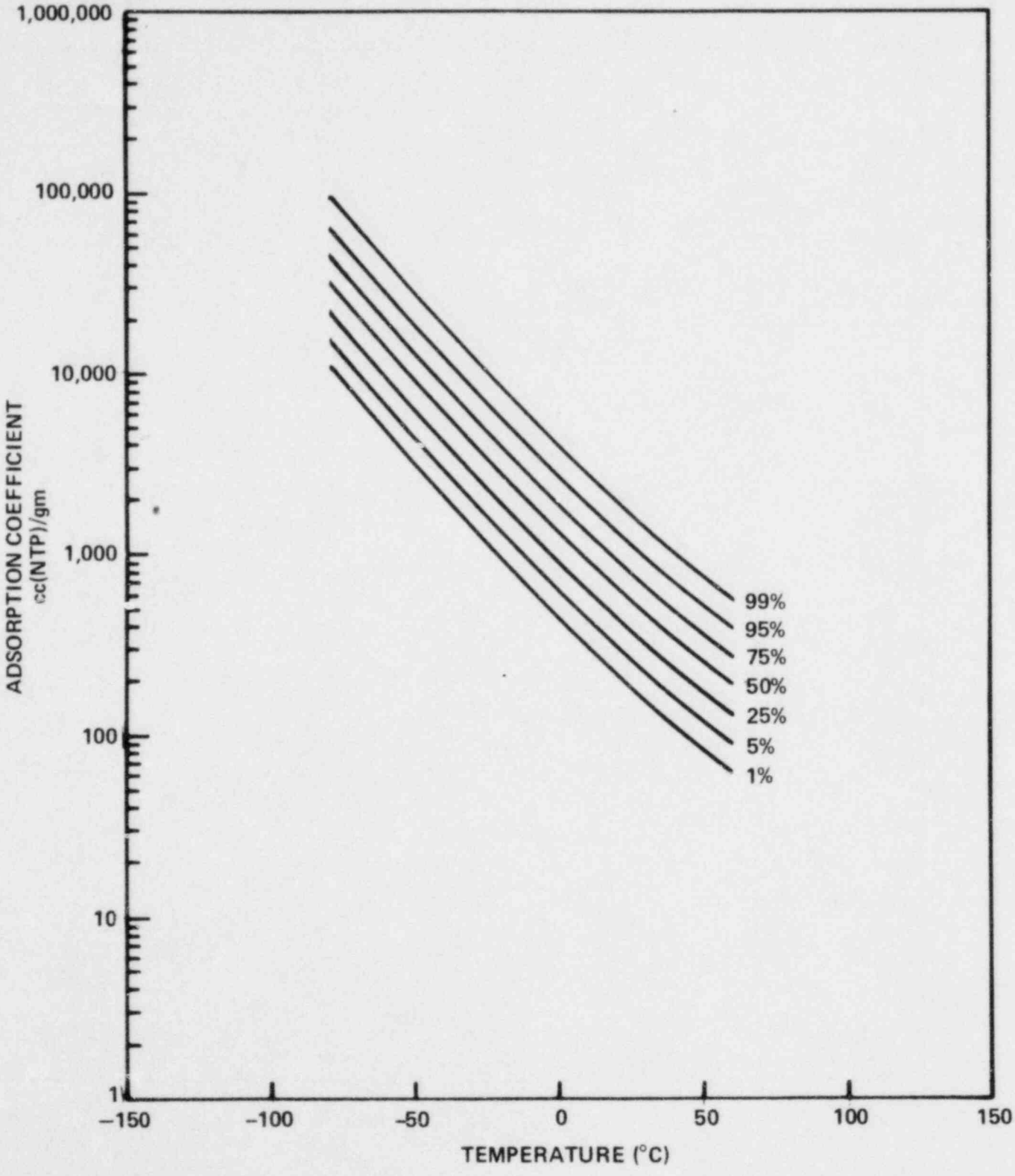

Figure 2.5 Adsorption of xenon from air: percent of adsorption coefficients expected to be less than stated value.

TABLE 2.1.1

Adsorption of Krypton from Hydrogen

Reference	Temperature (^{o}C)	Adsorption Coefficient /cc(NTP)/gm/	Comments
Razga (1975)	50	19.8	Adsorbent: Supersorbon (Particle Diameter: 0.20-0.25 mm)
	40	24.1	
	30	32.3	
	20	41.8	
	10	56.9	
	0	79.0	
	-10	105.5	
	-20	154.9	
	-30	232.2	
	-40	378.2	

TABLE 2.1.2

Adsorption of Krypton from Helium

Reference	Temperature (°C)	Adsorption Coefficient /cc(NTP)/gm/	Comments
Cooper, et al. (1975)	-100	7,200	Krypton concentration was 0.03 ppm.
	-120	68,000	Adsorbent: Pittsburgh PCB 12 x 30. Values here were taken from Cooper's Fig. 6. Data given for -140°C at a krypton concentration of 400 ppm will be discussed in a later section.
Browning and Bolta (1959)	- 5	264	Adsorbent: Columbia ACA.
	- 50	2,082	Adsorption coefficient determined by pulse input and fitting of output curve to a Poisson distribution.
Eshaya and Kalinowski (1967)	25	54	Adsorbent: Columbia HCC.
	50	34	Xenon Concentration: 0.025 mole %.
	75	25	
	100	18	
Madey (1961)	24	42	Adsorbent: Columbia HCC 12x28 Krypton Concentration: 10^{-6} ppm.
Burnette, et al. (1962)	25	55	Adsorbent: National Carbon CXC; Petroleum Base.
	25	59	National Carbon NXC; Petroleum Base.
	25	61	National Carbon G; Coconut Base.
	25	62	Pittsburgh PBC; Coconut Base.
	25	59	Barnebey Cheney 15578-2; Coconut Base.

TABLE 2.1.2 (Continued)

Adsorption of Krypton from Helium

Reference	Temperature (°C)	Adsorption Coefficient [cc(NTP)/gm]	Comments
	25	58	Barnebey Cheney AC4; Coconut Base
	25	48	Barnebey Cheney HH1; Coconut Base
	93	14	Barnebey Cheney 107; Coconut Base
	85	15	
	54	27	
	25	53	
	25	61	
	7	114	
	3	119	
	-25	312	
	-28	394	
	-50	859	
	-60	1,804	
First, et al. (1971a)	38	33	Adsorbent: North American Carbon G212
	-78	7,300	
Ackley, et al. (1960)	25	67	Adsorbent: Columbia G
	100	10.5	
Trofimov and Pankov (1965)	60	24	Adsorbent: AG-2 Activated Charcoal
	40	34	
	20	49	
	0	80	
	60	35	Adsorbent: BAU Activated Charcoal
	40	58	
	20	84	
	0	140	

TABLE 2.1.2 (Continued)

Adsorption of Krypton from Helium

Reference	Temperature (°C)	Adsorption Coefficient /cc(NTP)/gm/	Comments
Collins, et al (1967)	20	60	Adsorbent: Sutcliffe-Speakman Coconut Base Activated Charcoal, probably Type 203c.
	0	121	
	-20	280	
	-40	625	
	-60	2,240	
Barilli, et al (1969)	-133	3,700,000	Concentration of Krypton: 0.98 ppm. Results were originally given in cc(STP) of adsorbed krypton. These points not used in the regression analysis (Table 2.2) as only smoothed data were given.
	-153	15,000,000	
	-173	52,000,000	
	-193	139,000,000	

Table 2.1.3

Adsorption of Krypton from Nitrogen

Reference	Temperature (°C)	Adsorption Coefficient /cc(NTP)/gm/	Comments
Schumann (1973)	-20	110	Adsorbent: WTK-14
	-30	132	Krypton Concentration: 13 ppm
	-55	221	
	-20	144	Adsorbent: R4
	-30	180	
	-55	281	Because these values were based on the time of initial breakthrough, they are lower than the true equilibrium adsorption coefficients and therefore were not included in the regression analysis. (Table 2.2)
Kawazoe and Kawai (1972)	20	60	Adsorbent: Active Carbon HGR-510 In this case, the adsorption coefficient was extrapolated from a pressure of 1.22 Atm.
Kawazoe (1967)	20	56	Adsorbent: HGR-513
		38	Adsorbent: 2-GS
Nakhutin, et. al., (1969)	-100	1,579	Adsorbent: SKTM Activated Charcoal
	- 70	660	Packing density of 0.47 gm/cc was assumed by the reviewers.
	- 40	276	

TABLE 2.1.3 (Continued)

Adsorption of Krypton from Nitrogen

Reference	Temperature (°C)	Adsorption Coefficient [cc(NTP)/gm]	Comments
Kabele and Bohringer (1975)	-80	1,266	Adsorbent: Pittsburgh PCB 12x30
		1,200	The background Kr concentration was not stated.
	-120	4,900	Data were also given for N_2 + 1% O_2, and for N_2
		4,928	+ 1% O_2 + 100 ppm CO_2.
Browning and Bolta (1959)	15	48	Adsorbent: Columbia ACA
	0	71	The adsorption coefficient was determined by pulse
	-50	279	input and fitting of output curve to the Poisson
	-110	2,232	distribution.
Kitani, et al. (1968)	25	61	Adsorbent: Tsurumi GLS
	0	121	Columbia CXC
		86	Shirasagi G
		137	Columbia HCC
		96	Tsurumi 2G R-T*
		105	Tsurumi 2GM*
		123	Tsurumi GW*
		121	Tsurumi GLS*
		121	Takeda HGK-530
	-30	223	Adsorbent: Tsurumi GSL

* Primary wood based charcoals with added coal based charcoal.

TABLE 2.1.3 (Continued)

Adsorption of Krypton from Nitrogen

Reference	Temperature (°C)	Adsorption Coefficient /cc(NTP)/gm/	Comments
Lepold (1965)	20 10 0 -10 -20	79 116 143 193 218	Adsorbent: Not given. These measurements were conducted in a gas chromatography column designed to separate short lived isotopes.

TABLE 2.1.4

Adsorption of Krypton from Air

Reference	Temperature (°C)	Adsorption Coefficient /cc(NTP)/gm/	Comments
Yuasa, et al. (1975)	-50	360	Adsorbent: Coconut Base Charcoal. Krypton Concentration: 1 ppm.
		578	
	-100	2,600	
		2,400	
		2,600	
	-130	7,600	
	-150	16,000	
		17,000	
		15,000	
Yakshin, et al (1973)	40	40	Adsorbent not specified, but the reference cited is the design data for a Soviet reactor.
	20	57	
	0	84	
	-20	130	
	-40	230	
	-60	420	
Yoder and Imbarro (1965)	28	35	Adsorbent: Pittsburgh BPL 18x30
	-13	65	
	-13	65	Adsorbent: Pittsburgh BPL 6x16
	0	48	
	25	32	
	-20	70	Analysis: Frontal input with calculation of the adsorption coefficient from volume of effluent at point of 50% breakthrough.
	0	49	
	28	33	

TABLE 2.1.4 (Continued)

Adsorption of Krypton from Air

Reference	Temperature (°C)	Adsorption Coefficient /cc(NTP)/gm/	Comments
Trofimov and Pankov (1965)	60	20	Adsorbent: AG-2 Activated Charcoal
	40	28	
	20	39	
	0	57	
	60	26	Adsorbent: BAU Activated Charcoal
	40	34	
	20	47	
	0	68	
Underhill (1975) *	4	82	Adsorbent: "B"
	-29	205	
	4	75	Adsorbert: "I"
	-29	200	
Nakhutin, et al. (1976)	-80	560	Adsorbent: SKT-2B
	-30	135	
	0	67	
	20	44	

*Underhill, D. W. (1975): Unpublished Results.

TABLE 2.1.4 (Continued)

Adsorption of Krypton from Air

Reference	Temperature (°C)	Adsorption Coefficient /cc(NTP)/gm/	Comments
Nakhutin, et al. (1976)	-80	520	Adsorbent: SKT-3.
	-30	120	
	0	60	
	20	40	
	-80	480	Adsorbent: ART-2.
	-30	100	
	0	56	
	20	35	
	-80	440	Adsorbent: SKT.
	-30	97	
	0	52	
	20	31	
	-80	420	Adsorbent: SKT-6A.
	-30	92	
	0	48	
	20	33	
	-80	390	Adsorbent: SKT-2A.
	-30	93	
	0	30	
	20	12	

TABLE 2.1.4 (Continued)

Adsorption of Krypton from Air

Reference	Temperature (°C)	Adsorption Coefficient [cc(NTP)/gm]	Comments
Kanazawa, et al. (1977)	40	40	Adsorbent: Activated charcoal type Shirasaga G-A
	20	56	
	-10	120	Data originally given in terms of moles adsorbed/gm per moles/cc at bed temperature and pressure.
	-50	350	
	-100	2,181	
	-150	11,200	
Siegwarth, et al. (1973)			Adsorption coefficient was measured at 25°C, 16.7 psia and normalized to NTP.
	25	57.4-60.3	Coconut Base: Calgon PCB*
		54.8	Coconut Base: North American - G-210
		63.0	Coconut Base: North American - GX-169
		60.5	Coconut Base: Barneby-Cheney - 483
		48.0	Coconut Base: Sutcliffe-Speakman - 208C
		50.7-51.5	Petroleum Base: Witco - 337*
		52.0	Petroleum Base: Witco - 888
		49.1	Petroleum Base: Union Carbide - JXC
		45.7	Coal Base: Calgon BPL
		37.6	Coal Base: Westvaco - Nuchar

* K Measured on carbon samples received at different times.

TABLE 2.1.5

Adsorption of Krypton from Oxygen

Reference	Temperature (°C)	Adsorption Coefficient /cc(NTP)/gm/	Comments
Ackley, et al. (1960)	25	60	Adsorbent: Columbia G 8x14
	23	48	Fisher 6x14
	23	46	Columbia ACA 8x14
	24	39	Columbia CXA 4x6
	24	38	Columbia BPL 6x16
	149	6.2	Columbia ACA 8x14
	145	7.3	Columbia G 8x14
	145	5.8	Fisher 6x14
	145	5.6	Columbia CXA 4x6
	145	5.3	Pittsburgh BPL 6x16
	25	50	Columbia G.
	100	7.0	Columbia G.
Adams and Browning (1958)	15	64	
Madey, et al. (1962)	24	65	Adsorbent: Columbia G.
		59	Bulk density of charcoal calculated by reviewer
		58	using bed dimensions and weight.
		62	
Kitani, et al. (1968)	0	178	Adsorbent: Tsurumi GLS.

TABLE 2.1.6

Adsorption of Krypton from Argon

Reference	Temperature (°C)	Adsorption Coefficient [cc(NTP)/gm]	Comments
Kabele, et al. (1973)	-75	1,528	Adsorbent: Pittsburgh PCB 12x30
	-125	8,574	
	-160	31,600	
		29,500	
	-25	431	
		470	
First, et al. (1971b)	38	36	Adsorbent: National ACC
		39	NACAR G210
		36	NACAR G212
		25	NACAR G352
		41	Pittsburgh PCB
	-78	940	NACAR G212
		1,190	Pittsburgh PCB
First, et al. (1971a)	38	35	Adsorbent: North American Carbon G212.
	-78	880	
Collins, et al. (1967)	20	66	Adsorbent: Coconut Base Activated Charcoal.
	10	99	Krypton Concentration: 50 ppm
	0	130	Authors state that most tests were carried out using
	-10	170	Sutcliffe-Speakman 203c.
	-20	210	
	-30	280	
	-40	400	
	-50	540	

TABLE 2.1.6 (Continued)

Adsorption of Krypton from Argon

Reference	Temperature (°C)	Adsorption Coefficient /cc(NTP)/gm/	Comments
	-60	710	
	-70	950	
Aristarkhov, et al. (1975)	25	60	Adsorbent: SKT-2M

TABLE 2.1.7

Adsorption of Krypton from Carbon Dioxide

Reference	Temperature (°C)	Adsorption Coefficient /cc(NTP)/gm/	Comments
Trofimov and Pankov (1965)	60	17	Adsorbent: AG-2 Activated Charcoal.
	40	19	
	20	21	
	0	24	
	60	16	Adsorbent: BAU Activated Charcoal.
	40	19	
	20	21	
	0	25	
Ackley, et al. (1960)	24	15	Adsorbent: Columbia G.

TABLE 2.1.8

Adsorption of Krypton from Freon 12

Reference	Temperature (°C)	Adsorption Coefficient /cc(NTP)/gm/	Comments
Ackley, et al. (1960)	25 100	22 0.68	Adsorbent: Columbia G.

TABLE 2.1.9

Adsorption of Xenon from Hydrogen

Reference	Temperature (°C)	Adsorption Coefficient [cc(NTP)/gm]	Comments
Razga (1975)	50	232	Adsorbent: Supersorbon (Particle Diameter: 0.20-0.25 mm)
	40	291	
	30	429	
	20	544	
	10	718	
	0	1,159	

TABLE 2.1.10

Adsorption of Xenon from Helium

Reference	Temperature (°C)	Adsorption Coefficient /cc(NTP)/gm/	Comments
Kenney and Eshaya (1960)	25	624	Xenon Concentration: 0.5 volume %. Adsorbent: Columbia HCC.
	50	300	
	75	150	
	100	94	
	100	90	
	25	804	Adsorbent: Columbia CXC.
	50	390	
	75	184	
	100	110	
Burnette, et al. (1962)	90	105	Adsorbent: Barnebey-Cheney 107.
	75	143	
	75	169	
	25	947	
	25	1,180	
	0	2,700	
	-28	16,500	
	-45	53,000	
Trofimov and Pankov (1965)	60	220	Adsorbent: AG-2 Activated Charcoal.
	40	381	
	20	659	
	0	1,450	

TABLE 2.1.10 (Continued)

Adsorption of Xenon from Helium

Reference	Temperature (°C)	Adsorption Coefficient [cc(NTP)/gm]	Comments
	60	289	Adsorbent: BAU Activated Charcoal
	40	518	
	20	782	
	0	1,426	
Collins, et al (1967)	60	126	Adsorbent: Sutcliffe-Speakman Coconut Base Activated Charcoal, probably Type 203c
	50	173	
	40	256	
	30	375	Xenon Concentration: 0.0001 ppm
	20	546	
	10	906	
	0	1,460	
	-10	2,660	
	-20	4,420	
	-30	9,700	
	-40	19,200	
	-50	36,000	
	-60	66,000	
	-70	146,000	
Barilli, et al (1969)	-13	5,000	Xenon Concentration: 6.5 ppm
	-33	20,000	These points represent smoothed data and for this reason they were not included in the regression analysis (Table 2.2).
	-53	89,000	
	-73	330,000	

TABLE 2.1.10 (Continued)

Adsorption of Xenon from Helium

Reference	Temperature (°C)	Adsorption Coefficient /cc(NTP)/gm/	Comments
	-93	1,230,000	At these low temperatures the xenon concentration was sufficiently high to cause multilayer adsorption.
	-113	3,900,000	
	-133	10,500,000	
	-153	19,800,000	
	-173	30,000,000	
Nakhutin, et al. (1976)	-80	494,000	Adsorbent: SKT 2B
	20	880	
	-80	223,000	Adsorbent: SKT 6A
	-30	4,900	
	0	860	
	20	360	

TABLE 2.1.11

Adsorption of Xenon from Nitrogen

Reference	Temperature (°C)	Adsorption Coefficient /cc(NTP)/gm/	Comments
Lepold (1965)	20 10 0 -10 -20	762 988 1,141 1,459 1,901	These data were obtained in a gas chromatograph used to separate fission gas isotopes.
Collard, et al. (1977)	25	754	Adsorption on European Type Charcoal RBL-3. Adsorption coefficient was calculated from experiments in which xenon concentration ranged from 50 to 600 ppm.
Nakhutin, et al. (1969)	3	2,500	Adsorbent: SKTM activated charcoal. For this analysis, a packing density of 0.47 gm/cc was assumed by the reviewers. This result was not included in the regression analyses (Table 2.2).

TABLE 2.1.12

Adsorption of Xenon from Air

Reference	Temperature (°C)	Adsorption Coefficient [cc(NTP)/gm]	Comments
Yakshin, et al. (1973)	40 20 0 -20 -40 -60	530 1,000 1,800 3,600 8,400 24,400	Adsorbent not specified; reference cited relates to design data for adsorption system for USSR reactor.
Lee and Madey (1971)	~25, "Room temp")	66 83 87	Adsorbent: Cliffchar Adsorbent: BC Adsorbite Adsorbent: BC adsorbite These data were not included in the regression analysis (Table 2.2). Xenon-133 concentration: 0.09 ppm
Underhill (1975)*	4 -29 4 -29	2,460 8,500 1,840 7,200	Adsorbent: Charcoal "B". Adsorbent: Charcoal: "I".

*Underhill, D. W. (1975): Unpublished Results.

TABLE 2.1.12 (Continued)

Adsorption of Xenon from Air

Reference	Temperature (°C)	Adsorption Coefficient /cc(NTP)/gm/	Comments
Siegwarth, et al. (1973)	25	857-993*	Adsorbent: Coconut Base: Calgon PCB
		840	Coconut Base: North American - G-210
		1,010	Coconut Base: North American - GX-169
		1,060	Coconut Base: Barneby-Cheney - 483
		753	Coconut Base: Sutcliffe-Speakman - 208C
		715-742*	Petroleum Base: Witco - 337
		676	Petroleum Base: Witco - 888
		785	Petroleum Base: Union Carbide - JXC
		742	Coal Base: Calgon BPL
		502	Coal Base: Westvaco - Nuchar
			Adsorption coefficients were measured at 25°C, 16.7 psia and normalized to NTP.
Trofimov and Pankov (1965)	60	173	Adsorbent: AG-2 Activated Charcoal.
	40	235	
	20	368	
	0	536	
	60	220	Adsorbent: BAU activated charcoal
	40	321	
	20	468	
	0	756	

* These coefficients were obtained at different times.

TABLE 2.1.12 (Continued)

Adsorption of Xenon from Air

Reference	Temperature (°C)	Adsorption Coefficient /cc(NTP)/gm/	Comments
Nakhutin, et al. (1976)	-80	35,000	Adsorbent: SKT-2B
	-30	4,400	
	0	1,370	
	20	530	
	-80	31,000	Adsorbent: SKT-3.
	-30	4,100	
	0	1,230	
	20	428	
	-80	25,000	Adsorbent: SKT-2A
	-30	3,500	
	0	1,000	
	20	357	
	-80	20,000	Adsorbent: SKT-6A
	-30	2,400	
	0	700	
	20	328	

TABLE 2.1.13

Adsorption of Xenon from Argon

Reference	Temperature (°C)	Adsorption Coefficient /cc(NTP)/gm/	Comments
Kabele, et al. (1973)	30	796	Adsorbent: Pittsburgh PCB 12x30
	30	895	
	-30	10,900	
	-30	11,800	
	-75	108,000	
	-100	250,000	
	-100	305,000	
First, et al. (1971b)	38	489	Adsorbent: National ACC
	38	531	NACAR G210
	38	481	NACAR G212
	38	314	NACAR G352
	38	581	Pittsburgh PCB
	38	460	Witco 888
	38	485	Witco 337
	-78	100,000	NCAR G210
	-78	107,000	Pittsburgh PCB
Collins, et al. (1967)	60	260	Adsorbent: Coconut Base Activated Charcoal.
	50	350	Xenon Concentration: <1ppm
	40	500	Authors state that most tests were performed with
	30	750	Sutcliffe-Speakman 203c.
	20	1,000	These results are from their Table 1. To obtain
	10	1,570	cc(NTP)/gm, their values must be multiplied by
	0	2,300	298/T(abs.)

TABLE 2.1.13 (Continued)

Adsorption of Xenon from Argon

Reference	Temperature (°C)	Adsorption Coefficient /cc(NTP)/gm/	Comments
Collins, et al. (1967)	-10	3,600	
	-20	6,800	
	-30	10,500	
	-40	17,900	
	-50	26,700	
	-60	39,000	
	-70	63,100	Xenon concentration: <10 ppm.
Barilli, et al. (1969)	-13	1,650	Xenon concentration: 6.5 ppm.
	-33	10,800	These results were originally given in cc(STP)/gm.
	-53	29,000	These data were not used in the regression analysis
	-73	75,000	since they had been smoothed for purposes of analysis
	-93	193,000	Multilayer adsorption may have occurred at the
	-113	510,000	lower temperatures.
	-133	1,320,000	
	-153	3,500,000	
	-173	10,100,000	

TABLE 2.1.14

Adsorption of Xenon from Carbon Dioxide

Reference	Temperature (°C)	Adsorption Coefficient /cc(NTP)/gm/	Comments
Trofimov and Pankov (1965)	60	81	Adsorbent: AG-2 Activated Charcoal.
	40	91	
	20	136	
	0	167	
	60	60	Adsorbent: BAU Activated Charcoal.
	40	80	
	20	111	
	0	175	

TABLE 2.2

Antoine Coefficients for the Adsorption of Krypton and Xenon

System (Adsorbed Gas - Carrier Gas)	Antoine Coefficients			Natural Logarithm of the Geometric Standard Deviation $/\overline{\ln(\sigma)}/$	Number of Data Points (n)	Temperature Range Over Which Data Were Taken (^{o}C)
	A	B	C			
Kr-H_2	-3.56769	1902.38190	240.58930	0.02	10	-40 to 50
Kr-He	-5.06934	3647.85210	332.05548	0.29	44	-120 to 100
Kr-N_2	-9.29824	7963.78580	570.95524	0.25	29	-120 to 25
Kr-Air	-4.68315	3480.87430	391.32352	0.37	75	-150 to 60
Kr-O_2	-0.05476	419.06211	31.63314	0.18	18	0 to 100
Kr-Ar	-19.96366	21305.31700	862.32458	0.26	26	-160 to 38
Kr-CO_2	2.5936	21.50027	36.19603	0.11	9	0 to 60
Xe-H_2	-0.29532	1335.6667	182.50466	0.06	6	0 to 50
Xe-He	-2.57534	2284.49540	227.26565	0.37	45	-80 to 100
Xe-N_2	2.76102	871.51530	202.41475	0.04	6	-20 to 25
Xe-Air	-11.38411	10084.10400	542.88012	0.44	44	-80 to 60
Xe-Ar	-18.49801	16375.16900	622.35258	0.17	29	-100 to 60
Xe-CO_2	1.44594	673.45167	181.85625	0.12	8	0 to 60

TABLE 2.3

Adsorption of Krypton and Xenon from Various Gases on Charcoal as Calculated Using the Antoine Equation

Temperature (°C)	Adsorption Coefficient /cc(NTP)/gm/					
	$Kr-H_2$	$Kr-O_2$	$Kr-CO_2$	$Xe-H_2$	$Xe-N_2$	$Xe-CO_2$
-40	371					
-35	295					
-30	236					
-25	192					
-20	157				1879	
-15	130				1654	
-10	108				1466	
-5	91				1307	
0	77		24	1120	1172	172
5	65		23	922	1057	156
10	56		21	767	957	142
15	48	71	20	644	871	129
20	42	58	20	545	796	118
25	35	48	19	466	730	110
30	32	41	19	399		102
35	28	35	18	346		95
40	25	30	18	301		88
45	22	27	17	264		83
50	20	24	17	232		78
55		21	17			73
60		19	17			69
65		17				
70		16				
75		14				
80		13				
85		12				
90		11				
95		10				
100		10				

TABLE 2.4

Adsorption of Krypton from Helium on Charcoal as Calculated Using the Antoine Equation

Temperature (°C)	Percent of Measured Adsorption Coefficients Expected to be Less Than Stated Value						
	1%	5%	25%	50%	75%	95%	99%
-120	34291	41972	55975	68392	83563	111442	136406
-115	23072	28240	37661	46016	56223	74981	91778
-110	15803	19343	25796	31518	38510	51358	62862
-105	11006	13471	17966	21951	26820	35768	43781
-100	7786	9529	12709	15528	18973	25302	30970
-95	5588	5840	9122	11146	13619	18162	22230
-90	4067	4979	6638	8111	9910	13217	16177
-85	2998	3669	4893	5979	7305	9742	11925
-80	2237	2733	3651	4461	5450	7269	8897
-75	1688	2066	2755	3366	4113	5485	6714
-70	1287	1576	2102	2568	3137	4184	5121
-65	992	1214	1619	1979	2418	3224	3946
-60	772	945	1260	1539	1881	2508	3070
-55	606	742	989	1209	1477	1969	2410
-50	480	587	783	957	1169	1559	1909
-45	383	469	625	764	933	1245	1524
-40	308	377	503	615	751	1001	1226
-35	250	306	408	498	609	812	993
-30	204	249	333	406	497	662	811
-25	167	205	273	334	408	544	666
-20	138	169	226	276	337	450	550
-15	115	141	188	230	280	374	458
-10	96	118	157	192	235	313	383
-5	81	99	132	161	197	263	322
0	68	84	112	137	167	222	272
5	58	71	95	116	142	189	231
10	50	61	81	99	121	161	197
15	43	52	69	85	104	138	169
20	37	45	60	73	89	119	146
25	32	39	52	63	77	103	126
30	28	34	45	55	67	90	110
35	24	29	39	48	59	78	96
40	21	26	34	42	51	68	84
45	18	23	30	37	45	60	73

TABLE 2.4 (Continued)

Adsorption of Krypton from Helium on Charcoal as Calculated Using the Antoine Equation

Temperature (°C)	Percent of Measured Adsorption Coefficients Expected to be Less Than Stated Value						
	1%	5%	25%	50%	75%	95%	99%
50	16	20	27	32	40	53	65
55	14	18	23	29	35	47	57
60	13	16	21	25	31	41	51
65	11	14	18	23	28	37	45
70	10	12	16	20	25	33	40
75	9	11	15	18	22	29	36
80	8	10	13	16	20	26	32
85	7	9	12	15	18	24	29
90	7	8	11	13	16	21	26
95	6	7	10	12	14	19	24
100	5	7	9	11	13	17	21

TABLE 2.5

Adsorption of Krypton from Nitrogen on Charcoal as Calculated Using the Antoine Equation

Temperature (°C)	Percent of Measured Adsorption Coefficients Expected to be Less Than Stated Value						
	1%	5%	25%	50%	75%	95%	99%
-120	2339	2791	3591	4279	5100	6561	7830
-115	1927	2300	2959	3526	4202	5406	6452
-110	1594	1903	2449	2917	3477	4473	5338
-105	1325	1581	2034	2424	2888	3716	4435
-100	1105	1319	1696	2022	2409	3099	3699
-95	925	1104	1420	1693	2017	2595	3097
-90	777	928	1194	1422	1695	2180	2602
-85	656	782	1007	1199	1429	1839	2195
-80	555	662	852	1015	1210	1556	1857
-75	471	562	723	862	1027	1321	1577
-70	401	479	616	734	875	1126	1344
-65	343	409	527	628	748	962	1149
-60	294	351	451	538	641	825	984
-55	253	302	388	463	551	709	846
-50	218	260	335	399	475	612	730
-45	189	225	289	345	411	529	631
-40	163	195	251	299	355	459	547
-35	142	170	218	260	310	399	476
-30	124	148	190	227	270	347	415
-25	108	129	166	198	236	304	362
-20	95	113	146	174	207	266	317
-15	83	99	128	152	182	234	279
-10	73	87	113	134	160	206	245
-5	65	77	99	118	141	181	216
0	57	68	88	105	125	160	191
5	51	60	78	93	110	142	170
10	45	54	69	82	98	126	151
15	40	48	61	73	87	112	134
20	36	43	55	65	78	100	119
25	33	39	50	60	70	89	98

TABLE 2.6

Adsorption of Krypton from Air on Charcoal as Calculated Using the Antoine Equation

Temperature (°C)	Percent of Measured Adsorption Coefficients Expected to be Less Than Stated Value						
	1%	5%	25%	50%	75%	95%	99%
-150	7253	9307	13277	17000	21767	31051	39846
-145	5412	6945	9907	12685	16242	23169	29732
-140	4086	5243	7479	9576	12261	17491	22445
-135	3118	4002	5708	7309	9359	13350	17131
-130	2405	3086	4402	5637	7217	10295	13211
-125	1873	2403	3428	4389	5620	8017	10288
-120	1472	1889	2694	3450	4417	6301	8086
-115	1167	1497	2136	2735	3502	4996	6411
-110	933	1197	1708	2186	2800	3994	5125
-105	752	964	1376	1762	2256	3218	4129
-100	610	783	1117	1430	1831	2612	3351
-95	499	640	913	1169	1497	2135	2740
-90	410	527	751	962	1232	1757	2254
-85	340	435	622	797	1020	1455	1867
-80	283	363	518	664	850	1212	1556
-75	237	304	434	556	712	1016	1304
-70	200	257	366	469	600	856	1098
-65	169	217	310	397	508	725	930
-60	144	185	264	338	433	617	792
-55	123	158	226	289	370	528	678
-50	106	136	194	248	318	454	582
-45	91	117	167	214	275	392	503
-40	79	102	145	186	238	339	436
-35	69	89	126	162	207	295	379
-30	60	77	110	141	181	258	331
-25	53	68	97	124	159	226	290
-20	46	60	85	109	140	199	255
-15	41	53	75	96	123	176	226
-10	36	47	67	85	109	156	200
-5	32	41	59	76	97	138	177

TABLE 2.6 (Continued)

Adsorption of Krypton from Air on Charcoal as Calculated Using the Antoine Equation

Temperature (°C)	Percent of Measured Adsorption Coefficients Expected to be Less Than Stated Value						
	1%	5%	25%	50%	75%	95%	99%
0	29	37	53	67	86	123	158
5	26	33	47	60	77	110	141
10	23	30	42	54	69	99	127
15	21	27	38	49	62	89	114
20	19	24	34	44	56	80	103
25	17	22	31	40	51	72	93
30	15	20	28	36	46	65	84
35	14	18	25	33	42	59	76
40	13	16	23	30	38	54	69
45	12	15	21	27	35	49	63
50	11	18	19	25	32	45	58
55	10	12	18	23	29	41	53
60	9	11	16	21	26	38	48
65	8	10	15	19	24	35	45
70	7	10	14	18	22	32	41
75	7	9	13	16	21	29	38
80	6	8	12	15	19	27	35
85	6	8	11	14	18	25	32
90	5	7	10	13	16	23	30
95	5	7	9	12	15	22	28
100	5	6	9	11	14	20	26

TABLE 2.7

Adsorption of Krypton from Argon on Charcoal as Calculated Using the Antoine Equation

Temperature (°C)	Percent of Measured Adsorption Coefficients Expected to be Less Than Stated Value						
	1%	5%	25%	50%	75%	95%	99%
-160	17552	20916	26849	31945	38008	48790	58140
-155	14165	16879	21667	25780	30672	39373	46919
-150	11465	13662	17538	20867	24827	31870	37977
-145	9308	11091	14238	16940	20155	25872	30830
-140	7578	9030	11592	13792	16409	21064	25101
-135	6187	7373	9464	11261	13398	17198	20494
-130	5066	6036	7749	9219	10969	14081	16779
-125	4159	4956	6361	7569	9005	11560	13775
-120	3423	4079	5236	6230	7413	9515	11339
-115	2825	3366	4321	5142	6118	7853	9358
-110	2337	2785	3576	4254	5062	6497	7743
-105	1939	2310	2966	3529	4198	5389	6422
-100	1612	1921	2466	2934	3491	4481	5340
-95	1344	1601	2056	2446	2910	3735	4451
-90	1123	1338	1717	2043	2431	3121	3719
-85	940	1120	1438	1711	2036	2613	3114
-80	789	940	1207	1436	1709	2193	2614
-75	664	791	1015	1208	1437	1845	2199
-70	560	667	856	1018	1212	1555	1853
-65	473	563	723	860	1024	1314	1566
-60	400	477	612	728	867	1112	1326
-55	340	405	519	618	735	944	1125
-50	289	344	441	525	625	802	956
-45	246	293	376	447	532	683	814
-40	210	250	321	382	454	583	695
-35	179	214	274	326	388	499	594
-30	154	183	235	280	333	427	509
-25	132	157	202	240	286	367	437
-20	113	135	173	206	246	315	376
-15	98	116	149	178	212	272	324

TABLE 2.7 (Continued)

Adsorption of Krypton from Argon on Charcoal as Calculated Using the Antoine Equation

Temperature (°C)	Percent of Measured Adsorption Coefficients Expected to be Less Than Stated Value						
	1%	5%	25%	50%	75%	95%	99%
-10	84	100	129	153	183	234	279
-5	73	87	111	133	158	203	241
0	63	75	96	115	137	175	209
5	55	65	84	100	118	152	181
10	48	57	73	86	103	132	157
15	41	49	63	75	90	115	137
20	36	43	55	66	78	100	119
25	31	37	48	57	68	87	104
30	27	33	42	50	60	76	91
35	24	29	37	44	52	67	80
40	21	25	32	38	46	59	70

TABLE 2.8

Adsorption of Xenon from Helium on Charcoal as Calculated Using the Antoine Equation

Temperature (°C)	Percent of Measured Adsorption Coefficients Expected to be Less Than Stated Value						
	1%	5%	25%	50%	75%	95%	99%
-80	174499	224971	323060	415570	534571	767647	989681
-75	104849	135176	194113	249698	321201	461247	594657
-70	65073	83895	120474	154972	199350	286267	369067
-65	41592	53622	77001	99051	127415	182969	235891
-60	27305	35202	50551	65026	83647	120117	154860
-55	18369	23681	34007	43745	56271	80806	104178
-50	12636	16291	23394	30094	38711	55589	71668
-45	8873	11440	16428	21132	27183	39035	50325
-40	6350	8186	11755	15122	19452	27933	36012
-35	4623	5961	8560	11011	14164	20339	26222
-30	3421	4411	6334	8147	10481	15050	19403
-25	2569	3313	4757	6119	7871	11303	14573
-20	1957	2523	3622	4660	5994	8608	11097
-15	1509	1946	2794	3594	4623	6639	8560
-10	1178	1519	2181	2806	3609	5183	6682
-5	930	1199	1722	2215	2849	4091	5274
0	742	956	1373	1766	2272	3263	4207
5	597	770	1106	1423	1830	2628	3386
10	486	626	899	1156	1488	2136	2754
15	398	513	737	948	1219	1751	2258
20	329	424	609	783	1008	1447	1866
25	274	353	507	652	839	1205	1554
30	230	296	425	547	704	1011	1303
35	194	250	359	462	594	853	1100
40	165	212	305	392	505	725	935
45	141	182	261	335	431	620	799
50	121	156	224	288	371	533	687
55	105	135	194	249	321	460	593
60	91	117	168	216	278	400	515
65	79	102	147	189	243	349	450

TABLE 2.8 (Continued)

Adsorption of Xenon from Helium on Charcoal as Calculated Using the Antoine Equation

Temperature (°C)	Percent of Measured Adsorption Coefficients Expected to be Less Than Stated Value						
	1%	5%	25%	50%	75%	95%	99%
70	70	90	129	166	213	306	394
75	61	79	113	146	188	269	347
80	54	70	100	129	166	238	307
85	48	62	89	114	147	211	273
90	43	55	79	102	131	188	243
95	38	49	71	91	117	169	217
100	34	44	64	82	105	151	195

TABLE 2.9

Adsorption of Xenon from Air on Charcoal as Calculated Using Antoine Equation

Temperature (°C)	Percent of Measured Adsorption Coefficients Expected to be Less Than Stated Value						
	1%	5%	25%	50%	75%	95%	99%
-80	11502	15647	24256	32903	44646	69209	94151
-75	9113	12397	19218	26073	35373	54835	74596
-70	7256	9871	15301	20759	28164	43660	59394
-65	5805	7897	12241	16608	22532	34929	47517
-60	4665	6347	9839	13348	18110	28073	38190
-55	3767	5124	7943	10776	14620	22664	30832
-50	3054	4155	6441	8788	11855	18377	25000
-45	2487	3383	5244	7115	9653	14964	20357
-40	2033	2766	4288	5817	7892	12235	16644
-35	1669	2270	3520	4775	6478	10043	13662
-30	1375	1871	2900	3935	5338	8275	11258
-25	1137	1547	2399	3254	4415	6845	9311
-20	944	1285	1991	2702	3665	5682	7729
-15	787	1070	1659	2251	3053	4733	6439
-10	658	894	1387	1881	2552	3956	5382
-5	551	750	1163	1578	2141	3318	4514
0	464	631	979	1328	1801	2792	3798
5	392	533	826	1121	1520	2357	3206
10	332	451	699	949	1287	1995	2714
15	282	383	594	806	1093	1694	2305
20	240	326	506	686	931	1443	1963
25	205	279	432	586	795	1232	1677
30	175	239	370	502	681	1056	1436
35	151	205	318	431	585	906	1233
40	130	176	274	371	503	780	1062
45	112	152	236	320	435	674	916
50	97	132	204	277	376	583	793
55	84	114	177	240	326	506	688
60	73	99	154	209	284	440	598

TABLE 2.10

Adsorption of Xenon from Argon as Calculated Using the Antoine Equation

Temperature (°C)	Percent of Measured Adsorption Coefficients Expected to be Less Than Stated Value						
	1%	5%	25%	50%	75%	95%	99%
-100	252969	285220	338383	381121	429257	509268	574195
-95	187924	211883	251376	283125	318884	378322	426555
-90	140385	158283	187786	211504	238217	282619	318650
-85	105443	118886	141046	158860	178924	212275	239338
-80	79617	89768	106500	119951	135101	160283	180718
-75	60426	68130	80829	91038	102536	121648	137157
-70	46091	51967	61653	69440	78210	92788	104618
-65	35327	39831	47255	53224	59946	71120	80187
-60	27206	30674	36392	40988	46165	54770	61752
-55	21048	23731	28155	31711	35716	42373	47775
-50	16357	18443	21880	24644	27756	32930	37128
-45	12767	14395	[illegible]	19235	21665	25703	28980
-40	10008	11284	[illegible]	15078	16982	20148	22716
-35	7877	8882	[illegible]0537	11868	13367	15859	17881
-30	6226	7019	8328	9380	10564	12533	14131
-25	4940	5569	6607	7442	8382	9944	11212
-20	3934	4436	5263	5927	6676	7920	8930
-15	3145	3546	4207	4739	5337	6332	7139
-10	2524	2846	3376	3802	4283	5081	5729
-5	2032	2291	2719	3062	3449	4092	4613
0	1642	1852	2197	2474	2787	3306	3728
5	1332	1501	1781	2006	2260	2681	3023
10	1083	1221	1449	1632	1838	2181	2459
15	884	997	1183	1332	1500	1780	2007
20	724	816	968	1091	1228	1457	1643
25	595	670	795	896	1009	1197	1349
30	490	552	655	738	831	986	1112
35	405	456	541	610	687	815	918
40	335	378	448	505	569	675	761
45	279	314	373	420	473	561	632
50	232	262	310	350	394	467	527
55	194	219	259	292	329	390	440
60	162	183	217	245	276	327	369

TABLE 2.11

Reproducibility of Laboratory Determinations of Krypton and Xenon Adsorption Coefficients

Moisture Content (% by weight)	Run No.	Krypton Adsorption Coefficient /cc(NTP)/gm/	Xenon Adsorption Coefficient /cc(NTP)/gm/
2.05 ± 0.05	1	60.6	1,080
	2	60.5	1,065
	3	60.5	1,092
	Average	60.5	1,078
	Run No.		
1.0 ± 0.05	1	68.8	1,112
	2	68.6	1,097
	3	68.8	1,103
	Average	68.7	1,104

Reference: Littlefield, et al., (1975)

TABLE 2.12

Krypton Adsorption Coefficients Obtained at Various Stages in the Design and Construction of an Off-Gas System

Data Source and Test Conditions	Krypton Adsorption Coefficient /cc(NTP)/gm/
1. Carbon Supplier Laboratory Test	49*
2. Equipment Manufacturer Laboratory Test	
a. 1% moisture	55
b. 0% moisture	58
3. Independent Laboratory Test (1% moisture)	69
4. Off-Gas System Pre-Op Test	48
5. Off-Gas System in Operation	70**

* Bed temperature = $25^{o}C$
Krypton partial pressure = 7.6×10^{-3} mm Hg

** Average of all evaluations, corrected to 760 mm Hg

Reference: Littlefield et al. (1975)

TABLE 2.13

Adsorption Coefficients for Krypton Obtained Under Operating Conditions in an Off-Gas System

Date	Krypton Adsorption Coefficient /cc(NTP)/gm/			
	First Adsorber Bed		Second Adsorber Bed	
	^{85m}Kr	^{88}Kr	^{85m}Kr	^{88}Kr
December 28, 1973	68	61	67	--
January 16, 1974	62	64	66	--
January 21	61	61	62	--
January 29	--	--	59	60
February 4	48	53	--	--
February 15	55	61	--	--
March 12	51	53	60	60
March 20	51	55	--	--
April 10	51	54	59	61
April 24	52	56	50	53
April 26	56	60	54	56
May 14	55*	58*	55*	58*
May 15	59*	62*	59*	62*
May 16	62*	64*	62*	64*
May 17	58*	62*	58*	62*
June 10	--	--	60	63
June 11	--	--	63	63
June 12	--	--	71	68
June 14	--	--	69	69
June 17	--	--	67	70
June 18	--	--	76	76
June 20	--	--	71	71
June 21	65	71	--	--
June 24	68	75	80	80
June 25	71	71	82	84
June 26	71	71	82	82
June 28	71	72	86	85
July 1	84	94	96	96
July 3	67	78	--	--
July 12	65	65	68	68
July 15	70	70	78	78
July 16	71	69	76	78

* Average value across both beds

Reference: Littlefield et al. (1975)

CHAPTER 3

THE EFFECTS OF MOISTURE ON THE ADSORPTION OF KRYPTON AND XENON

A number of published papers contain data on the effects of moisture on the adsorption of krypton and xenon on charcoal. Experimental data are usually reported either in terms of the relative humidity of the carrier gas or in terms of the water content of the charcoal. Both factors are significant. It is important to know the effect of a given relative humidity since this determines the input of water into an adsorption bed.

Most charcoals saturate very slowly with water -- 16 hours exposure being required for equilibrium in some adsorption experiments. In addition, because of hysteresis effects, what appears to represent a steady state saturation of the charcoal may actually correspond to one of several water contents. For these reasons, measurements of the reduction in adsorption capacity as a function of water content of the charcoal may be more reproducible than similar measurements made as a function of the relative humidity of the incoming carrier gas.

3.1 Krypton Adsorption on Charcoal

3.1.1 Effect of Relative Humidity (RH) of the Carrier Gas

Figure 3.1 from Castellani, et al. (1975), shows the effect of the RH of the carrier gas on the adsorption coefficient for krypton on charcoal. The adsorbent was Barnebey-Cheney Type 592, 8/14 mesh, activated coconut base shell charcoal. The RH was calculated from the temperatures of the

bed and of a water condenser through which the input air was passed. The data have considerable scatter, but by a least square analysis Castellani, et al.(1975), found that the percent loss in the adsorption coefficient, from the value at zero percent RH, could be expressed by the following equation:

$$\Delta k = (0.0037 \pm 0.0007)\ RH \qquad (3.1)$$

The effect of the RH of the carrier gas and the water content of an activated charcoal native to India has been examined by Khan, et al. (1976). Figure 3.2 shows that at 100% RH the charcoal had lost 50% of its capacity for krypton. At intermediate RH levels, the dew point rather than the RH is given, so that correlation of these results with RH is not possible. Examination of Figure 3.2, however, makes it clear that the water content of the charcoal is more important than the momentary RH of the input air. A major difficulty in using Khan's adsorption coefficients is that they are strongly influenced by the carrier gas velocity. According to the theory developed in Chapter 6, the adsorption coefficient should be independent of the carrier gas velocity.

Roemberg (1964) developed values for the adsorption coefficient as a function of both the RH and the weight of adsorbed water. For this reason his data (Table 3.1) are especially valuable. At a low RH, the loss in the adsorption coefficient--about a 1.2% loss for each percent increase in the relative humidity--is far less than that given by Cardile and Bellamy (1979). These latter authors observed that at 25°C the reduction in the adsorption coefficient for krypton was 64% at a RH of 4% and 74% at a RH of 32%.

The percent decrease in the adsorption coefficient for each percent increase in RH (at low RH values), as reported by the above authors, is given in Table 3.2. As may be noted, these values show considerable variation. If a decision were to be made at this time, the data of Roemberg (1964) could probably best be defended, as his are the only data which include both the relative humidity of the incoming gas stream and the water content of the charcoals. In obtaining such a correlation, Roemberg clearly indicated his awareness of potential sources of error, such as incomplete saturation and hysteresis.

3.1.2 Effect of Water Content of the Charcoal

Foerster (1971) examined the effect of the water content of charcoal on the adsorption of krypton from argon. His results (Figure 3.3) show that over the range of 0% to 35% adsorbed water by weight, the adsorption coefficient is reduced by a factor of nearly 10. For the first several percent of adsorbed water, the loss in the adsorption coefficient is 6% for each 1% increase in water content. Above 5% water by weight, the average reduction is about 1.5% for each 1% of additional water. A confounding factor in these data is that results obtained from wood, coal and peat base charcoals are plotted on the same graph without any identification as to the type of charcoal.

Data reported by Ackley, et al. (1960), shown in Figure 3.4, also indicated that above loadings of 3% water by weight, the effect of additional water becomes less important. However, the magnitude of the

effect as determined by Ackley, et al., is much greater than that determined by other investigators. This can be seen by comparing Figure 3.4 with Figures 3.1 through 3.3. The reason for this difference is unknown.

Littlefield, et al. (1975), determined the effect of water over the range of 0.0 to 2.5 weight percent. The large number of experimental points in their data (Figure 3.5) show considerable scatter, but are consistent with a linear reduction in the adsorption coefficient of 6% for each 1% of added water at loadings below 3% to 5% by weight.

Roemberg (1964) observed an initial loss of adsorption capacity of about 10% for each added percent of water up to a 2% water content, and a leveling off in the effect of added water at higher water contents (Table 3.1). His correlations between RH and water loading, given in Table 3.3, are useful in assessing the effects of both factors on the adsorption behavior of charcoal.

The effect of low water loadings on the adsorption of krypton is summarized in Table 3.4. Except for the data from Ackley, et al. (1960), these results are consistent. At high water contents, only the data of Foerster (1971) are available, so no further comparisons can be made.

3.2 Xenon Adsorption on Charcoal

3.2.1 Effect of the Relative Humidity (RH) of the Carrier Gas

Considerably less information exists on the effect of the relative

humidity of the carrier gas on the adsorption of xenon. Based on studies conducted at 25°C, Cardile and Bellamy (1979) reported adsorption coefficient reductions of 62% and 72%, at relative humidities of 4% and 32%, respectively.

Collard, et al. (1977), using a European charcoal designated as Type RBL-3, found a factor of three reduction in the adsorption coefficient when the relative humidity was increased from 0% to about 62%.

Underhill (1974)*found a ninefold reduction in the adsorption coefficient at -29°C in passing from 0% to 100% relative humidity.

Although not apparent from the results cited here, under the same conditions the adsorption of xenon appears to be more affected by coadsorbates than is the adsorption of krypton. Whether adsorbed water differentially affects the adsorption coefficients of krypton and xenon can be determined only after more data have been accumulated.

3.2.2 Effect of the Water Content of the Charcoal

Few data on this subject could be located in the published literature. Those that were are given in Table 2.11. Because no test results were reported for dry charcoals, however, the overall effect of water content on the adsorption coefficient for xenon on charcoal cannot be calculated.

3.3 Experimental Difficulties

Results obtained from charcoals from India, the United States, the Federal Republic of Germany and the United Kingdom have been presented here. Because different base materials and manufacturing technologies

*Underhill, D. W. (1974): Unpublished Results.

are employed in these countries, differences are to be expected in the surface areas and the pore structures of the charcoals produced. Because smaller pores become filled with adsorbed water at much lower RH values, a charcoal with relatively small micropores will probably lose its effectiveness at a lower RH. Unfortunately, the effects of relative humidity on the adsorption coefficient are generally presented without concurrent data on the pore structure of the charcoal. As a result, available data on the effects of the RH of the carrier gas and the water content of the charcoal are deficient in this respect. In addition, it should be noted that a number of carrier gases, i.e., helium, air, oxygen and argon, were used in these studies. Whatever effect, if any, that this had is probably more important at low than at high RH values.

It is unfortunate that the published papers in this field often do not contain sufficient information to permit a subsequent investigator to fully reproduce the experimental conditions. A related factor is that frequently each investigator uses his own technique to determine the effects of relative humidity. The resulting differences make intercomparisons difficult.

Given the wide variation in experimental techniques and results, it would appear that the most pressing need is not to obtain more experimental data, but to caution researchers to be more careful in specifying the properties of the charcoals used in their tests, and to better define the experimental conditions under which their tests are conducted.

Only when these conditions are met, can reproducible data be generated. Specific features of a protocol that we believe should be considered for future tests include:

3.3.1 The pore size distribution and surface area of the charcoal should be reported. Also it is important that the base material and the manufacturer's designation be given. Generally, most of this information is available from the manufacturer or vendor of the charcoal. Unless this information is published with the experimental data, there will be no means for future investigators to correlate the observed effects of moisture with the physical properties of the charcoal.

3.3.2 The charcoal should be dried overnight in a stream of nitrogen gas at a temperature greater than 100°C. Drying is necessary to remove water and organic contaminants that may have been picked up by the charcoal. The reason that nitrogen rather than air should be used as the drying agent is that the use of the former eliminates the possibility of modifying the surface of the charcoal by oxidation during the drying procedure.

3.3.3 The charcoal should be allowed to come into equilibrium with a stream of air at a known relative humidity. It is necessary that humidification be continued until equilibrium is established; otherwise, the bed being tested will contain charcoal of varying degrees of saturation and the experimental results will be impossible to interpret.

3.3.4 The adsorption test should be made, after the above equilibrium has been established, by the injection of a tracer of either ^{85}Kr or ^{133}Xe into

the humidified air entering the bed. The adsorption coefficient can then be determined from the breakthrough curve.

3.3.5 After the dynamic measurement has been made, the charcoal should be removed from the system and the amount of adsorbed water determined by weighing before and after a second drying.

This permits the adsorption coefficient to be determined as a function of the weight of adsorbed water and, as discussed above, this may prove to be a more reliable correlation. These steps also permit the construction of water vapor isotherms, and their comparison with water vapor isotherms obtained by other procedures can be useful in identifying experimental error.

3.4 Recommendations and Conclusions

3.4.1. Only a very limited amount of data could be found regarding the effect of relative humidity of the carrier gas on the adsorption of xenon. Because xenon adsorption may be more strongly affected by moisture than krypton adsorption, obtaining additional xenon data should be given priority.

3.4.2 The effects of moisture on the adsorption of radioactive fission gases are better correlated with the water content of the charcoal than with the transient RH of the carrier air. Future experiments should include provisions to obtain measurements of both the RH of the air

in equilibrium with the charcoal as well as the water content of the charcoal under these conditions.

3.2.3 A protocol for reproducible experimental procedures needs to be established.

3.4.4 Excluding the results of one investigator, the effects of adsorbed water on the adsorption of krypton was found to be a 6% to 10% loss in the adsorption coefficient for each percent of adsorbed water (by weight) in the range of 1% to 2%.

3.4.5. As the water content increased beyond 2%, the data indicate a reduction in the effects of additional water.

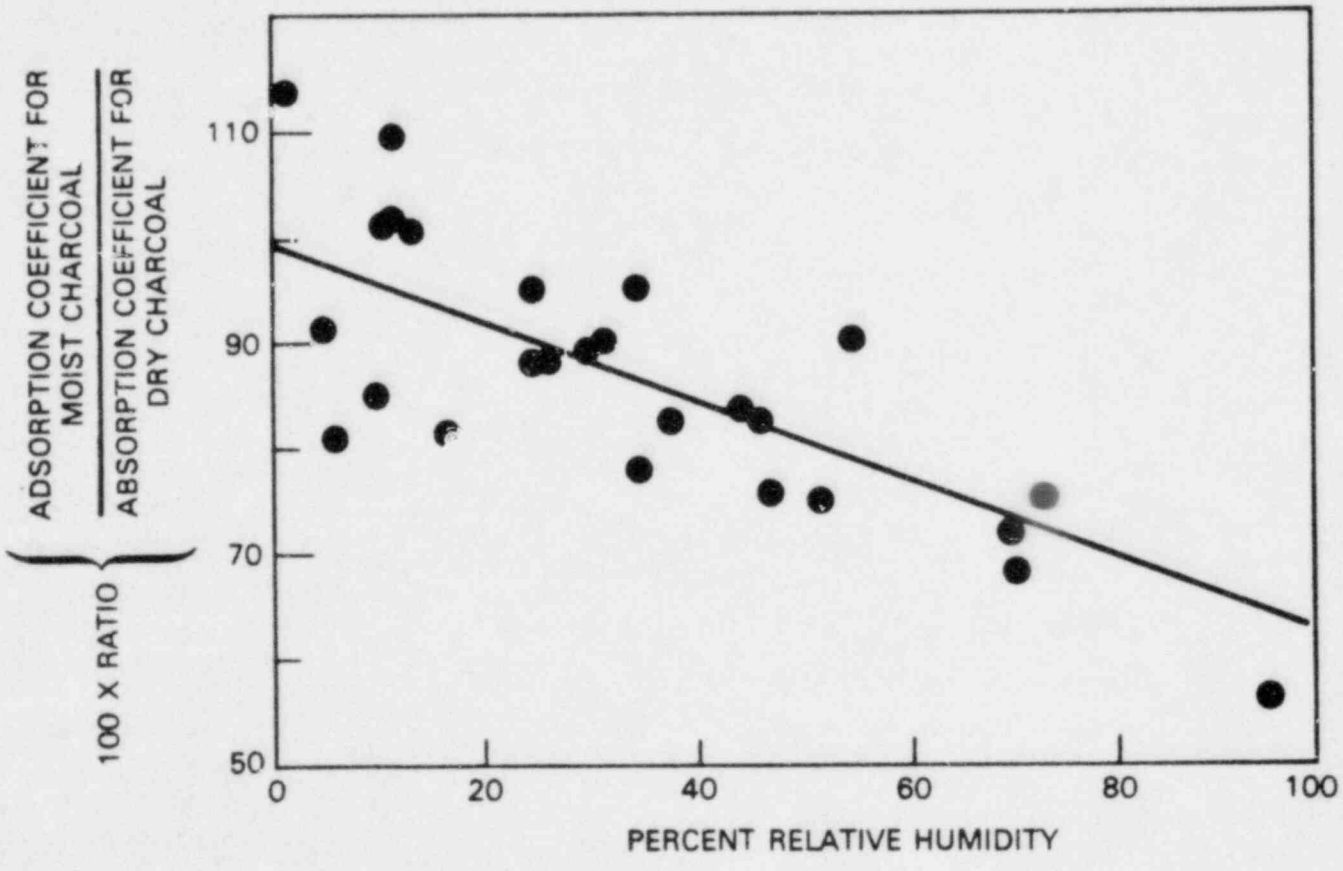

Figure 3.1 Effect of relative humidity on the adsorption coefficient of charcoal for krypton.
Adsorbent: Barnebey-Cheney Type 592. 8/14 mesh activated coconut base shell carbon.
Reference: Castellani et al. (1975).

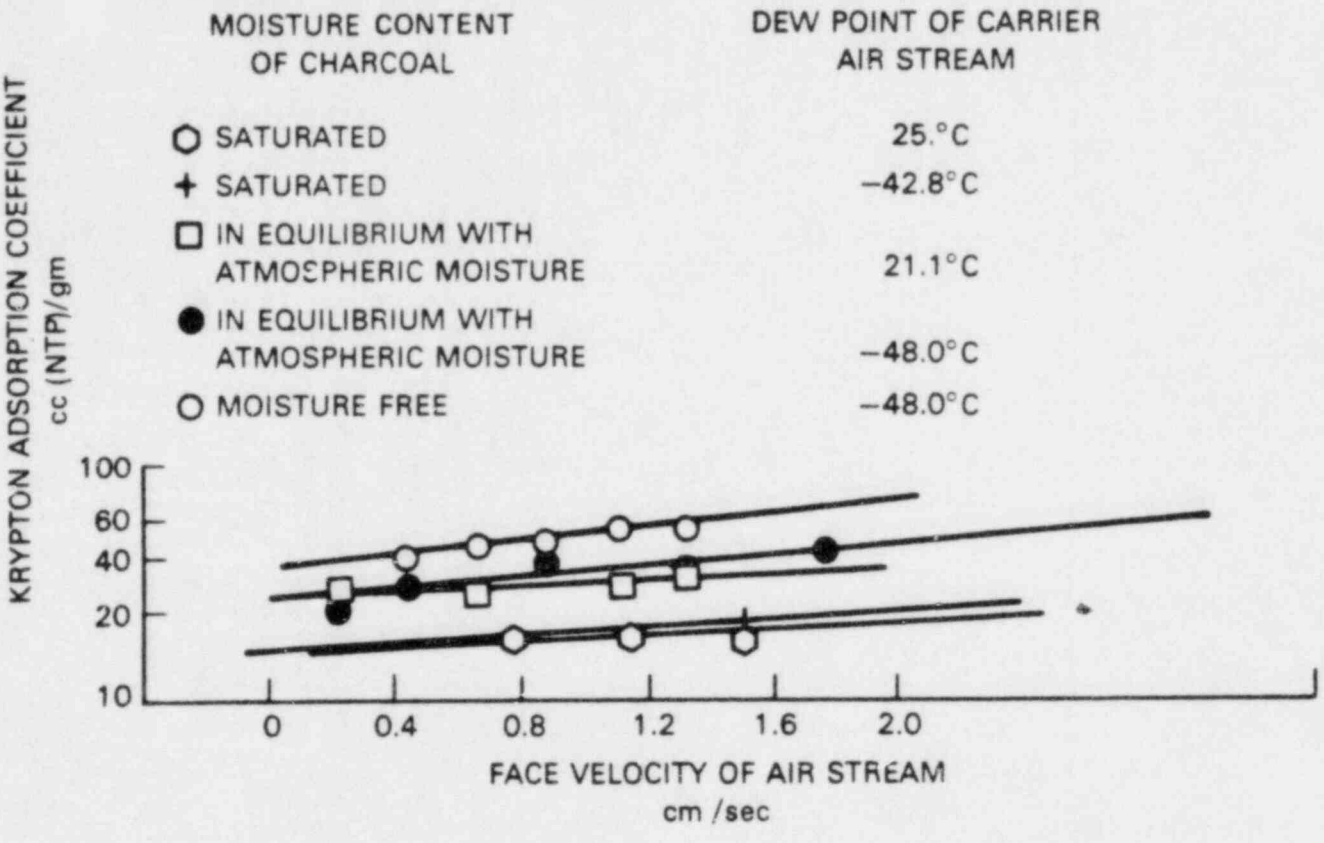

Figure 3.2 Effect of moisture content on the adsorption of krypton on activated charcoal at ambient temperature.
Reference: Khan et al. (1976).

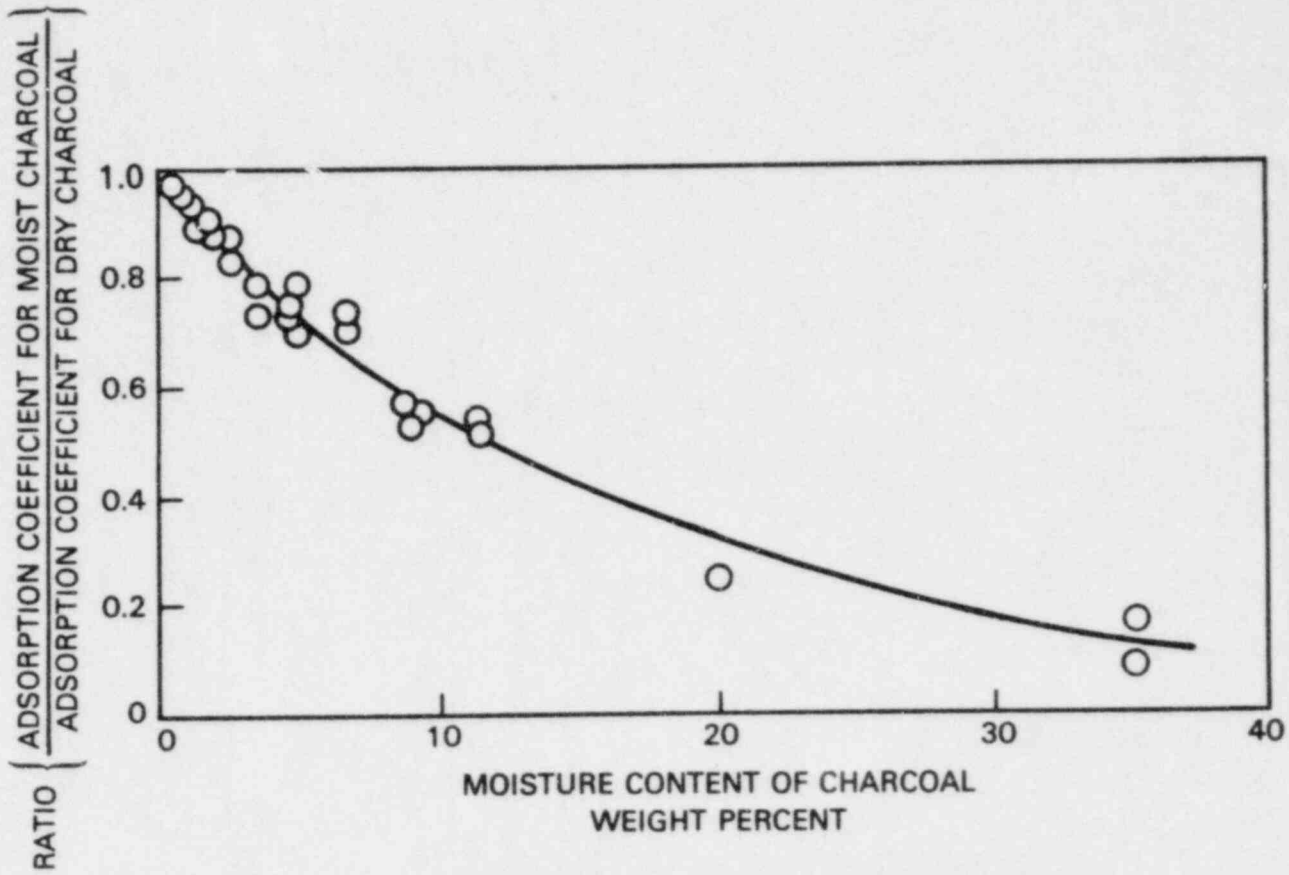

Figure 3.3 Effect of moisture contents of various charcoals on their adsorption coefficients for krypton.
Carrier gas: argon
Reference: Foerster (1971).

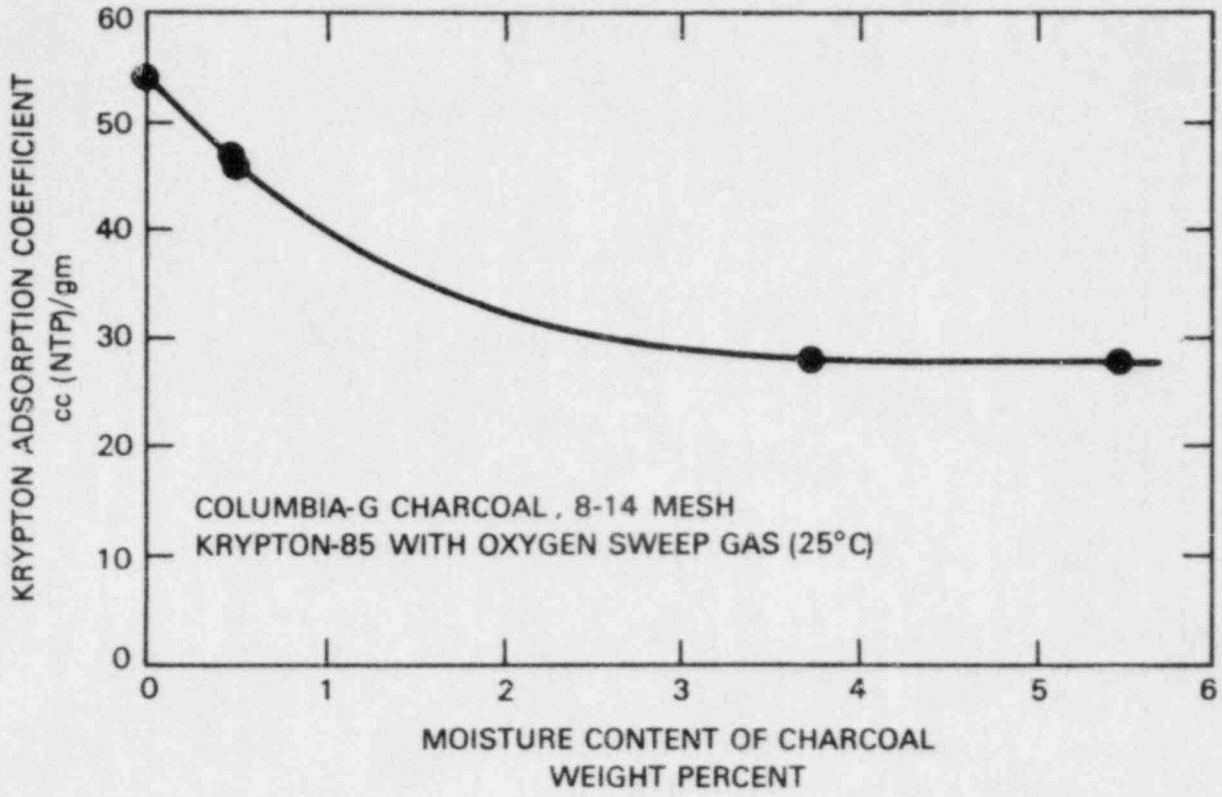

Figure 3.4 Effect of moisture content on the adsorption of krypton.
Reference: Ackley et al. (1960).

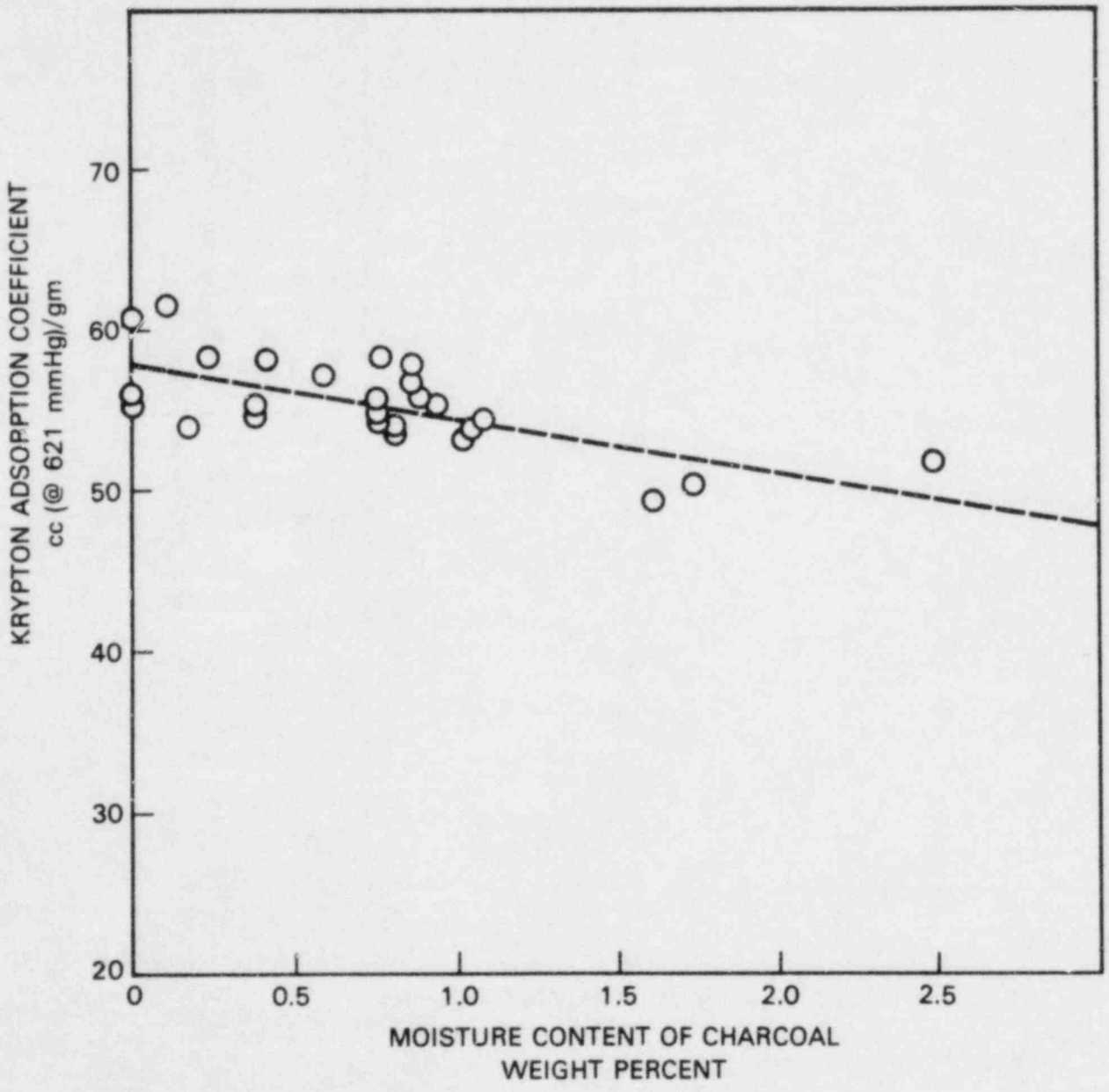

Figure 3.5 Vendor's measurements of the effect of moisture content on the adsorption of krypton.
Reference: Littlefield et al. (1975).

TABLE 3.1

Effect of Moisture on the Adsorption Coefficient of Coconut Base Shell Charcoal for Krypton

Moisture Content, (Wt. %)	Relative Humidity, (%)	Reduction in Krypton Adsorption Coefficient (%)
1.2	10	12.5
2.0	20	22
3.2	25	25

Adsorbent: Sutcliffe-Speakman 208[C]

Temperature: 50°C

Krypton Concentration: 1000 ppm

Reference: Roemberg (1964)

TABLE 3.2

Effect of Low Relative Humidities on the Adsorption of Krypton on Charcoal

Reference	Percent Decrease in Adsorption Coefficient for Each 1% Increase in Relative Humidity
Castellani, et al. (1975)	0.37
Roemberg (1964)	1.2
Cardile and Bellamy (1979)	16

TABLE 3.3

Water Vapor Isotherms for Charcoal
At Various Temperatures

0°C		25°C		50°C	
Relative Humidity (%)	Moisture Content (Wt. %)	Relative Humidity (%)	Moisture Content (Wt. %)	Relative Humidity (%)	Moisture Content (Wt. %)
4.5	1.00	6.1	1.00	7.4	1.00
12.8	1.83	17.6	1.83	20.7	1.83
25.1	3.3	31.4	3.3	33.7	3.3
30.8	4.2	42.5	5.7	38.6	4.2
44.7	7.4	51.8	9.0	53.4	7.5
50.4	14.0	53.9	12.9	61.4	17.8
55.9	23.8	57.7	19.2	66.6	26.1
64.2	30.9	66.5	28.7	71.6	30.9
72.0	33.9	77.4	34.1	89.1	35.8
93.2	36.8	88.8	35.7	100.0	36.3
100.0	37.9	100.0	36.8		
91.5	37.2	60.2	31.2	71.6	32.7
58.5	31.9	57.7	30.4	59.5	30.0
57.6	31.2	50.5	26.9	56.2	28.0
45.9	28.2	47.6	21.0	53.9	22.1
43.2	21.2	46.0	13.5	51.9	17.8
39.4	14.8	41.3	7.9	5.0	13.2
40.2	10.6			4.5	6.0
36.7	7.3				

Adsorbent: Sutcliffe-Speakman 208c Coconut Base Shell Charcoal

Reference: Roemberg (1964)

TABLE 3.4

Effect of Small Quantities of Adsorbed Moisture on the Krypton Adsorption Coefficient

Reference	Percent Decrease, at Low Moisture Content, in the Adsorption Coefficient of Krypton for Each 1% (by weight) of Adsorbed Moisture
Foerster (1971)	6
Littlefield, et al. (1975)	6
Roemberg (1964)	10
Ackley, et al. (1960)	26

CHAPTER 4

THE EFFECTS OF CONCENTRATION ON THE ADSORPTION OF KRYPTON AND XENON

When krypton and xenon are present at high concentrations, their adsorption coefficients are reduced. If this reduction becomes significant, adsorption beds could become ineffective under the very circumstances where they are most needed. Summarized in this Chapter are a number of published reports relating to the effects of concentration on the adsorption coefficients for these two gases.

4.1 Concentration Effects in the Presence of a Helium Carrier Gas

Because helium does not compete with krypton and xenon for adsorption sites, the krypton and xenon isotherms obtained in the presence of helium should be the same as those obtained in the absence of a carrier gas. Figure 4.1 (Eshaya and Kalinowski, 1961) demonstrates this point. The lines in this figure represent isotherms determined statically by Amphlett and Greenfield (1958) in the absence of a carrier gas. The data points are from dynamic adsorption experiments conducted by Eshaya and Kalinowski (1961) using the same types of charcoal, but this time in the presence of a helium carrier gas. Within the limits of experimental error there is no difference between the results obtained by these procedures.

Adsorption isotherms often follow the Freundlich isotherm,

$$q = aP^b \qquad (4.1)$$

where

q = volume (cc at NTP) of adsorbed gas per gram of adsorbent;

P = partial pressure of the adsorbed gas;

a,b = coefficients for the Freundlich isotherm.

This definition omits the contribution of the interparticle gases, which for bulk charcoal at NTP amounts to about 0.8 cc/gm.

As may be noted from Figure 4.1, a plot of isotherm data on log-log coordinates results in a straight line. This demonstrates that the Freundlich isotherm is applicable to the data of Eshaya and Kalinowski (1961).

A relationship between the adsorption coefficient and the Freundlich isotherm is:

$$k = aP^{b-1} \qquad (4.2)$$

where k = adsorption coefficient, cc(NTP)/gm.

Tables 4.1, 4.2, and 4.3 and Figs. 4.2 and 4.3 present adsorption coefficients determined by Kenney and Eshaya (1960) and Eshaya and Kalinowski (1961). The xenon adsorption coefficient shows a definite increase with decreasing xenon concentration, whereas the krypton adsorption coefficient appears to decrease only slightly under the same conditions. This latter result is probably an artifact since the factor, "b", is expected to have a value less than 1.

Ackley and Browning (1961) also observed that the adsorption of krypton and xenon in the absence of a carrier gas followed the

Freundlich isotherm. Table 4.4 gives their values for "a" and "b" for the Freundlich isotherm over the pressure range, 0.1 to 2.0 mm Hg. The adsorption coefficients are calculated for a pressure of 0.1 mm Hg. Ackley and Browning have pointed out that these isotherms would also be representative of the adsorption coefficients obtained in the presence of helium.

Zeldowitsch (1934) determined that the Freundlich isotherm was consistent with the assumption that the adsorbent surface consists of sites having an exponential distribution of energies of adsorption. In general, "b" will be less than unity, but will approach unity as the temperature increases. For two gases at the same temperature, "b" will be less for the more strongly adsorbed gas. These predictions are in good agreement with the data cited above.

According to the Freundlich isotherm, the adsorption coefficient increases indefinitely as the concentration of adsorbate (adsorbed gas) decreases. In actuality this cannot occur. When the concentration is decreased below the point where there is appreciable coverage of the most active sites, the number of adsorbed atoms at all sites should become proportional to the partial pressure of the adsorbate. At this point the adsorption coefficient becomes independent of the partial pressure and "b" is equal to unity. It is not known how low the concentration of fission gas must be for the isotherm to become linear, but for some gases nonlinear effects may be found well below 10^{-6} Atm.

Cooper, et al. (1975), found evidence that at -140°C the adsorption coefficient for 400 ppm krypton in helium is nonlinear. This is based on their observation that measurements of the krypton adsorption coefficient by frontal and by pulse chromatography gave different results. Their explanation for this phenomenon is that in pulse chromatography the injected pulse, as it passes through the bed, spreads, and the krypton concentration in the pulse becomes far less than the injected value. If the adsorption coefficient is affected by concentration, then by definition the adsorption isotherm is nonlinear.

Below their critical temperatures, adsorption of krypton and xenon from helium can be represented by a Polanyi isostere, which gives the combined effects of temperature and pressure on a single curve. Figure 4.4 shows the Dubinin modification of this method applied by de Bruijn, et al. (1964), to the adsorption of both krypton and xenon. Here the volume of condensed adsorbate, per gram of charcoal, is plotted as a function of the free energy required for adsorption.

This change in free energy per mole of adsorbate is approximately equal to:

$$\Delta F = RT \ln (P_o/P) \qquad (4.3)$$

where:

R = the ideal gas constant

T = the absolute temperature

P = the partial pressure of vapor in contact with the charcoal

P_o = the vapor pressure of the pure liquid at the temperature of the measurement.

Using this method, de Bruijn, et al., combined data from different temperatures, pressures and adsorbates into a single curve. Above the critical temperature, this procedure begins to break down as it becomes necessary to calculate artificial vapor pressures and liquid densities (Hotchkiss, 1976).

4.2 Concentration Effects in the Adsorption of Krypton from Carrier Gases other than Helium.

Carrier gases other than helium compete with the fission gases for adsorption sites. At low concentrations of fission gases, this competition linearizes their adsorption isotherms by converting their heat of adsorption on very active sites into the lesser value of a heat of displacement. The net result is that at moderate and low concentrations of fission gases, the adsorption isotherm is either linear or very nearly linear. At high concentrations the isotherm is nonlinear.

This prediction of the effects of high fission gas concentrations is supported by experimental studies. Ackley, et al. (1960), measured the effect of a high concentration of krypton on its adsorption from oxygen at room temperature. From their results (Figure 4.5) it can be seen that raising the krypton concentration from trace levels to 100% reduced the adsorption coefficient from an initial value of 50 cc(NTP)/gm to a final value of 32 cc(NTP)/gm. Khan, et al.(1976), observed a 10% loss in the adsorption coefficient for krypton at ambient temperature when the krypton concentration was raised from trace levels to 0.2% in an air carrier. Foerster (1971) found a 4% reduction in the krypton adsorption coefficient when the

concentration of krypton in argon was raised from trace levels to 2%. The possible effects of an argon carrier gas should be considered if Foerster's results (Figure 4.6) are used to predict similar effects in other carrier gases.

At low concentrations of fission gases, the independence or near independence of the adsorption coefficient on concentration has been substantiated by several studies. Schumann's (1973) results (Figure 4.7) are consistent with a linear isotherm for trace levels of krypton at -20°C. The adsorption isotherm for trace levels of krypton should remain linear at higher temperatures, and the values of Kitani, et al. (1968), plotted by Schumann (1973) in Figure 4.7 are consistent with this conclusion. The data in Table 4.5, from Kitani, et al. (1968), show that the krypton adsorption coefficient is independent of the krypton concentration at krypton concentrations of 63, 100, and 630 ppm, temperatures of 25, 0, and -30°C, and pressures of 1 and 10 atmospheres.

Wirsing, et al. (1970), observed that, at -170°C in air and at -128°C and -66°C in nitrogen, the krypton adsorption coefficient remained independent of concentration up to 4000 ppm. It will be noted later that these adsorption coefficients were strongly dependent on the carrier gas velocity and that this casts doubt on their reliability.

Kovach (1972) found a nonlinear isotherm for the adsorption of krypton at extremely low concentrations from air. It should be noted from Table 4.7 that two of his three krypton concentrations were below the level

usually present in the atmosphere and cannot be taken as typical of ambient air.

Collins, et al. (1967), reported a large number of measurements of the effect of concentration on the adsorption of krypton and xenon from argon. Their data permit correlations to be made between temperature, krypton concentration, and the adsorption coefficient. From the Langmuir coefficients derived from data published by Collins, et al.(Table 4.8), the effect of krypton concentration on its adsorption coefficient can be calculated for a wide range of krypton concentrations at temperatures from -70 to 60°C. It is found, for example, that at -70°C the loss of adsorption capacity will be less than 1% at krypton concentrations of 100 ppm or less. At 20°C the loss of adsorption capacity will be less than 1% for krypton concentrations up to 10,000 ppm.

It is interesting to apply this analysis to the measurements of Ackley, et al. (1960), for the adsorption of krypton from oxygen. At krypton concentrations of 21% and 100%, the reductions were 21% and 46%, respectively (Figure 4.5), whereas the values calculated from the coefficients in Table 4.8 were 15% and 46%, respectively. This agreement suggests that the coefficients in Table 4.8 may be applicable to results obtained from other carrier gases. It is probable that the coefficients in Table 4.8 are the best available parameters for determining the effects of high krypton concentrations on the adsorption of krypton from air, but it should be

kept in mind that these coefficients were determined using an argon carrier gas.

4.3 Effects of Concentration on the Adsorption of Xenon from Carrier Gases other than Helium

Collard, et al. (1977), found the adsorption coefficient for xenon at room temperatures to be independent of concentration at concentrations in the range of 50 to 600 ppm. Nakhutin, et al. (1976), (Figure 4.2) similarly found the adsorption coefficient for xenon at 21°C to be independent of its concentration at xenon partial pressures approaching 1 mm Hg. However, at -82°C, as the xenon partial pressure approached 0.1 mm Hg, a small but definite nonlinearity was observed.

Table 4.9 from Kovach (1972) shows a concentration effect on xenon adsorption in the ultra-low range of 0.013 ppm to 1.3 ppm xenon in air. Again, it should be noted that the lowest concentration cited by Kovach is below the ambient level of xenon in air.

Again, the most extensive study was by Collins, et al. (1967), in which the effect of xenon concentration on the adsorption of xenon from argon was examined. At low and intermediate xenon concentrations, the Langmuir isotherm (Equation 4.4) closely represents the experimental data (Table 4.8). At the very highest concentrations (i.e., those experiments where the initial xenon concentration was 10% or more), the Langmuir isotherm did not fit the data well, probably because of multilayer adsorption.

An appreciable reduction in the adsorption coefficient occurs at much lower concentrations for xenon than for krypton under comparable circumstances. At 20°C the reductions in their adsorption coefficients are comparable when the xenon concentration is one twentieth of the krypton concentration. Since the fission yield for xenon is greater than that for krypton, it appears that if reductions in the adsorption coefficients due to high concentrations occur, the effect is likely to be greater for the xenon isotopes.

4.4 Cross Interferences in the Adsorption of Krypton and Xenon

The effects of the presence of krypton on the adsorption of xenon (or the effects of xenon on the adsorption of krypton) are important because, in an operational nuclear facility, these two gases are generally found in combination. Measurements (Figure 4.6) by Foerster (1971) show that, at 20°C, the addition of 1% xenon to a trace concentration of krypton in argon reduced the krypton adsorption coefficient by 16%. At -50°C, the same concentration of xenon reduced the krypton adsorption coefficient by 36%.

In apparent contradiction to the above results, Eshaya and Kalinowski (1961) found that in helium at room temperature, raising the xenon concentration from 0.25% to 1% had no effect on the adsorption coefficient of krypton.

A more extensive study of the interference of krypton on the adsorption of xenon is reported by Collins, et al. (1967). Their krypton concentrations were either below 0.1% or above 20%, and this gap in their data certainly complicated our effort to analyze them.

Nonetheless, the Langmuir isotherm (Equation 4.4, Table 4.8) permits calculation of the simultaneous adsorption of krypton and xenon. From the Langmuir coefficients given in Table 4.8, it may be seen that the effect of krypton in reducing the adsorption coefficient of xenon is less than the reduction in the krypton adsorption coefficient brought about by the presence of an equivalent concentration of xenon.

The reverse effect--the reduction in the adsorption coefficient of krypton brought about by the presence of xenon--is expected to be greater because xenon is the more strongly adsorbed gas and therefore would more easily displace the krypton. Unfortunately, there are insufficient data to determine the Langmuir coefficients for this phenomenon.

4.5 Conclusions

A number of reports describing measurements of th effect of noble gas concentrations on their adsorption coefficients have been reviewed in this Chapter. The important findings and recommendations are:

4.5.1 In helium, at temperatures below the critical temperatures of the fission gases, the Polanyi isostere is useful in correlating the combined effects of temperature and concentration. At higher temperatures, the Freundlich isotherm more closely fits the experimental data.

4.5.2 In gases other than helium, the adsorption coefficients of krypton and xenon at low concentrations are independent of, or only very slightly influenced by their concentrations.

4.5.3 For the adsorption of krypton and xenon from argon, the Langmuir isotherm provides a simple procedure for estimating the effects of concentration on the adsorption coefficient. The validity of these coefficients for the adsorption of krypton and xenon from air needs to be confirmed.

4.5.4 The Langmuir coefficient for the effect of xenon on the adsorption of krypton needs to be determined.

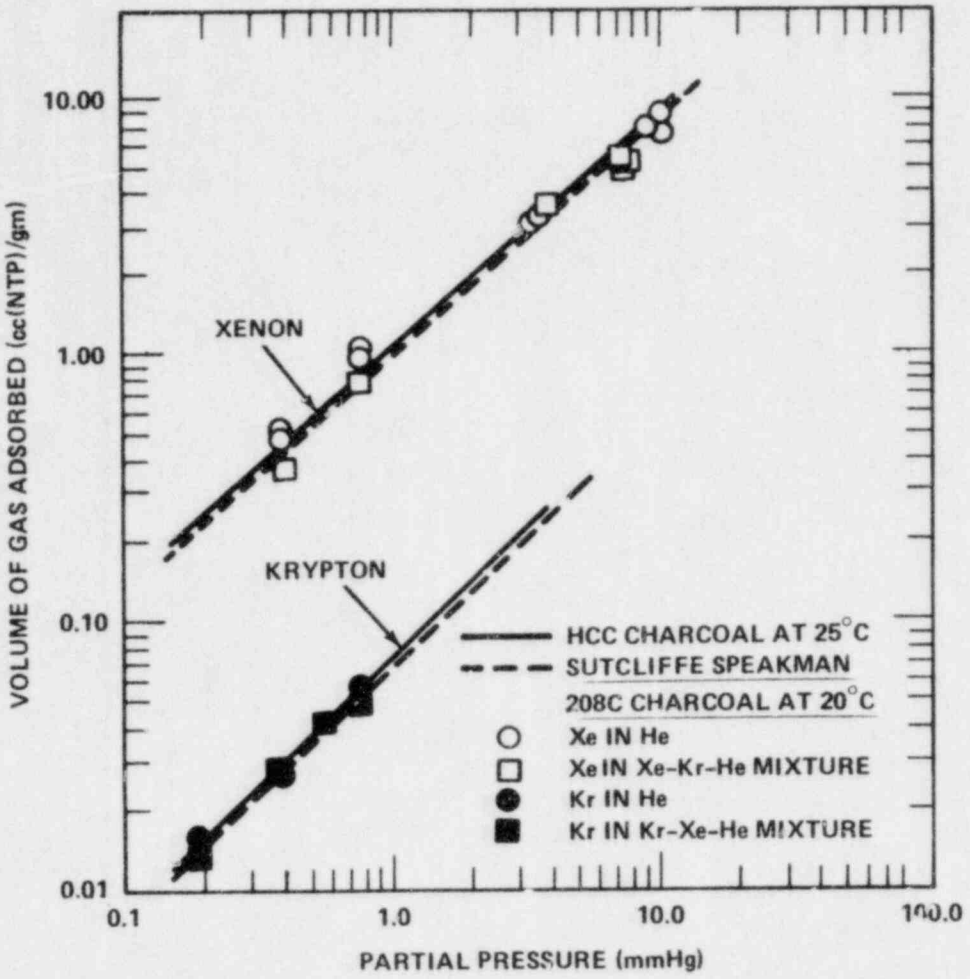

Figure 4.1 Comparison of static and dynamic adsorption coefficients for xenon and krypton and xenon-krypton mixtures in helium.

Reference: Eshaya and Kalinowski (1961)

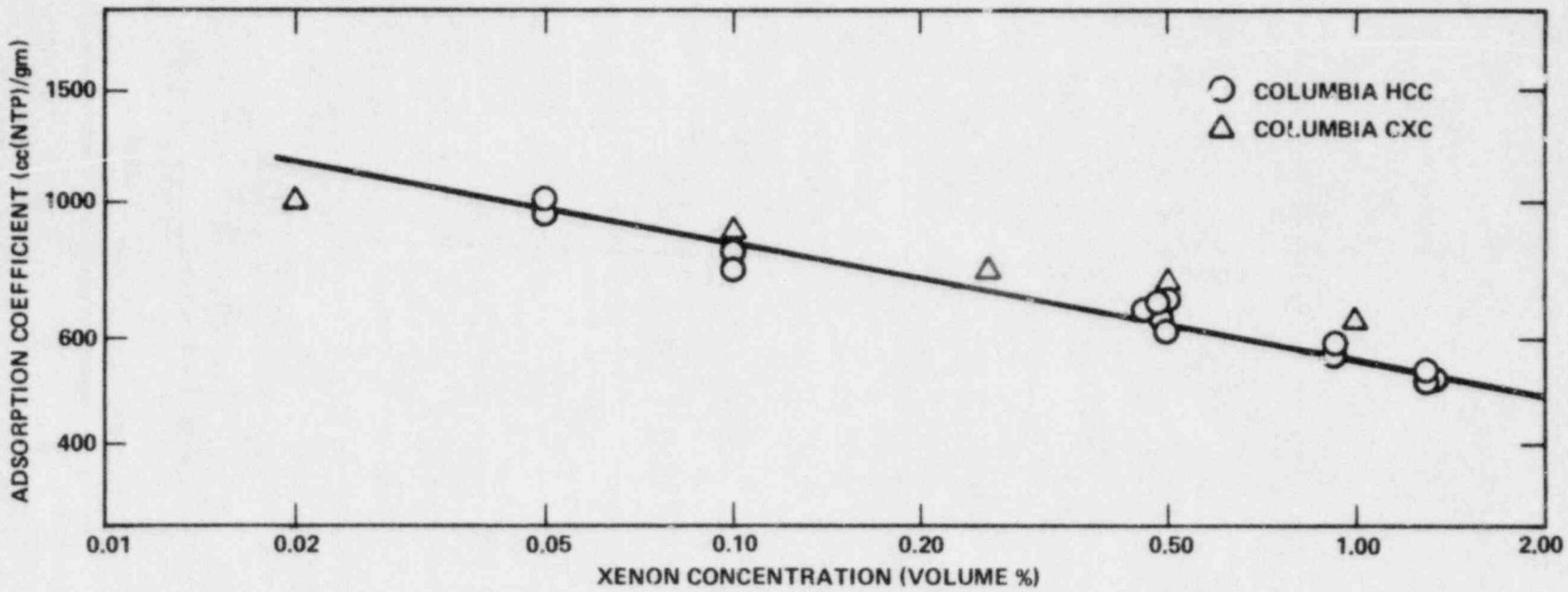

Figure 4.2 Effect of concentration on xenon adsorption coefficient.
Reference: Kenney and Eshaya (1960).

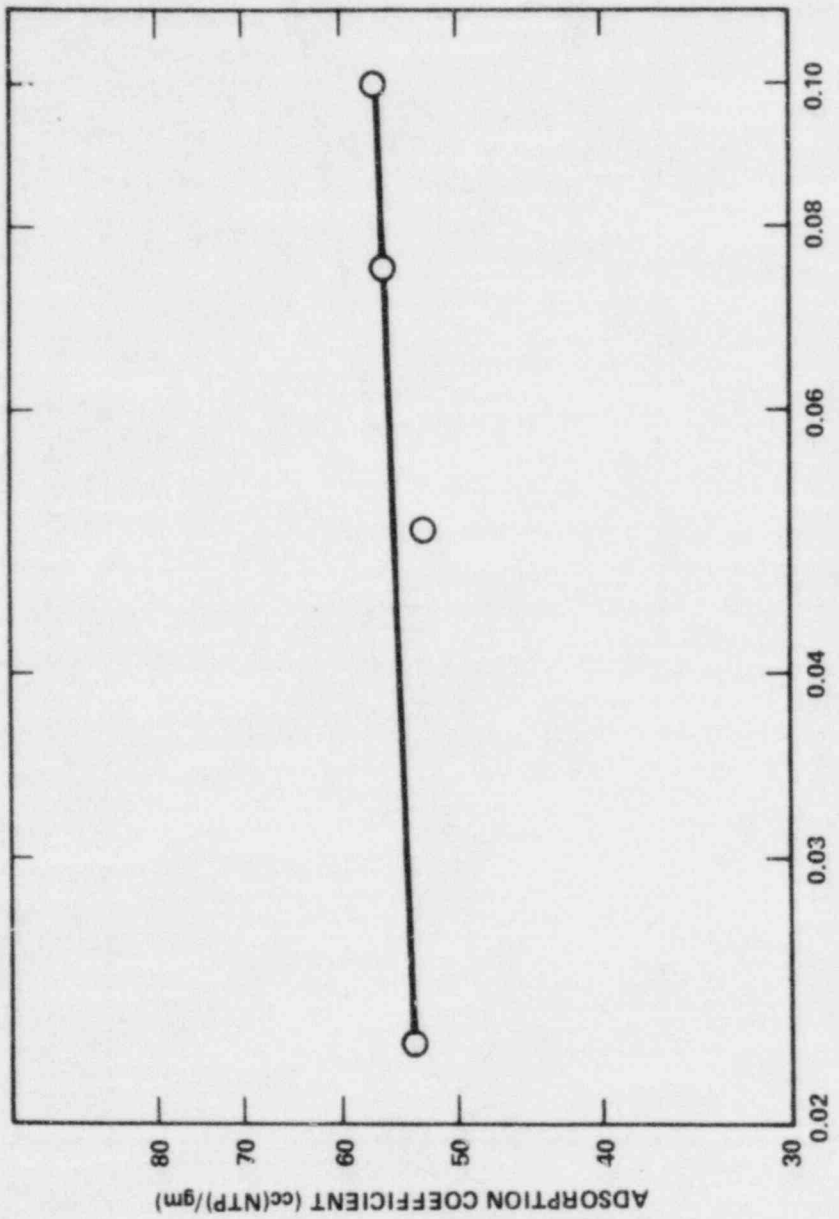

Figure 4.3 Effect of concentration on krypton adsorption coefficient.
Reference: Eshaya and Kalinowski (1961).

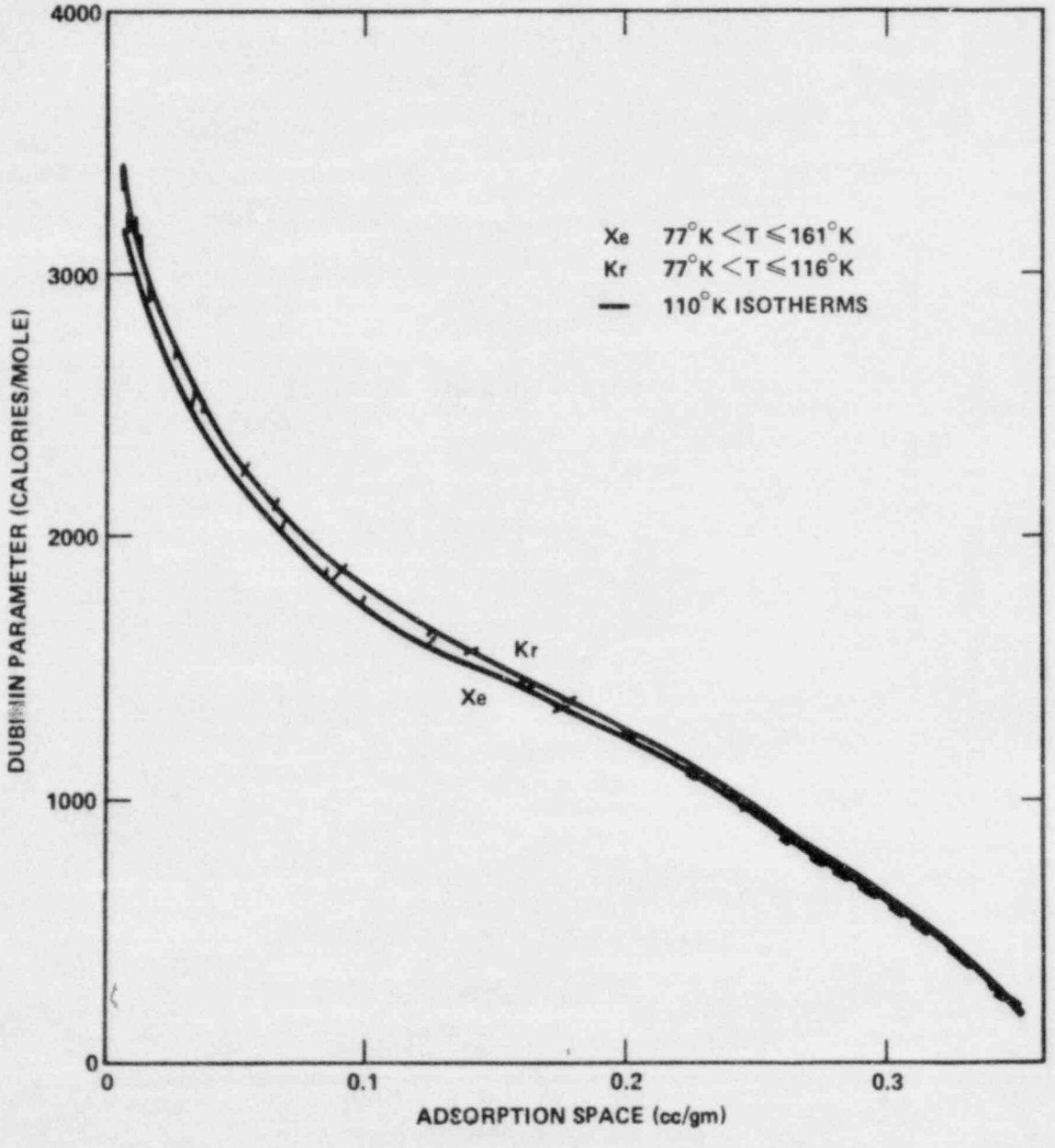

Figure 4.4 Adsorption isosteres for krypton and xenon.
Reference: de Bruijn et al (1964)

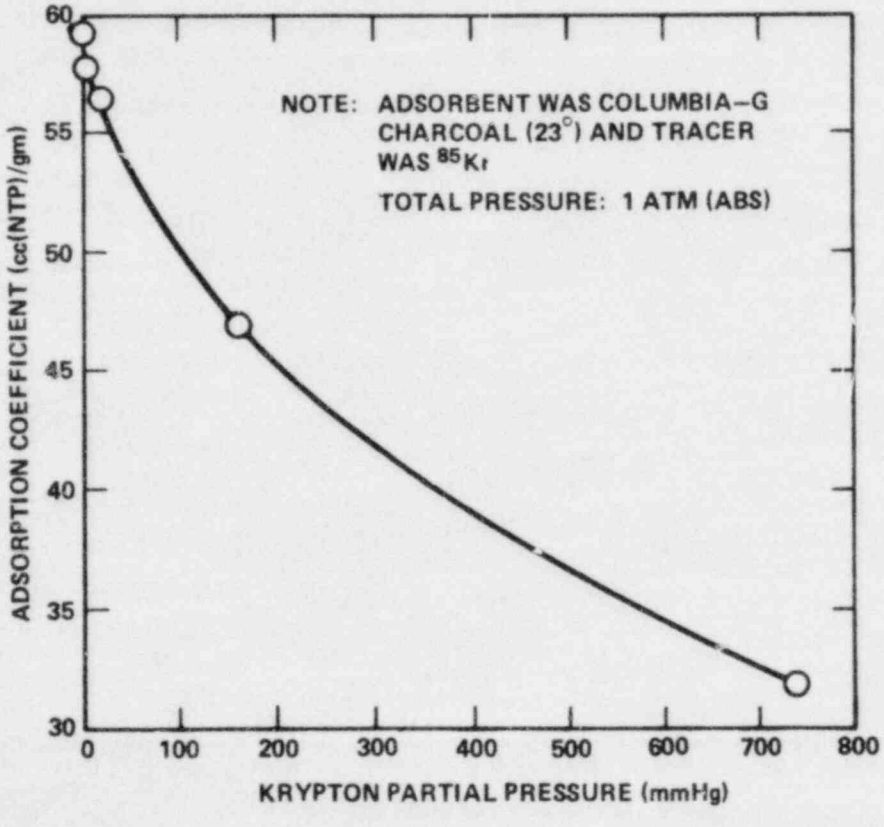

Figure 4.5 Adsorption coefficient for highly concentrated krypton
Reference: Ackley et al (1960)

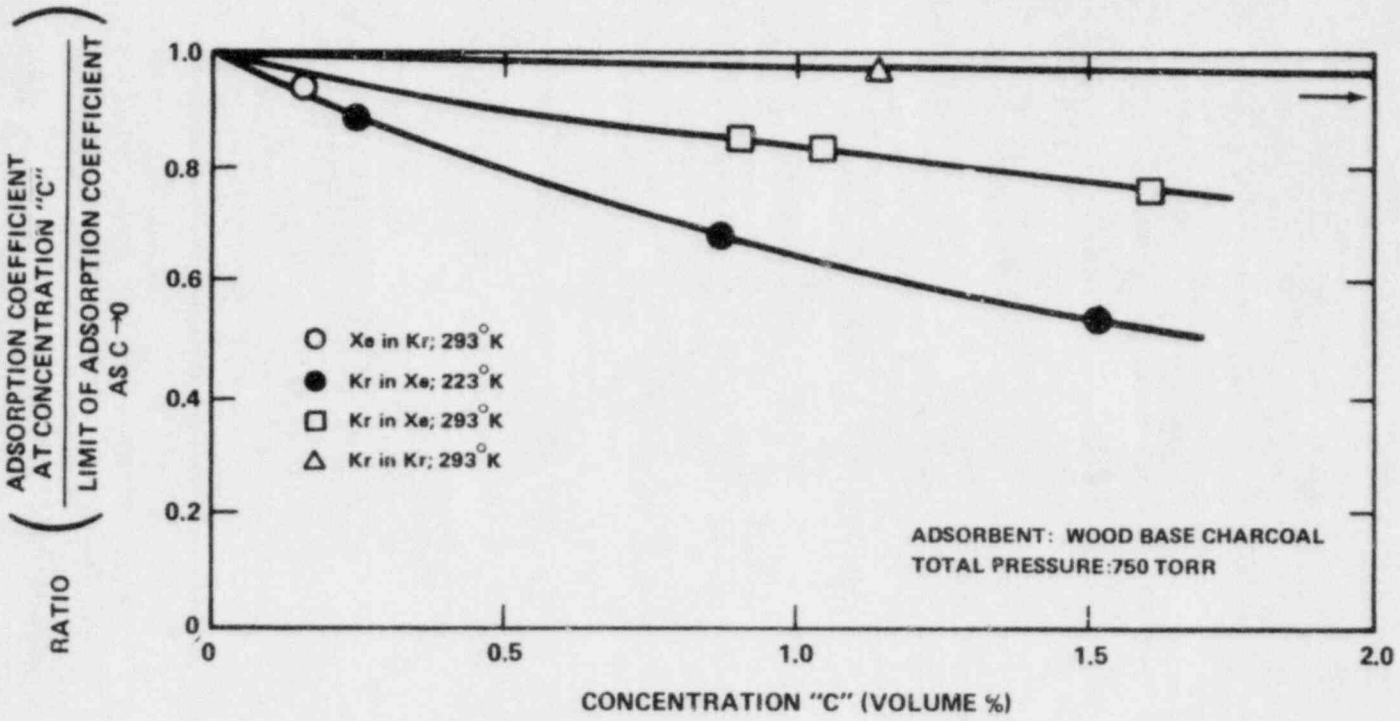

Figure 4.6 Effect of concentration on adsorption of krypton and xenon from argon.
Reference: Foerster (1971)

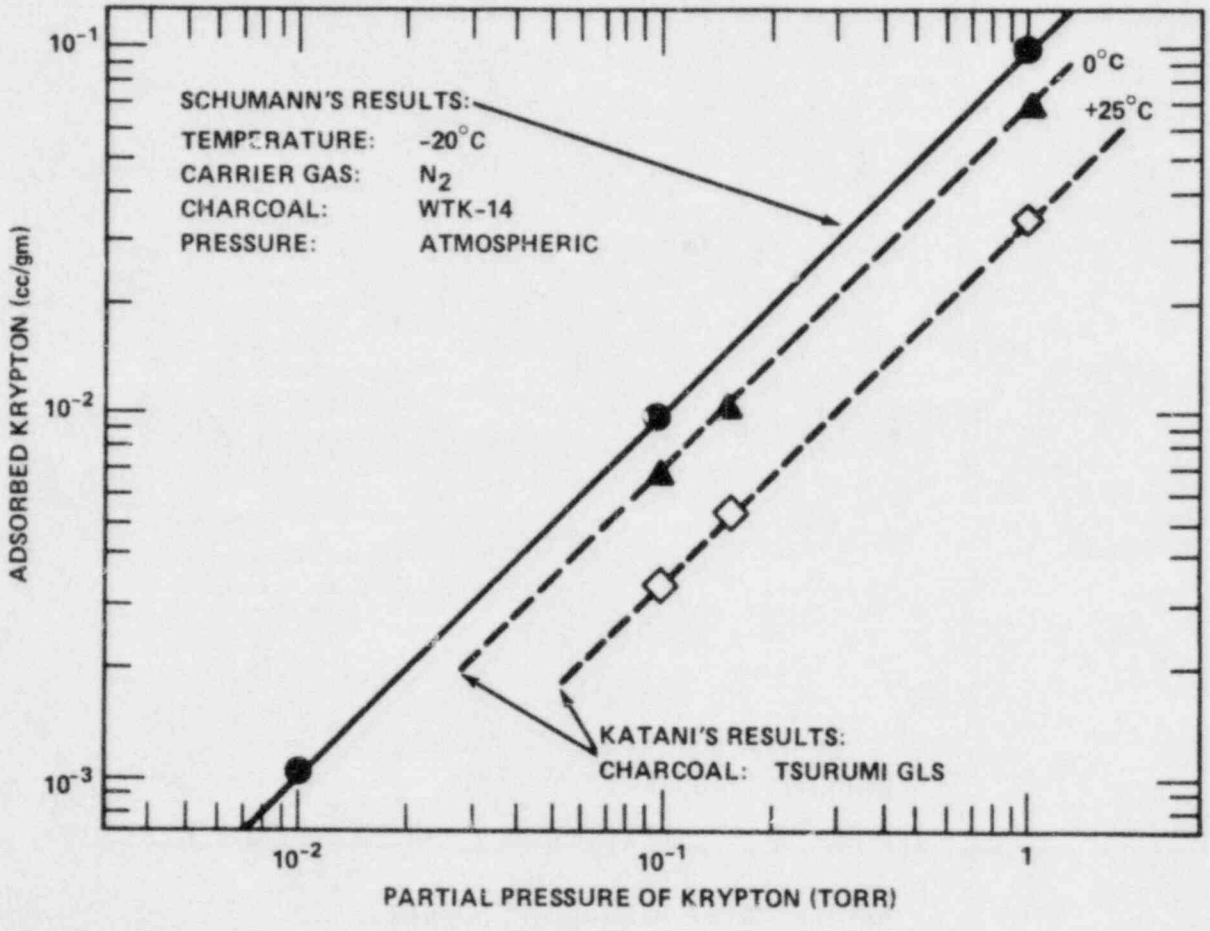

Figure 4.7 Effect of concentration on adsorption of krypton.
Reference: Schumann (1973)

n.b. The adsorption coefficient can be determined from these data by dividing the volume of adsorbed krypton by the partial pressure of krypton.

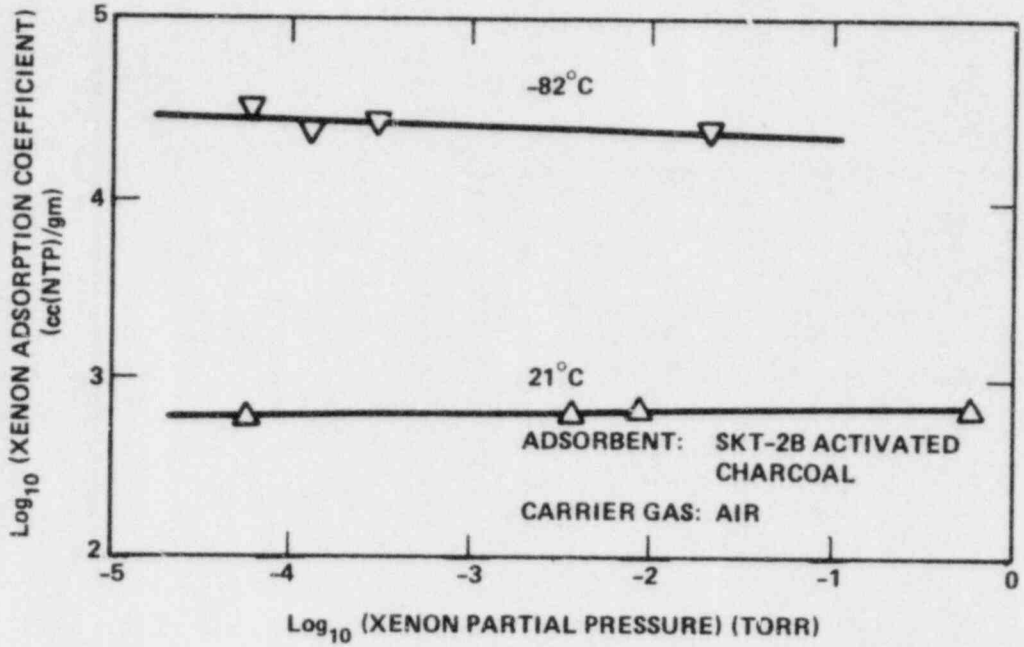

Figure 4.8 Effect of concentration on the xenon adsorption coefficient.
Reference: Nakhutin et al (1976)

TABLE 4.1

Effect of Concentration on Xenon Adsorption Coefficient

Test Conditions	Xenon Concentration (Volume %)	Adsorption Coefficient /cc(NTP)/gm/
Adsorbent: Columbia CXC Activated Charcoal	0.02	1,000
	0.10	890
Carrier Gas: Helium	0.26	769
Temperature 25 ± 0.5°C	0.50	754
	1.00	646

Reference: Kenney and Eshaya (1960)

TABLE 4.2

Effect of Concentration on Xenon Adsorption Coefficient

Test Conditions	Xenon Concentration (Volume %)	Adsorption Coefficient /cc(NTP)/gm/
Adsorbent: Columbia HCC Activated Charcoal Carrier Gas: Helium Temperature: 24 ± 2°C	0.05	1,020
	0.05	960
	0.10	800
	0.10	830
	0.47	668
	0.49	690
	0.49	673
	0.50	710
	0.50	622
	0.91	577
	0.93	596
	0.93	596
	1.30	544
	1.30	538
	1.31	517

Reference: Kenney and Eshaya (1960)

TABLE 4.3

Effect of Concentration on Krypton Adsorption Coefficient

Test Conditions	Krypton Concentration (Volume %)	Adsorption Coefficient, /cc(NTP)/gm/
Adsorbent: Columbia HCC Activated Charcoal Carrier Gas: Helium Temperature: 25°C	0.025	54
	0.050	53
	0.075	56
	0.100	57

Reference: Eshaya and Kalinowski (1961)

TABLE 4.4

Freundlich Constants for Adsorption of Krypton and Xenon on Charcoal

$k\ [cc(STP)/gm] = a(P_{mmHg})^b$; $k\ [cc(NTP)/gm] = 1.09\ a(P_{mmHg})^b$

Adsorbent Type	Adsorbate	Isotherm Temperature (°C)	Freundlich Constants		Number of Isotherm Points	Adsorption Coefficient at 0.1 mm Hg [cc(STP)/gm]
			a	b		
Columbia G Activated Carbon, 8/14 mesh	Xe	0	3.7827	0.89667	15	3647.2
	Xe	25	1.3338	0.92901	9	1193.7
	Xe	60	0.44020	0.90350	11	417.79
	Kr	0	0.18465	1.01149	10	136.67
	Kr	25	0.080505	1.00334	15	60.716
	Kr	60	0.031981	1.04785	11	21.770
Pittsburgh PCB Activated Carbon, 12/30 mesh	Xe	0	3.0302	0.90074	16	2894.3
	Xe	25	1.2716	0.88444	5	1261.1
	Xe	60	0.29196	0.81650	5	338.44
	Kr	0	0.17203	0.96261	7	142.50
	Kr	25	0.073542	0.96874	5	60.063
	Kr	60	0.026494	0.81051	5	31.149
Columbia ACC Activated Carbon, 6/14 mesh	Xe	0	2.7049	0.91782	6	2484.0
	Xe	25	1.0983	0.92820	5	984.81
	Xe	60	0.32095	0.92631	6	289.02
	Kr	0	0.14696	0.93595	7	124.18
	Kr	25	0.064717	0.96635	5	53.148
	Kr	60	0.028871	0.95799	5	24.170
Columbia HCC Activated Carbon, 12/28 mesh	Xe	0	2.8877	1.00172	5	2186.0
	Xe	25	1.1946	0.90211	5	1137.5
	Xe	60	0.34275	0.96886	5	279.86
	Kr	0	0.14621	0.93548	7	128.92
	Kr	25	0.066833	0.97958	5	53.238
	Kr	60	0.018836	0.93745	5	16.532

Reference: Ackley and Browning (1961)

TABLE 4.5

Effect of Concentration on Krypton Adsorption Coefficient

Temperature (°C)	Absolute Pressure (Atm)	Krypton Concentration (ppm)	Adsorption Coefficient /cc(NTP)/gm/	Percent Change in the Adsorption Coefficient at Constant Temperature and Pressure
25	1	63	60.6	--
		100	61.7	1.8
		630	61.5	1.4
	10	63	181	--
		100	174	-3.8
		630	183	1.10
0	1	63	122	--
		100	106	-13.
		630	113	-7.4
	10	63	312	--
		100	251	-19.
		630	260	-16.
-30	1	63	203	--
		100	223	9.8
		630	225	10.8
	10	63	447	--
		100	445	0.5
		630	447	0.0

Adsorbent: Tsurumi - GLS Activated Charcoal
Carrier Gas: Nitrogen

Reference: Kitani, et al. (1968)

TABLE 4.6

Effect of Temperature and Concentration on Krypton Adsorption Coefficient

Temperature (°C)	Adsorption Coefficient (in liters(NTP)/gm) at Stated Temperature and Krypton Concentration						
	1 ppm	10 ppm	25 ppm	50 ppm	100 ppm	1000 ppm	4000 ppm
-170		19.5	19.7	20.3	20.5	19.7	19.9
-128	4.1	4.1			3.5		3.7
-66	1.40				1.21		1.31

Adsorbent: Fisher Coconut Base Activated Charcoal
Carrier Gas: Air at -170°C and N_2 at -128 and -66°C

Reference: Wirsing, et al. (1970)

TABLE 4.7

Effect of Temperature and Concentration on Krypton Adsorption Coefficient

Krypton Concentration (ppm)	Adsorption Coefficient at Stated Temperature and Krypton Concentration /cc(NTP)/gm/			
	10°C	20°C	40°C	50°C
1.3	92	65	48	38
0.13	98	68	53	
0.013	100	72	55	

Adsorbent: NACAR G210 Activated Charcoal
Carrier Gas: Air

Reference: Kovach (1972)

TABLE 4.8
Langmuir Coefficients for the Adsorption of Krypton and Xenon from Argon as Calculated from Data by Collins, et al. (1967)

Temperature (°C)	Langmuir Coefficients for the Effects of the Krypton Concentration on the Adsorption of Krypton	Xenon Concentration on the Adsorption of Xenon	Krypton Concentration on the Adsorption of Xenon
-70	129,000	1,055	28,000
-60	173,000	1,800	49,000
-50	228,000	3,100	81,000
-40	290,000	5,000	125,000
-30	370,000	7,900	185,000
-20	470,000	12,000	262,000
-10	580,000	18,000	360,000
0	710,000	26,000	480,000
10	850,000	37,000	617,000
20	1,020,000	51,000	780,000
30	1,200,000	70,000	
40	1,410,000	93,000	
50	1,640,000	160,000	
60	1,910,000	210,000	

Through application of the Langmuir isotherm, the coefficients given above can be used to calculate the adsorption of noble gases at low and intermediate concentrations. The equation for the Langmuir isotherm is as follows:

$$k = k_1/(1 + C_1/\overline{C}_1 + C_2/\overline{C}_2) \qquad (4.4)$$

where

- k = adsorption coefficient of xenon (krypton)
- k_1 = adsorption coefficient of xenon (krypton) at infinitely low xenon and krypton concentrations
- C_1 = concentration of xenon (krypton), ppm
- $\overline{C}_1$ = Langmuir coefficient for the effect of the xenon (krypton) concentration on the adsorption of xenon (krypton)
- C_2 = concentration of krypton (xenon), ppm
- $\overline{C}_2$ = Langmuir coefficient for the effect of the krypton (xenon) concentration on the adsorption of xenon (krypton)

The geometric standard deviation, σ, between the measured and the predicted adsorption coefficients was 1.11 and 1.19, respectively, for the adsorption of krypton in the absence of xenon and for the adsorption of xenon in the absence of krypton. For the adsorption of xenon from argon containing appreciable concentrations of krypton, the geometric standard deviation between the measured and the predicted values was 1.16.

TABLE 4.9

Effect of Temperature and Concentration on Xenon Adsorption Coefficient

Xenon Concentration (ppm)	Adsorption Coefficient at Stated Temperature and Xenon Concentration /cc(NTP)/gm/			
	10°C	20°C	40°C	50°C
1.3	1,750	1,300	620	400
0.13	1,850	1,380	690	450
0.013	1,940	1,450	730	490

Adsorbent: NACAR G210 Activated Charcoal (8x16 mesh, 1100 m^2/gm)
Carrier Gas: Air

Reference: Kovach (1972)

CHAPTER 5

THE EFFECTS OF PRESSURE ON THE ADSORPTION OF KRYPTON AND XENON

Although operation of pressurized systems has been considered in the design of fission gas holdup beds, most current systems are operated near atmospheric pressure. Under abnormal conditions it may be possible to increase the holdup in such beds by operation at higher pressures. The data in this chapter should permit designers of such systems to estimate, in advance, the effectiveness of pressurization.

5.1 Effect of Pressure on the Adsorption of Krypton and Xenon from Nitrogen and Air

Goldin and Trindade (1973) measured the adsorption of krypton and xenon from both air and nitrogen as a function of pressure at temperatures ranging from ambient to -100°C. Table 5.1 and Figure 5.1 give their original presentation of these data. If, as in Figure 5.1, the logarithm of the adsorption coefficient is plotted versus the pressure, the resultant isotherms are highly curved. In evaluating these data, it was found that very nearly linear results could be obtained by reversing the plot, that is, by plotting the log of the pressure vs. the adsorption coefficient. This approach is shown in Figures 5.2 through 5.4, which present different segments of the pressure and temperature ranges studied.

Kabele and Bohringer (1975) studied the adsorption of krypton from gas mixtures, primarily nitrogen, at temperatures of -80°C and -120°C. Their data (Table 5.2, Figure 5.2) are consistent with the earlier results of Goldin and Trindade.

The data of Kawazoe and Kawai (1972) are unique in describing the effects of very high pressures on the adsorption of krypton. Even at pressures up to 123 Atm, their data show a nearly linear relationship between the adsorption coefficient for krypton and the logarithm of pressure (Figure 5.5).

A dimensionless factor, the pressure coefficient, α, has been derived here to characterize the slope of these adsorption isotherms. This factor may be expressed as:

$$\alpha = \frac{K_2 - K_1}{K_1 (\ln P_2)} \qquad (5.1)$$

where α = pressure coefficient, dimensionless

K_1 = adsorption coefficient at 1 Atm (abs)

K_2 = adsorption coefficient at pressure, P_2

Figure 5.6 shows a plot of the pressure coefficient vs temperature, as calculated using the data discussed above. From this Figure, it is relatively simple to estimate the effects of pressure on the adsorption coefficient for either krypton or xenon. It is apparent from Figure 5.6 that, for a given temperature, an increase in pressure is more effective in increasing the adsorption coefficient for krypton than for xenon. From the standpoint of safety analyses, this shows that pressurization will affect unequally the retention of krypton and xenon isotopes. Another important observation is that the effectiveness of pressurization decreases as the temperature is reduced.

In 1968, Kitani, et al., published a number of measurements of the adsorption of krypton from nitrogen at 1 and 10 Atm. They determined adsorption coefficients for eight charcoals at a krypton concentration of 64 ppm at 0°C (Table 5.4), and for one of these charcoals at temperatures of 25°C and -30°C (Table 5.5 and Figure 5.7). On the basis of a review of these data, Kovach (1972) concluded that the effect of pressure on the adsorption coefficient is less than would have been expected. For example, at 0°C the increase in the adsorption coefficient is less than a factor of three for a tenfold increase in pressure. Although Wirsing, et al. (1970), have also made measurements of the adsorption of krypton from nitrogen and air, their data appear to be too inconsistent to be useful here.

The fact that the data reported by Kitani, et al., were obtained using a wide variety of charcoals (including some manufactured in the United States) points to experimental technique as being the main source of differences between their results and those published by other authors.

5.2 Effect of Pressure on the Adsorption of Krypton and Xenon from Argon

Kabele, et al.(1973), measured the adsorption of xenon from argon at 30°C and -30°C. The pressure coefficients calculated from their data (Table 5.6) are very close to values reported earlier for the adsorption of xenon from a nitrogen carrier gas.

Figure 5.8, from Foerster (1971), shows conclusively that the overall pressure has a nonlinear effect on krypton adsorption from an argon carrier gas. The pressure coefficient calculated from Foerster's data is 1.4 at 20°C.

At low temperatures, adsorbed argon interferes severely with the adsorption of krypton and xenon. Ratney and Underhill (1972) found a regime at -140°C where an increase in pressure actually decreased the adsorption of krypton from argon. This behavior can be explained by the formation of liquid argon in the micropores of the charcoal as the pressure was increased.

5.3 Effect of Pressure on the Adsorption of Krypton and Xenon from Helium

Figure 5.9 (Ratney and Underhill, 1972) shows three isotherms for the adsorption of krypton from helium at temperatures below 0°C. These isotherms are linear or very nearly linear, indicating little interference with adsorption by the helium carrier gas. Because helium is not expected to interfere with the adsorption of krypton or xenon, the adsorption of these latter two gases should be a function only of the temperature and their partial pressures..

If these data were obtained at temperatures below the critical temperature of krypton (-63.8C), the Polanyi isostere would be preferable, as it presents the data most concisely. At significantly higher temperatures, however, the assumptions underlying the Polanyi isostere lose their validity and, as is the case here, the isotherm graph is the better method of data presentation.

5.4 Adsorption of ^{41}Ar from an Argon Carrier Gas

The effects of pressure on the adsorption coefficient for ^{41}Ar from an argon carrier gas have been determined in conjunction with the use of argon as a cover gas for liquid metal cooled reactors. Tables 5.7 and 5.8, and Figures 5.10 and 5.11, present results obtained in parallel studies at the Harvard Air Cleaning Laboratory (Underhill, et al. 1973),

and at the Hanford Engineering Development Laboratory (Kabele, et al. 1973). Constants for the Freundlich isotherm for the adsorption of argon are given in Figure 5.12, but the range of pressures over which these constants are valid is not known.

5.5 Conclusions

By examining the available information concerning the effects of pressure on the adsorption of noble gases, a number of factors of importance in the design and evaluation of krypton and xenon holdup beds have been identified. These include:

5.5.1 The percent increase in the adsorption coefficient will be less than the percent increase in absolute pressure. An exception to this rule may occur if helium (and possibly hydrogen) is the carrier gas.

5.5.2 A plot of the adsorption coefficient vs. pressure is approximately linear if the absolute pressure is plotted on the log axis of semi log paper. Coefficients of the normalized slope of these plots, taken as a function of temperature, show promise as a means of correlating data from a wide number of experiments.

5.5.3 At the same temperature, an increase in pressure increases the adsorption coefficient of xenon by a lesser fraction than it increases the adsorption coefficient of krypton.

5.5.4 At reduced temperatures, pressurization is less effective in increasing the adsorption coefficients of noble gases.

5.5.5 There is sufficient information on the effects of temperature and pressure on the adsorption of ^{41}Ar from an argon carrier gas to permit estimates to be made of the adsorption coefficients under a range of conditions.

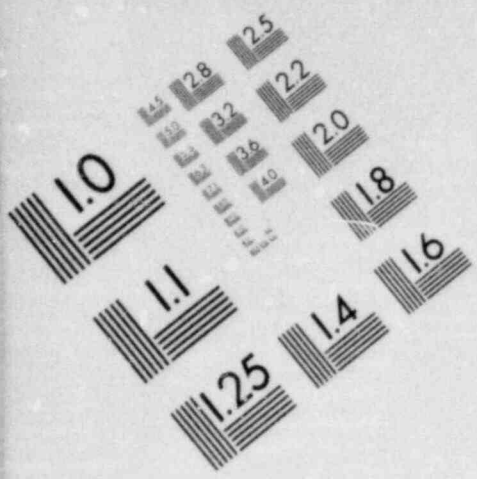

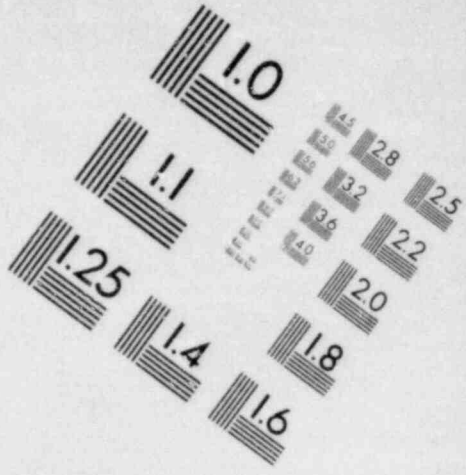

IMAGE EVALUATION
TEST TARGET (MT-3)

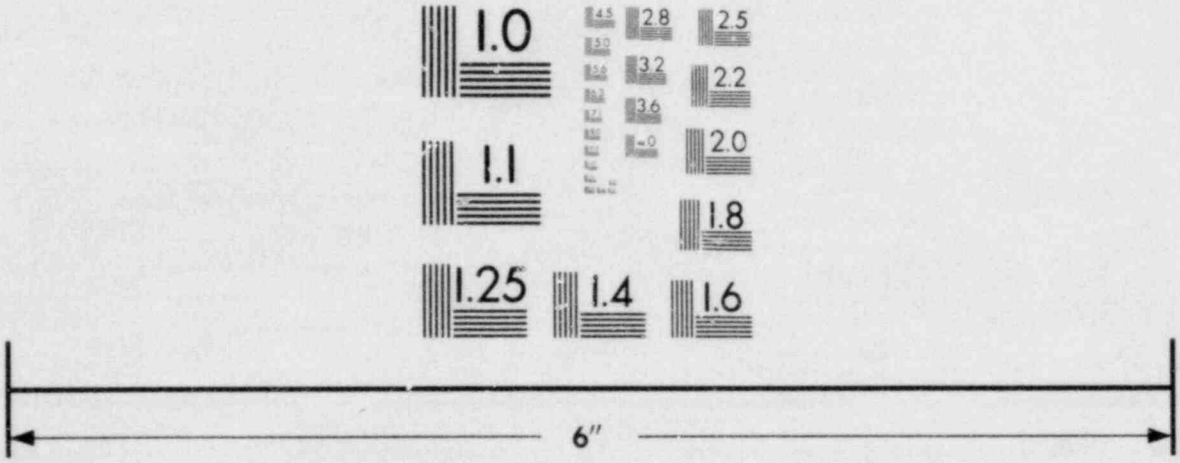

MICROCOPY RESOLUTION TEST CHART

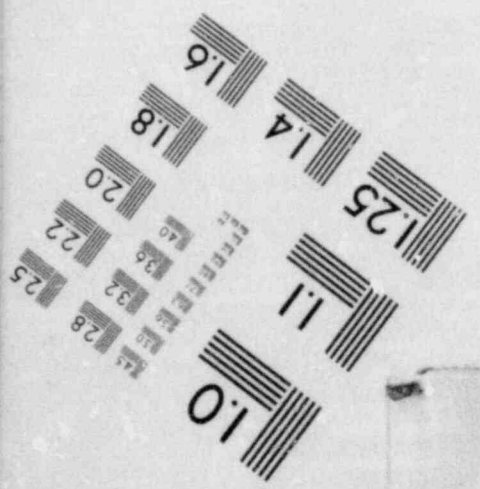

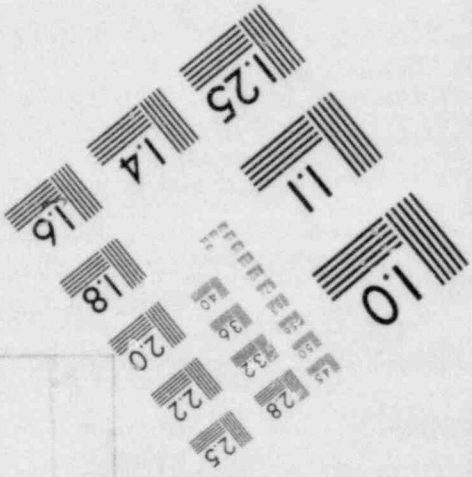

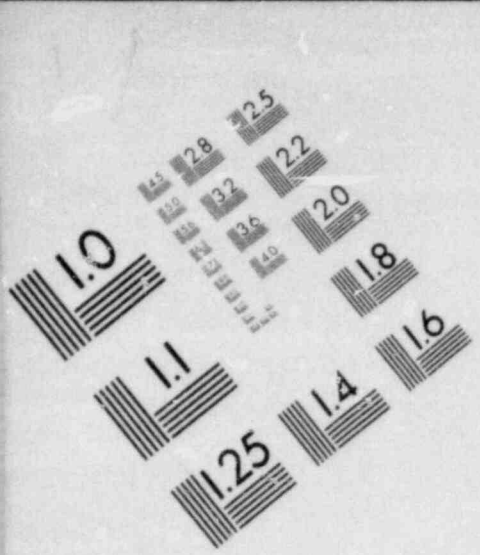

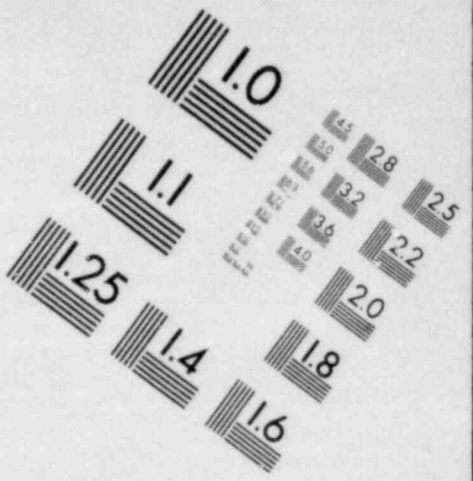

IMAGE EVALUATION
TEST TARGET (MT-3)

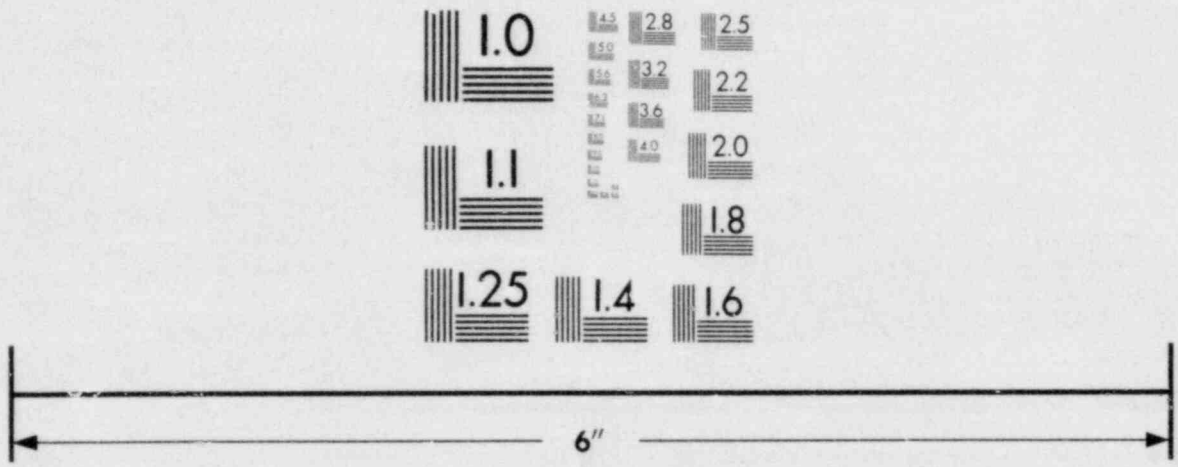

MICROCOPY RESOLUTION TEST CHART

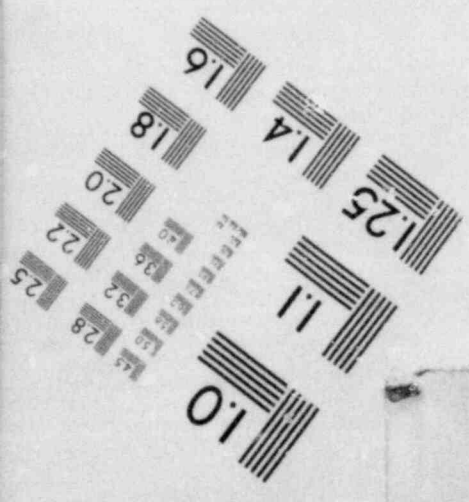

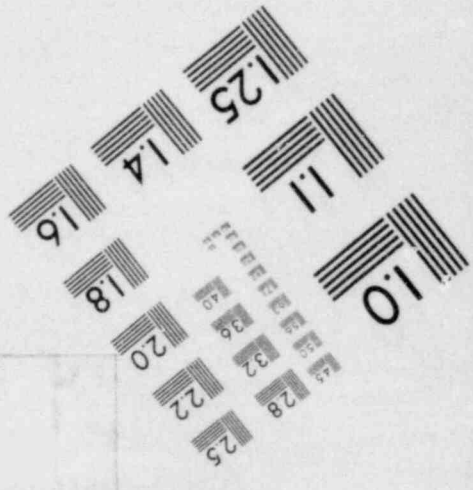

Figure 5.1 Effect of pressure on the adsorption of krypton and xenon from nitrogen.
Adsorbent: Pittsburgh PCB 12x30 charcoal.
Reference: Goldin and Trindade (1973).

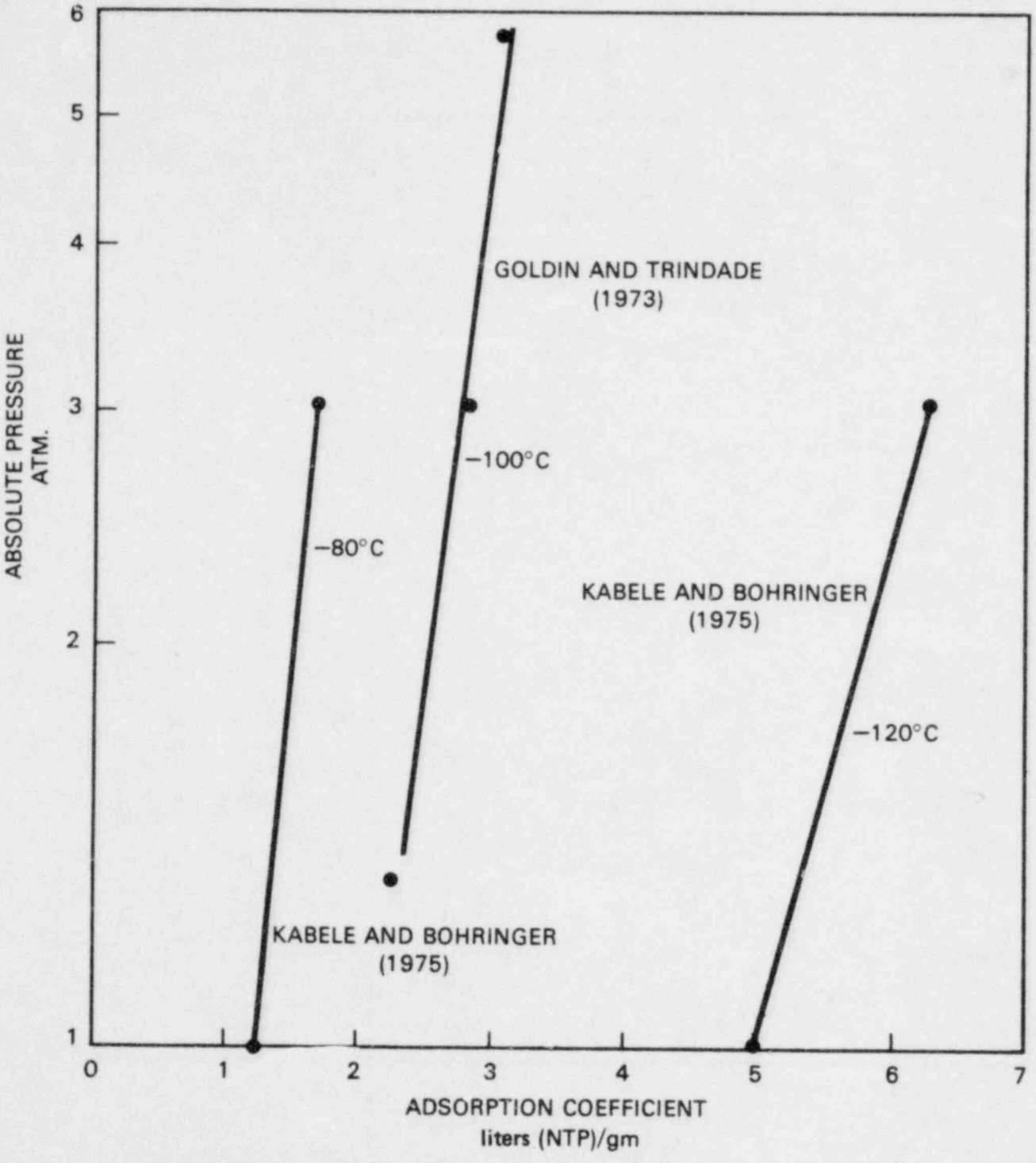

Figure 5.2 Effect of pressure on the adsorption of krypton from nitrogen at low temperatures. Adsorbent: Pittsburgh PCB 12 x 30 charcoal

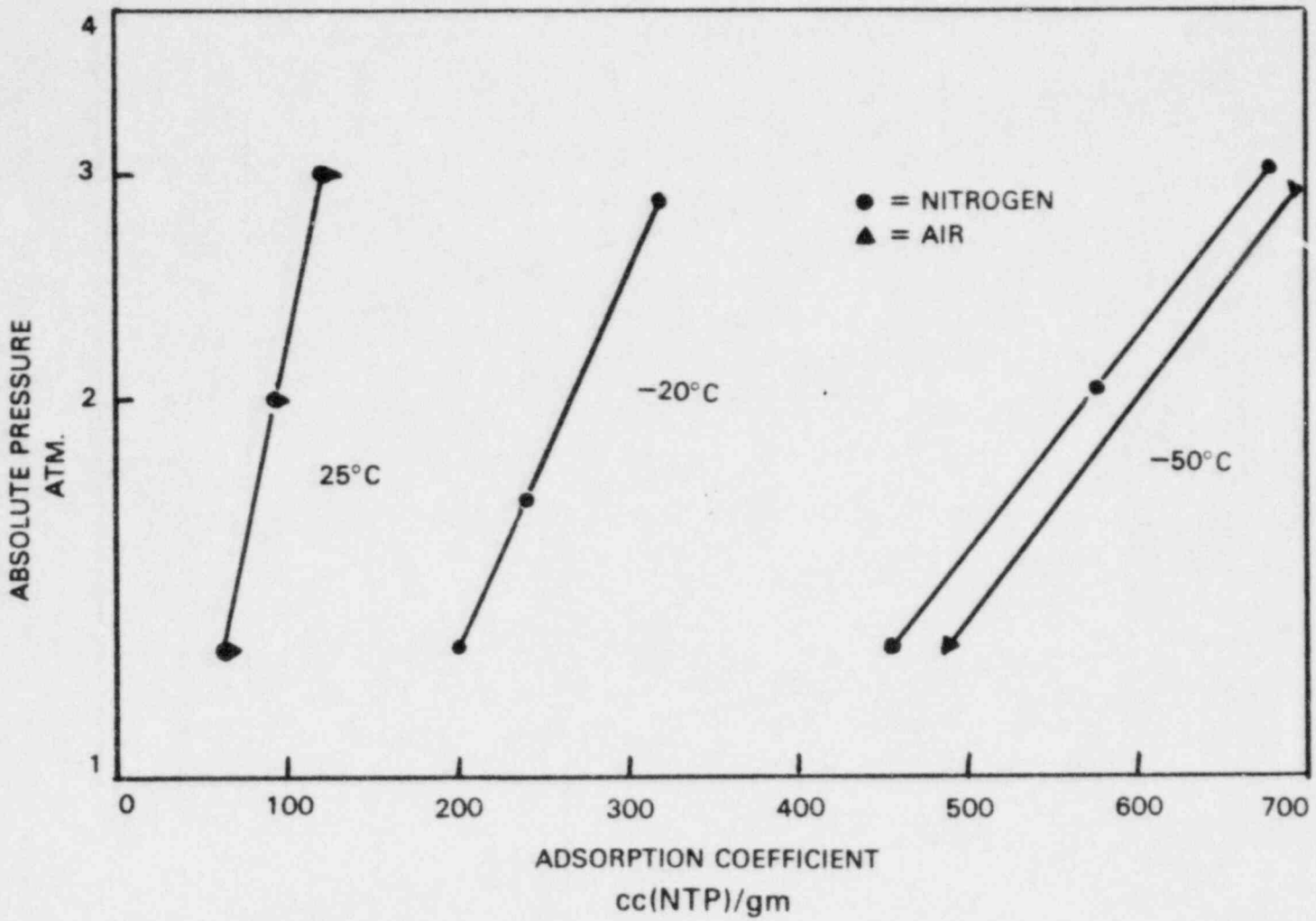

Figure 5.3 Effect of pressure on the adsorption of krypton from nitrogen and air.
Adsorbent: Pittsburgh PCB 12x30 charcoal.
Reference: Goldin and Trindade (1973).

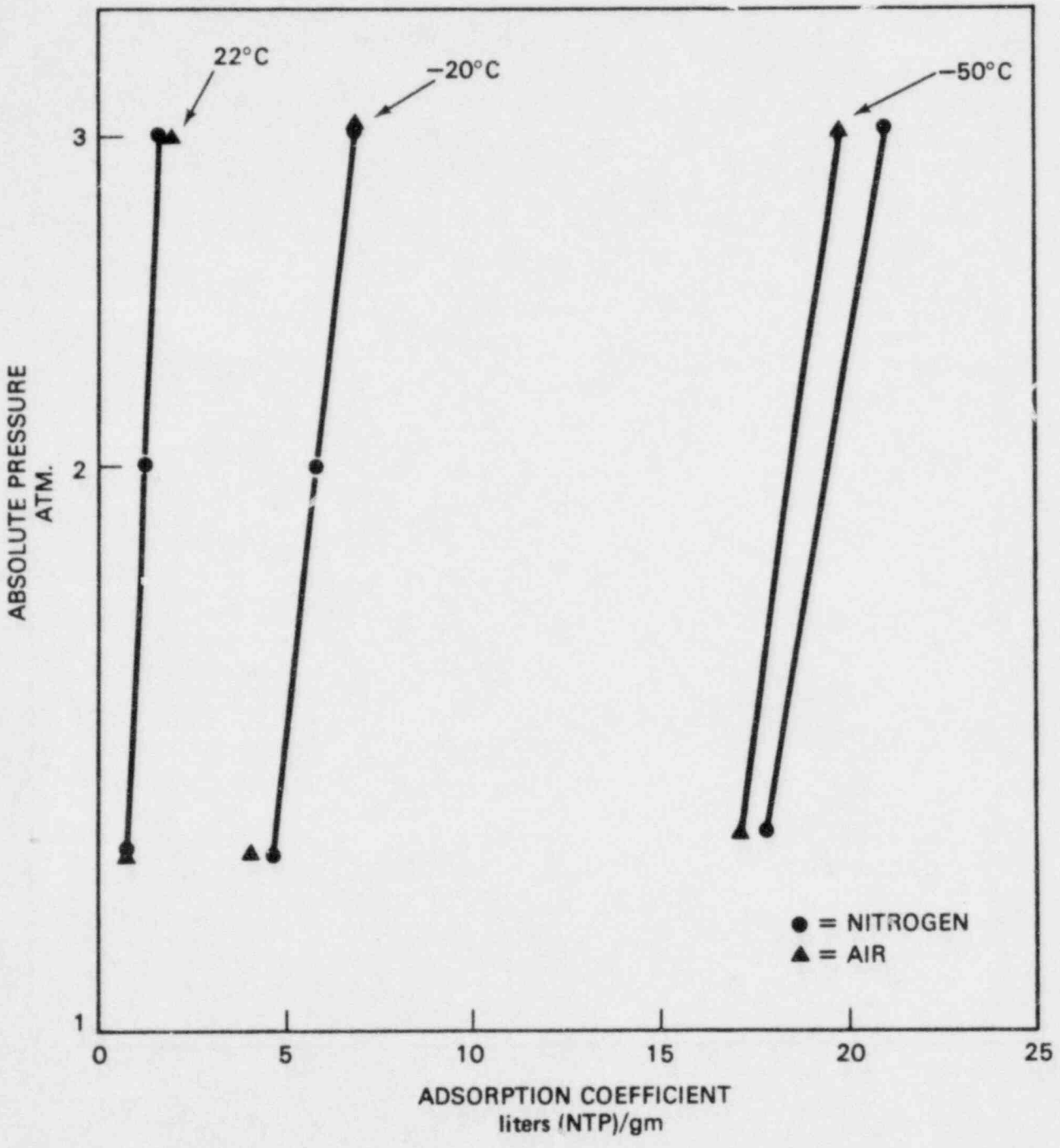

Figure 5.4 Effect of pressure on the adsorption of xenon from nitrogen and air.
Adsorbent: Pittsburgh PCB 12x30 charcoal.
Reference: Goldin and Trindade (1973).

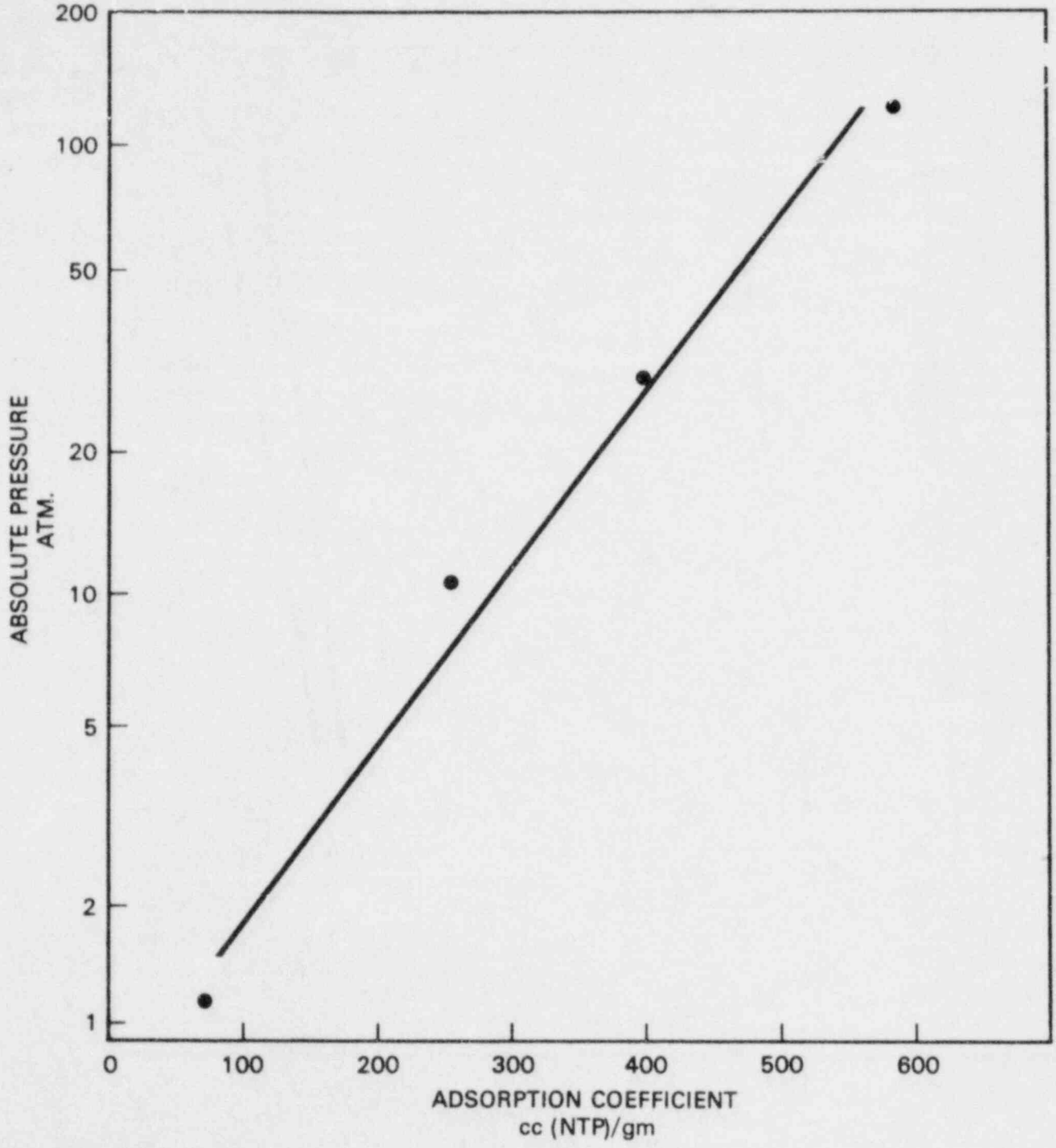

Figure 5.5 Effect of high pressure on the adsorption of krypton from nitrogen.
Adsorbent: activated charcoal type HGR-510.
Reference: Kawazoe and Kawai (1972).

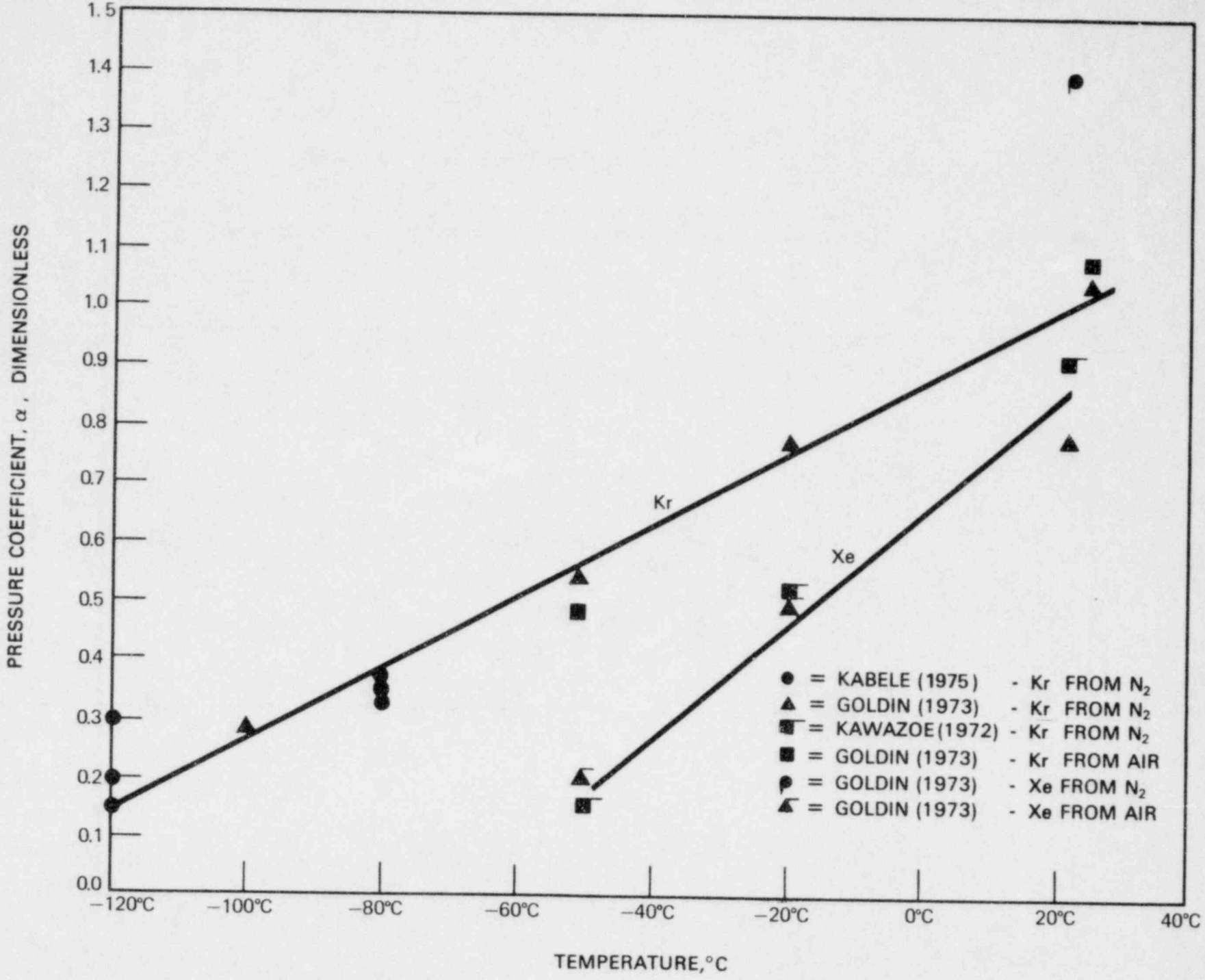

Figure 5.6 Coefficients for the effect of pressure on the adsorption of krypton and xenon from nitrogen and air.

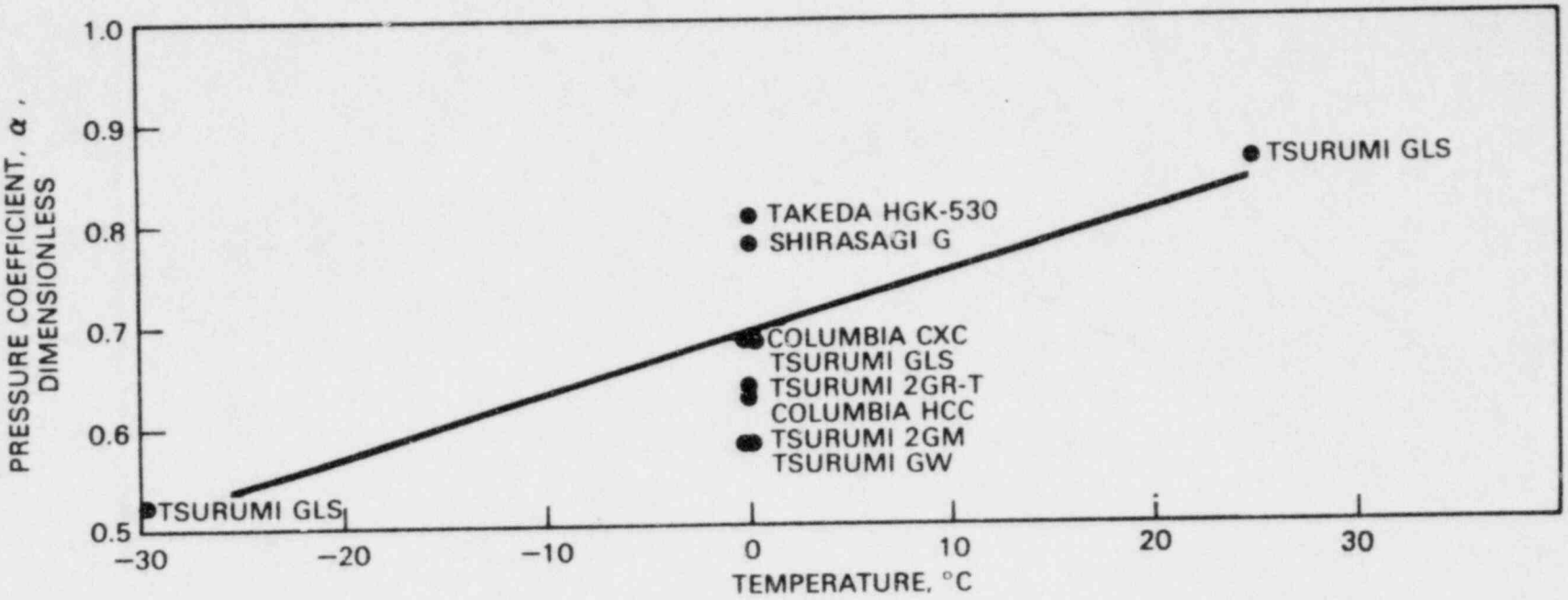

Figure 5.7 The effect of pressure on the adsorption of krypton from nitrogen. (Note: Table 1.2 gives important physical characteristics of these adsorbents.)
Reference: Kitani et al. (1968).

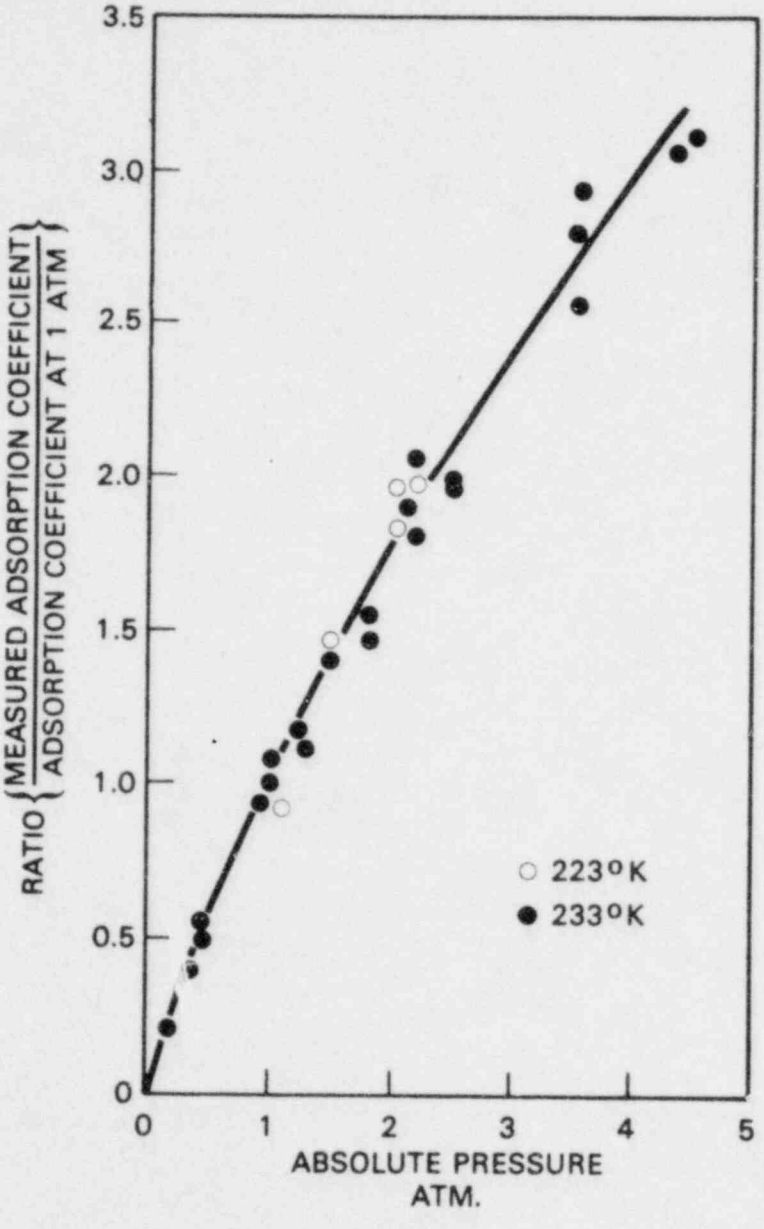

Figure 5.8 Effect of pressure on the adsorption of krypton from argon.
Adsorbent: wood base charcoal.
Reference: Foerster (1971).

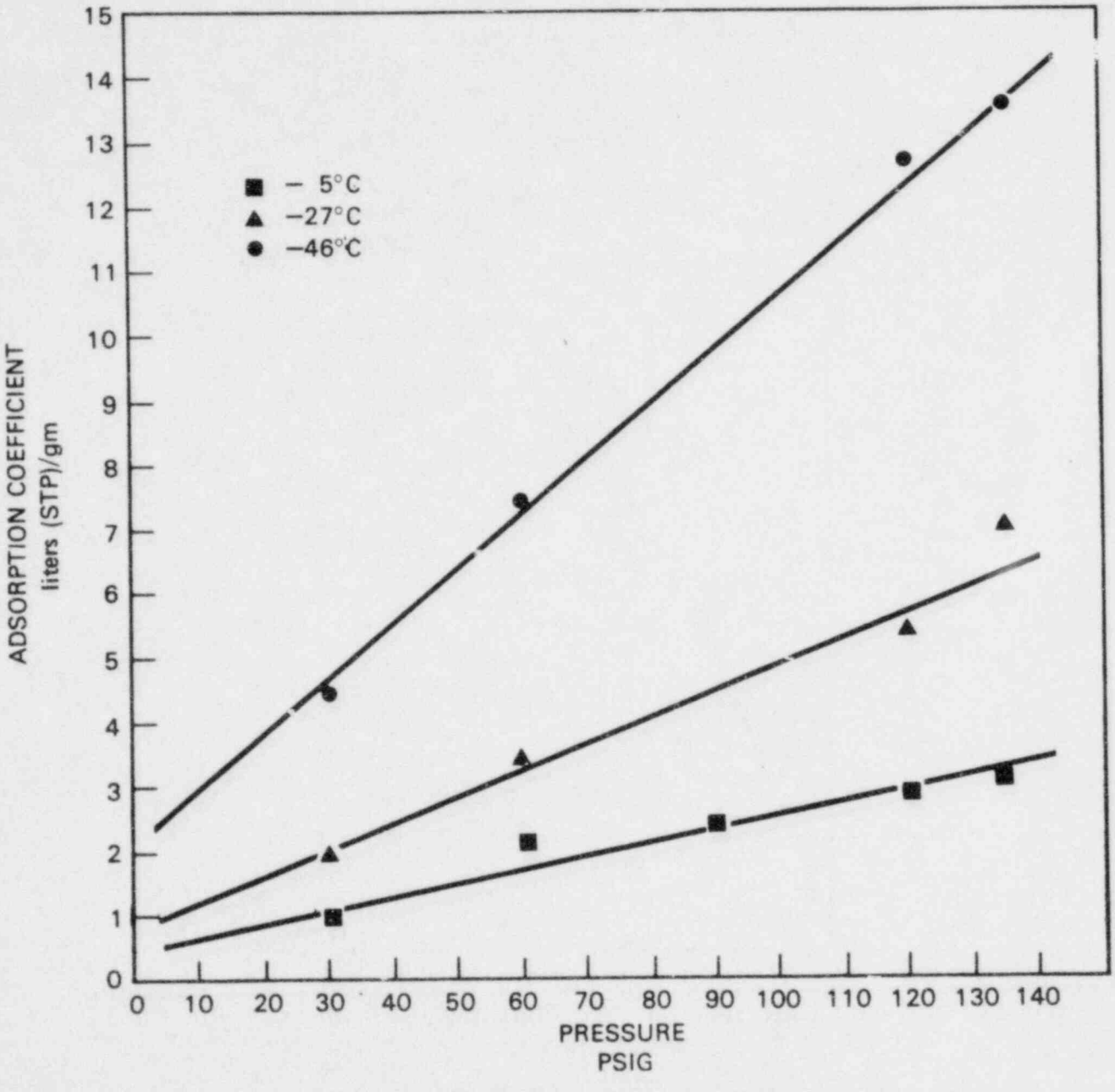

Figure 5.9 Effect of pressure on the adsorption of krypton from helium.
Adsorbent: Pittsburgh PCB 6x16 mesh charcoal.
Reference: Ratney and Underhill (1972).

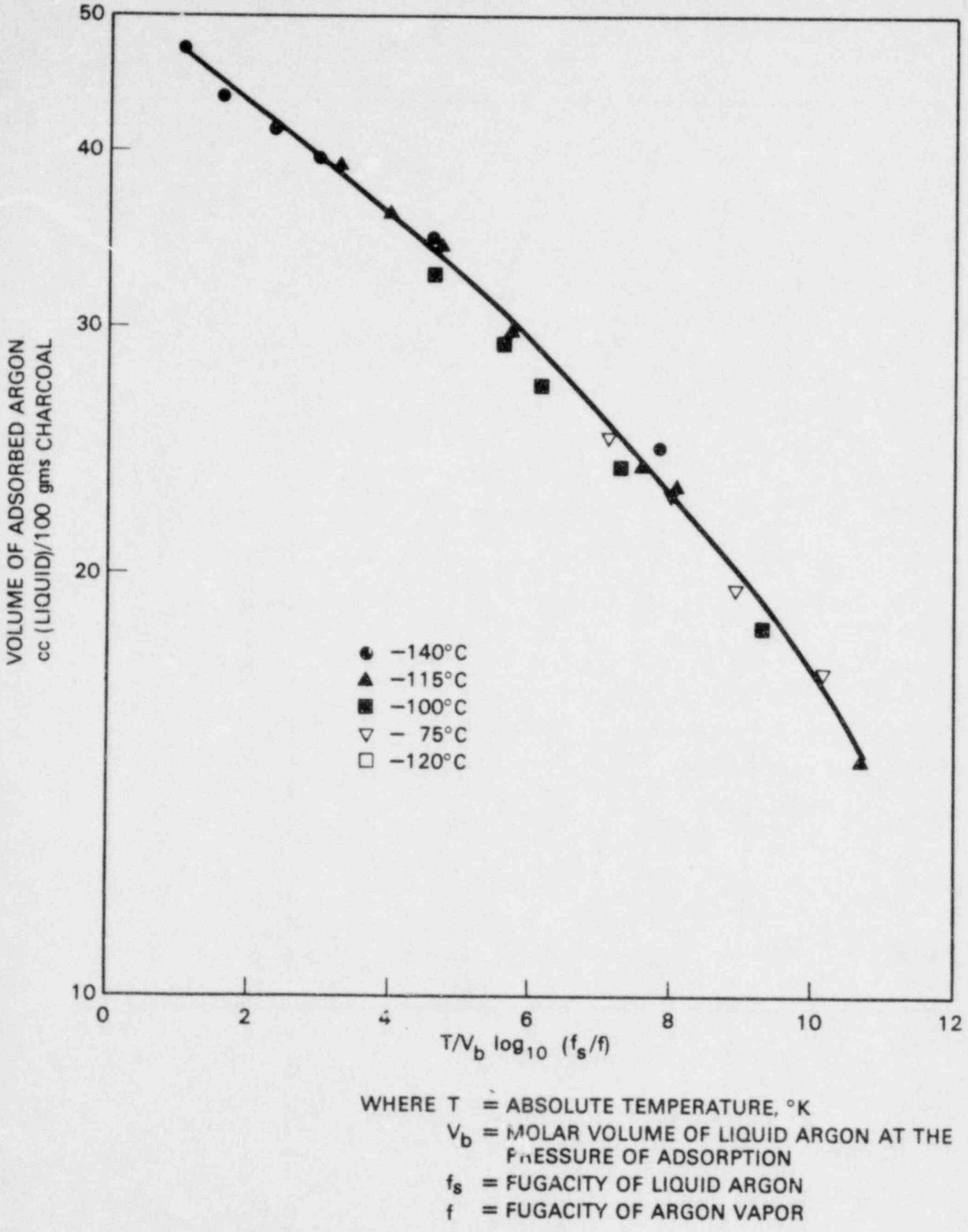

WHERE T = ABSOLUTE TEMPERATURE, °K
V_b = MOLAR VOLUME OF LIQUID ARGON AT THE PRESSURE OF ADSORPTION
f_s = FUGACITY OF LIQUID ARGON
f = FUGACITY OF ARGON VAPOR

Figure 5.10 Polanyi diagram for the adsorption of argon on Pittsburgh PCB charcoal. Reference: Underhill et al. (1973).

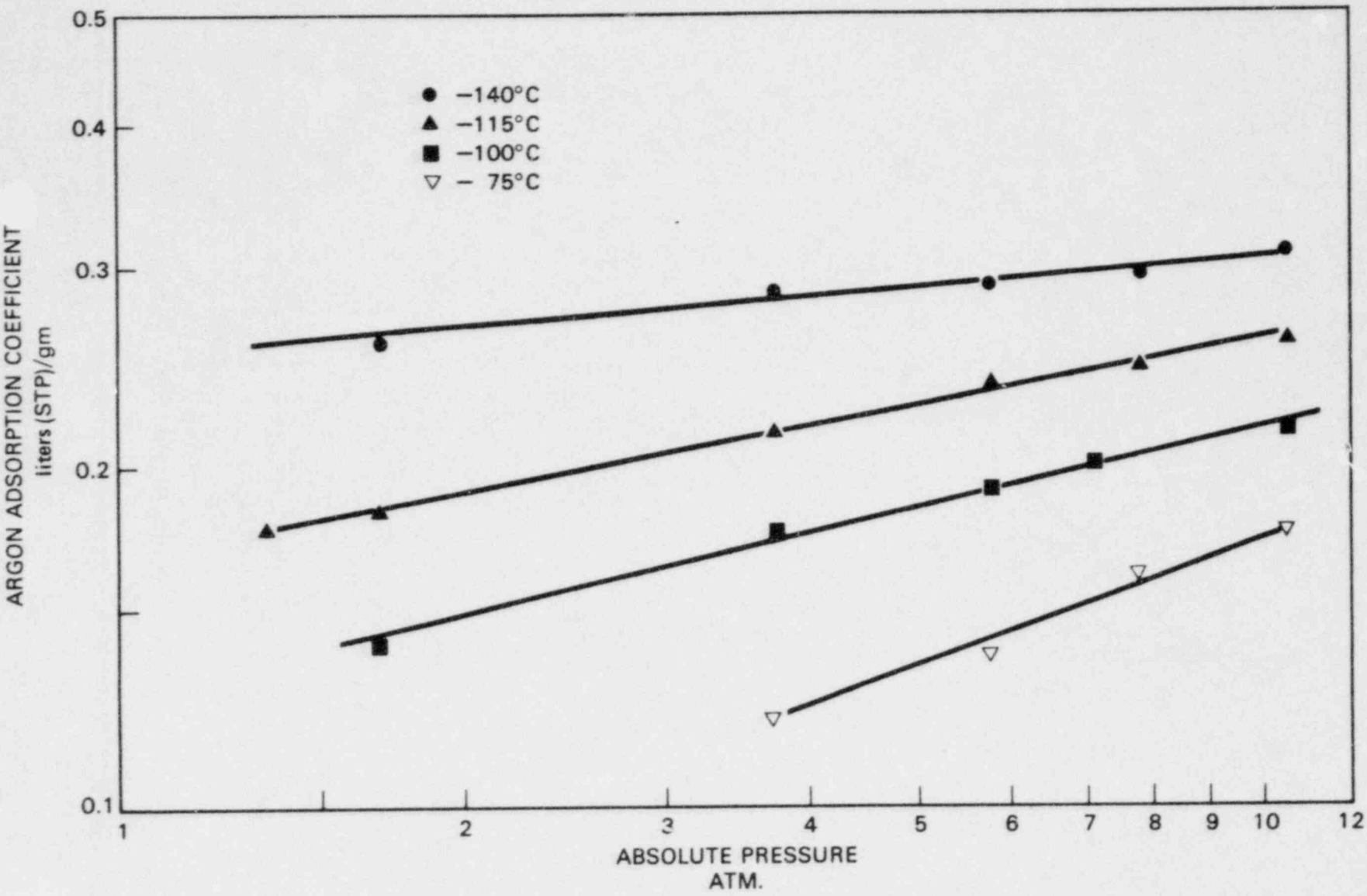

Figure 5.11 Effect of pressure on the adsorption of argon.
Adsorbent: Pittsburgh PCB 12x30 charcoal.
Reference: Underhill et al. (1973).

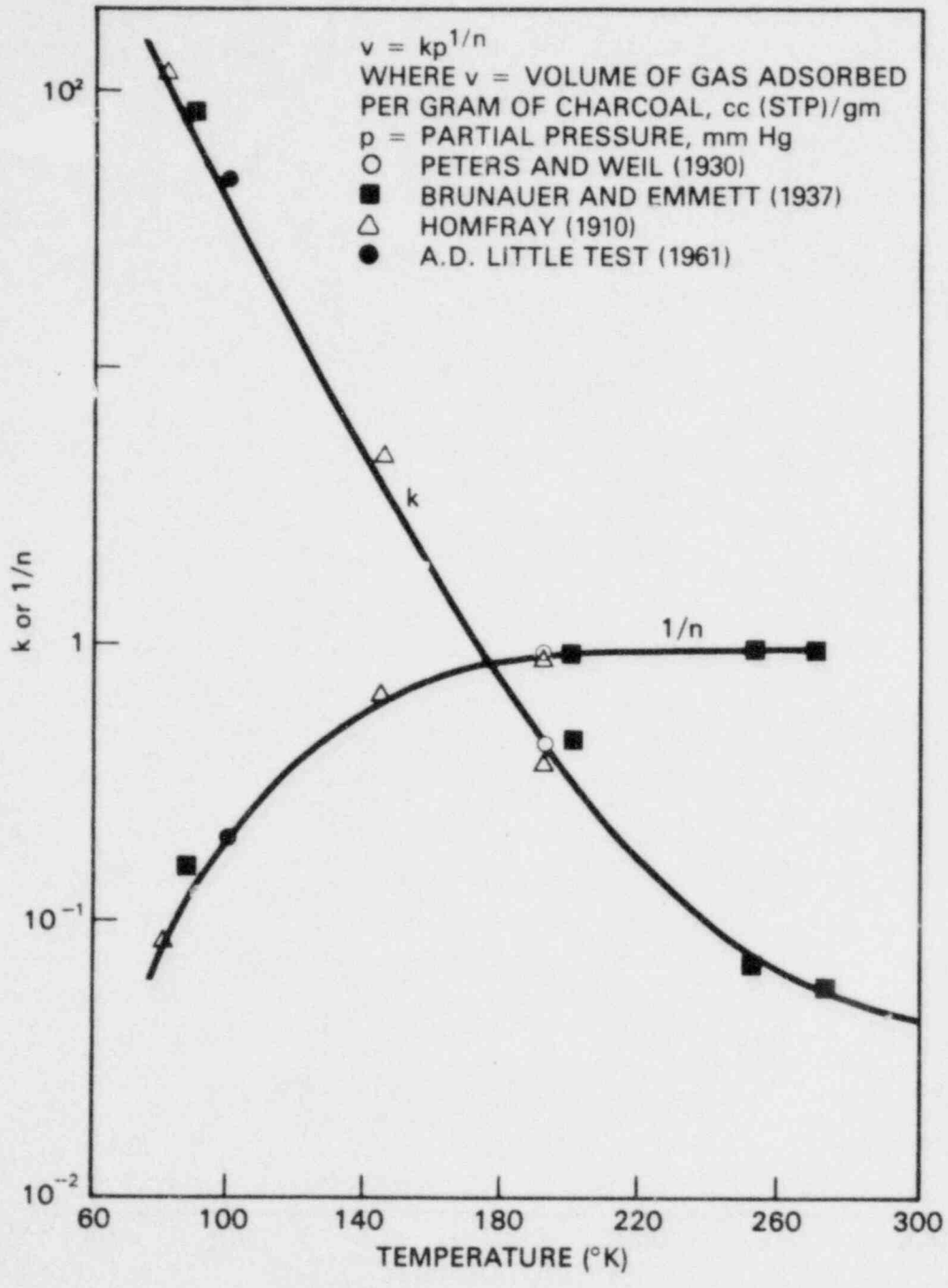

Figure 5.12 Coefficients of Freundlich isotherm for the adsorption of argon on charcoal.

Reference: Robinson (1961).

TABLE 5.1

Effect of Pressure on the Adsorption of Krypton and Xenon from Nitrogen and Air

1. Adsorption of Krypton from Nitrogen

Temperature °C	Absolute Pressure (Atm)	Adsorption Coefficient (liters(NTP)/gm)	Pressure Coefficient, α (Dimensionless)
-100	1.29	2.26	0.31
	1.95	2.61	
	3.04	2.82	
	5.76	3.06	
-50	1.29	0.46	0.65
	2.00	0.58	
	3.04	0.68	
-20	1.29	0.20	0.91
	1.68	0.24	
	2.90	0.32	
+25	1.29	0.067	1.39
	2.00	0.093	
	3.04	0.126	

2. Adsorption of Xenon from Nitrogen

Temperature °C	Absolute Pressure (Atm)	Adsorption Coefficient (liters(NTP)/gm)	Pressure Coefficient, α (Dimensionless)
-50	1.29	19.5	0.21
	3.04	22.9	
-20	1.29	5.16	0.58
	2.00	6.48	
	3.04	7.41	
+22	1.29	1.06	0.98
	2.00	1.39	
	3.04	1.77	

3. Adsorption of Krypton from Air

Temperature °C	Absolute Pressure (Atm)	Adsorption Coefficient (liters(NTP)/gm)	Pressure Coefficient, α (Dimensionless)
-50	1.29	0.49	0.57
	3.04	0.70	
+25	1.29	0.066	1.42
	2.00	0.096	
	3.04	0.125	

TABLE 5.1 (continued)

4. Adsorption of Xenon from Air

Temperature °C	Absolute Pressure (Atm)	Adsorption Coefficient (liters(NTP)/gm)	Pressure Coefficient α (Dimensionless)
-50	1.29	18.8	0.18
	3.04	21.5	
-20	1.29	5.16	0.58
	3.04	7.41	
+22	1.29	1.05	1.17
	3.04	1.86	

Adsorbent: Pittsburgh PCB 12x30 Mesh Charcoal

Reference: Goldin and Trindade(1973)

TABLE 5.2

Effect of Pressure on the Adsorption of Krypton
from Nitrogen Enriched Carrier Gases

Temperature (°C)	Carrier Gas	Absolute Pressure (Atm)	Adsorption Coefficient /cc(NTP)/gm/	Pressure Coefficient α (Dimensionless)
-80	Nitrogen	1.00 3.04	1,235 1,692	0.33
-120	Nitrogen	1.00 3.04	4,912 6,293	0.25
-80	N_2 + 1% O_2	1.00 3.04	1,277 1,768	0.34
-120	N_2 + 1% O_2	1.00 3.04	5,130 6,298	0.20
-80	N_2 + 1% O + 100 PPM CO_2	1.00 3.04	1,222 1,713	0.36
-120	N_2 + 1% O_2 + 100 PPM CO_2	1.00 3.04	4,966 5,916	0.17

Adsorbent: Pittsburgh PCB 12x30 mesh charcoal

Reference: Kabele and Bohringer (1975)

TABLE 5.3

Effect of High Pressure on the Adsorption

of Krypton from Nitrogen at 20°C

Absolute Pressure (Atm)	Adsorption Coefficient /cc(NTP)/gm/	Pressure Coefficient α (Dimensionless)
123	585	
30	396	
10.7	249	1.19
1.22	67.5	

Adsorbent: Activated Charcoal Type HGR-510

Reference: Kawazoe and Kawai (1972)

TABLE 5.4

Effect of Pressure on the Adsorption of Krypton from Nitrogen by Various Adsorbents at 0°C

Adsorbent (See Table 1.2 for additional information)	Adsorption Coefficient /cc(NTP)/gm/ Absolute Pressure		Pressure Coefficient α (Dimensionless)
	1 Atm	10 Atm	
Columbia CXC	121	309	0.67
Shirasagi G	87	243	0.78
Columbia HCC	136	335	0.64
Tsurumi 2GR-T	96	235	0.63
Tsurumi 2GM	103	239	0.58
Tsurumi GW	124	291	0.58
Tsurumi GLS	121	314	0.68
Takeda HGK-530	121	346	0.81

Krypton Concentration: 63 ppm.

Reference: Kitani, et al. (1968)

TABLE 5.5

Combined Effect of Temperature and Pressure

on the Adsorption of Krypton from Nitrogen

Temperature (°C)	Adsorption Coefficient /cc(NTP)/gm/ Absolute Pressure 1 Atm	10 Atm	Pressure Coefficient α (Dimensionless)
25	61	182	0.86
0	121	314	0.68
-30	203	447	0.52

Adsorbent: Tsurumi-GLS (See Table 1.2)

Krypton Concentration: 63 ppm

Reference: Kitani, et al. (1968)

TABLE 5.6

Effect of Pressure on the Adsorption of Xenon from Argon

Temperature (^{o}C)	Absolute Pressure (Atm)	Adsorption Coefficient /cc(NTP)/gm/	Pressure Coefficient, α (Dimensionless)
30	1	873	
30	3.04	1,800	0.96
-30	1	11,300	
-30	3.04	16,000	0.37

Adsorbent: Pittsburgh PCB 12x30 mesh charcoal

Reference: Kabele, et al. (1973)

TABLE 5.7

Adsorption of Argon at Various Temperatures and Pressures

Temperature (°C)	Absolute Pressure (Atm)	Adsorption Coefficient (liters(NTP)/gm)
-140	0.34*	0.211
	1.68	0.280
	3.72	0.311
	5.76	0.313
	7.79	0.321
	10.51	0.335
-120	0.34*	0.128
	1.34	0.192
	1.68	0.198
	3.72	0.233
	5.76	0.257
	7.79	0.265
	10.51	0.279
-100	0.34*	0.074
	1.68	0.152
	3.72	0.190
	5.76	0.207
	7.11	0.218
	10.51	0.237
-75	0.34*	0.035
	3.72	0.130
	5.76	0.149
	7.79	0.174
	10.51	0.189
-78	5.76	0.153
	7.79	0.169
+25	1.00	0.0060
	3.72	0.022
	6.44	0.035
	10.54	0.054

* 0.34 atmospheres partial pressure of Ar, from a 25:75 Ar-He mixture at 5 psig (=1.34 Atm)

Adsorbent: Pittsburgh PCB 12x30 mesh charcoal

Reference: Underhill, et al. (1973)

TABLE 5.8

Adsorption of ^{41}Ar from an Argon Carrier Gas

Temperature (°C)	Absolute Pressure (Atm)	Adsorption Coefficient /cc(NTP)/gm/
-30	1.00	46
	1.00	49
	3.04	57
	3.04	59
-75	1.00	97
	3.04	120
	3.04	129
-125	1.00	218
	1.00	234
	3.04	251
	3.04	262
-160	1.00	346
	1.00	371
	3.04	378
	3.04	396

Adsorbent: Pittsburgh PCB 12x30 charcoal

Reference: Kabele, et al. (1973)

CHAPTER 6

THE EFFECTS OF MASS TRANSFER ON THE ADSORPTION OF KRYPTON AND XENON

In a series of papers which examined the theoretical bases for mass transfer in fission gas adsorption beds, Underhill (1967, 1969, 1970) demonstrated that the method of moment analysis is the best procedure for determining mass transfer effects. Additional findings of practical importance to this subject are covered in this Chapter.

6.1 Fitting of Breakthrough Data to Theoretical Curves

All of the current knowledge regarding adsorption coefficients and mass transfer in a fission gas adsorption bed has been obtained from the study of breakthrough curves. Such curves are graphic presentations of the concentration of fission gas in the effluent from a bed following the introduction of a pulse or frontal input of fission gas into the carrier gas entering the bed.

J. M. Smith (1975)* developed a computer program that can be used to calculate breakthrough curves for any expected combination of mass transfer parameters, making it possible to determine if a given combination of mass transfer parameters can account for an observed breakthrough curve. This program is written in Fortran IV and uses a fast inverse Laplace transform. Copies of the program are available from the author.*

---

* Smith, J. M. (1975): Personal Communication.

Dr. J. M. Smith
University of California at Davis
Davis, CA 95616

In practice, equations less general than the inverse Laplace transform are frequently used to describe the data resulting from breakthrough experiments (Table 6.1). How well these theoretical equations fit actual data is not precisely known, but several instructive examples can be given. Figure 6.1, from Kenney and Eshaya (1960), shows data fitted to the theoretical breakthrough equations of Glueckauf (1955) and Jury and Licht (1952). In developing his equation, Glueckauf assumed that mass transfer was controlled by interparticle diffusion, whereas Jury and Licht assumed that mass transfer was controlled by a thin air film surrounding the adsorbent particles. It is interesting to note that both equations produced curves that fit the experimental data quite well, even though a third mechanism, intraparticle diffusion, probably controlled mass transfer in the experiments of Kenney and Eshaya. Perhaps the shape of breakthrough curves is not strongly dependent on the mechanisms of mass transfer.

The theoretical chamber model, which produces a simple breakthrough curve, was developed by Browning and Bolta (1959) at the Oak Ridge National Laboratory. In this model the adsorption bed is artificially divided into a series of chambers and rapid mixing of the fission gases is assumed to take place within each chamber. Although the equation developed from this model does not closely fit data obtained by Ackley, et al. (1960) (Figure 6.2), it does provide good agreement with data developed by Strong and Levins (1979) (Figure 6.3) for the adsorption of radon. There is no ready explanation why this equation worked well in one case and not in another.

Figure 6.4 shows the excellent fit of data of Collard, et al. (1977), to a Gaussian equation. This approach works best when the breakthrough curve can be characterized by a large number of theoretical plates; otherwise the curve will be too skewed to fit the symmetrical Gaussian equation. Three useful techniques for determining the number of theoretical plates from a Gaussian breakthrough curve are described in Figure 6.5.

For skewed breakthrough curves, it may be possible to obtain a straight line relationship between the fraction of the noble gas retained in the bed and the volume of effluent carrier gas by using log-probability coordinates (for example, compare Figures 6.6 and 6.7). In the Japanese literature, use of probability coordinates appears to be a common procedure (e.g., Kitani, et al., 1968).

6.2 Applicability of the van Deemter Equation

The applicability of the van Deemter equation to the analysis of noble gas holdup beds has been confirmed by a number of investigators, including Underhill (1967), Collard, et al. (1977), Castellani, et al. (1975), and Curzio and Gentili (1972). The basic equation may be expressed as:

$$H = \frac{2\varepsilon\gamma D_m}{V_s} + 2\lambda_p d_p + \frac{d_p^2 V_s (k - \varepsilon/\rho)}{30\rho k^2 D_p} \qquad (6.1)$$

where

H = height equivalent to one theoretical plate, cm

d_p = mean adsorbent particle diameter, cm

D_m = molecular diffusion coefficient for fission gas in carrier gas, cm^2/sec

k = adsorption coefficient, cc(at temperature and pressure of bed)/gm

V_s = superficial carrier gas velocity, cm/sec

γ = tortuosity factor for interparticle diffusion, dimensionless

ε = fraction of adsorption bed consisting of interparticle void volume, dimensionless

λ_p = coefficient for axial dispersion, dimensionless

ρ = bulk density of the adsorbent, gm/cc

This equation can be written in a nondimensional form by use of the following nondimensional parameters:

$$h = \frac{H}{d_p} \qquad (6.2)$$

$$v_i = \frac{V_s d_p}{\varepsilon D_m} \qquad (6.3)$$

where

h = reduced height equivalent to one theoretical plate

v_i = reduced interparticle velocity

Then

$$h = \frac{2\gamma}{v_i} + 2\lambda_p + cv_i \qquad (6.4)$$

where

$$c = \frac{\varepsilon D_m (k - \varepsilon/\rho)}{30\rho k^2 D_p} \qquad (6.5)$$

Shown in Figure 6.8 is a plot of H (the height equivalent to one theoretical plate) vs. V_s (the superficial velocity). This relation can be used to determine the coefficients for the van Deemter equation. As discussed below, Figures 6.9 through 6.13 show this equation to be applicable even under conditions of changing relative humidity and temperature.

6.2.1 Effects of Humidity

Castellani, et al. (1975), have observed that the mass transfer of krypton is unaffected by relative humidity (Figure 6.9). This is understandable at intermediate and low carrier gas velocities, because under these conditions, mass transfer is controlled by diffusion and flow patterns external to the granules of adsorbent, and these factors are only slightly altered by the relative humidity. Relative humidity also appears to have little effect on mass transfer at high carrier gas velocities, where mass transfer is controlled by diffusion within the adsorbent granules (intraparticle diffusion). This is an interesting finding, which may be explained by the fact that water first condenses in the micropores of the adsorbent, leaving the macropores (which many research workers believe control intraparticle diffusion) unaffected.

Similarly, Collard, et al. (1977), observed only a slight alteration in the mass transfer of xenon at room temperature when the relative humidity was increased from 0% to 65%.

6.2.2 Effects of Temperature

A straightforward way to determine the effects of temperature on mass

transfer is to plot data in the form of the reduced van Deemter equation (Equation 6.4). In this equation, the values for γ and λ_p should be independent of, or only very slightly affected by, temperature. The coefficient, "c" (Equation 6.5), contains three temperature dependent factors: D_m, D_p, and k. If intraparticle diffusion is controlled by diffusion in the macropores, then D_m and D_p should have the same temperature dependency and the net result would be that the coefficient "c" varies with temperature as the reciprocal of k. It follows from this reasoning that at high carrier gas velocities (where mass transfer is controlled by intra-particle diffusion), the value of h (Equation 6.4) should increase rapidly with increasing temperature, whereas at low and intermediate carrier gas velocities, the temperature effect should be small.

Experimental measurements, although fragmentary, are in agreement with these predictions. Lepold (1965), using a fine mesh charcoal in a gas chromatography column for the rapid separation of short-lived isotopes of krypton and xenon, observed a dependency of H on temperature that agrees very well with the theoretical predictions given here. As he decreased the flow rate of the carrier gas, the separation between the isotherms for both krypton and xenon decreased (Figures 6.10 and 6.11). Curzio and Gentili (1972) (Figure 6.12) found no temperature dependence for h at low values of v_i, but at the same time they found the temperature dependence of the inter-particle diffusion coefficient to be $T^{1/2}$. This latter result is puzzling because the kinetic theory of gases predicts that the

diffusion coefficient would vary as $T^{3/2}$. It is logical to seek some discrepancy in the procedure used by Curzio and Gentili in the analysis of their data. A factor that could account for their results is the temperature dependency of the carrier gas velocity. In this context, it is interesting to note that in plotting their data (Figure 6.13) these authors assumed that interparticle velocity was independent of temperature.*

Browning and Bolta (1959) injected pulses of ^{85}Kr into nitrogen passing through a bed of Columbia ACA activated charcoal and calculated a constant value of 4.3 cm for H at temperatures of 15°C, 5°C, -50°C, and 110°C. At their flow velocity of 5.6 cc (NTP)/cm^2-sec, the effects of temperature on H should have been important. It is not known why this was not the case.

6.2.3 Effects of Adsorbent Particle Size and Carrier Gas Composition

Trofimov and Pankov (1972ab) observed that at low carrier gas velocities, the particle size had little influence on mass transfer. At higher carrier gas velocities, however, particle size strongly influenced mass transfer. This result is consistent with the predictions of the van Deemter equation (Equation 6.1). These authors also found that intraparticle diffusion was more rapid in the presence of air than in the presence of carbon dioxide and still more

---

*Curzio and Gentili actually used a linear equation for the temperature dependence of the diffusion coefficient, but it can be shown that for small changes in the temperature this linear equation is equivalent to the square root relationship given above.

rapid in the presence of helium. This observation is strong evidence that intraparticle diffusion is rate-limited by diffusion in the macropores, where collisions between the molecules of the noble gas and the carrier gas are commonplace.

Figure 6.14 (Ayers, et al. 1975), shows a tenfold reduction in H when the adsorbent particle size is reduced by a factor of about 5. These data were obtained in a flow regime where mass transfer is controlled by intraparticle diffusion. As a result, they are compatible with theoretical predictions.

6.2.4 Effect of Pressure

Pressure affects three parameters that influence intraparticle diffusion. These are the adsorption coefficient, the intraparticle diffusion coefficient, and the carrier gas velocity. The net result is that, if the input to a bed remains constant (measured at NTP), an increase in pressure will increase the number of theoretical plates (Figures 6.14 and 6.15).

Data published by Kawazoe and Kawai (1972) (Table 6.2) show that both the film mass transfer coefficient and the rate of intraparticle diffusion vary inversely with absolute pressure. Again, this is compatible with theory.

6.3 Parameters Affecting Mass Transfer in Charcoal Beds

6.3.1 Effects of Interparticle and Intraparticle Diffusion

Experiments by Madey (1961), using ^{85m}Kr tracer in a helium carrier

gas, showed that interparticle diffusion can reduce the decontamination factor of a charcoal adsorption bed at low carrier gas velocities. These results are in agreement with his theoretical model (Madey, et al., 1962).

Using a rigorous experimental approach, Nakhutin, et al. (1969), studied the effect of intraparticle diffusion on the decontamination factor of a charcoal bed. In these studies, nitrogen containing short-lived krypton and xenon radioisotopes was passed through a bed monitored at various points by a collimated gamma spectrometer. Using this approach, it was possible to determine the concentration of individual radionuclides as a function of their distance from the bed entrance. These experiments showed that the adsorption coefficients for the radionuclides employed were independent of half life. This is in agreement with the hypothesis that under most conditions the effect of intraparticle diffusion is negligible. If this were not the case, the longer lived nuclides would have had a greater time to penetrate the adsorbent granules and to establish equilibrium, and their adsorption coefficient would have appeared to be greater (Thiele, 1939).

Nakhutin, et al. (1969), have also suggested that, at low temperatures (i.e., less than -100°C for krypton and less than 3°C for xenon), conditions may be found under which intraparticle diffusion does become important. However, this suggestion has not yet been tested experimentally.

6.3.2 Overall Effects of Mass Transfer on the Decontamination Factor

The effects of mass transfer on the decontamination factor of a charcoal bed can be determined from Figures 6.16 and 6.17, which were developed for interparticle and intraparticle diffusion, respectively. Many holdup beds operate with the parameter, z, less than 0.1. When this is the case, both Figures 6.16 and 6.17 give essentially the same result. Then the following simple approximate equation can also be used.

$$DF = 2^{\left(\frac{z}{1 + 2\ \ln(2)z/N}\right)} \qquad (6.6)$$

where

DF = Decontamination Factor, $\left(\frac{\text{Input Concentration}}{\text{Output Concentration}}\right)$

m = mass of adsorbent, gms

k = adsorption coefficient, cc/gm

$\dot{V}$ = flow of carrier gas, cc/sec

$t_{1/2}$ = isotopic half life, sec

N = number of theoretical plates, dimensionless

z = $mk/\dot{V}t_{1/2}$, dimensionless

Table 6.3 summarizes calculations obtained by applying Equation 6.6 to the mass transfer data of Collard, et al. (1977). It can be seen from these data that as long as the carrier gas velocity is 0.1 cm/sec or greater, the effects of mass transfer can be neglected. In summary, then, it appears that the effects of mass transfer on the efficiency of

a fission gas adsorption bed are usually quite small, except at very low carrier gas velocities.

6.4 Effects of Carrier Gas Velocity on the Adsorption Coefficient

Theory would predict that the adsorption coefficient for a charcoal bed should be independent of the carrier gas velocity. Any other result would have great impact on the design of noble gas holdup beds. There are, however, a number of studies in which some effect of carrier gas velocity on adsorption coefficient has been reported. For example, Wirsing, et al. (1977), at the Brookhaven National Laboratory conducted extensive measurements of the adsorption of krypton and xenon from air and nitrogen at low temperature. Parish (1979) showed that the adsorption coefficients obtained in these experiments were strongly dependent on the carrier gas velocity (Figure 6.18). Although data taken from the lowest flow regime used by Wirsing, et al., agreed with proprietary data of Parish, at higher carrier gas velocities, the adsorption coefficients obtained by Wirsing, et al., sharply decreased as the carrier gas velocity increased. Not only do the data of Wirsing, et al., show a velocity effect but they also have a high degree of scatter. Parish believes that at higher velocities Wirsing, et al., encountered fluidization and that this influenced their breakthrough curves. If fluidization is the explanation for their erratic results, then it should be noted that this difficulty could have been avoided if the carrier gas had passed down, rather than up, through the adsorbent bed.

Other data from the Brookhaven National Laboratory are in sharp contrast to the results reported by Wirsing, et al., Kenney and Eshaya (1960) and Eshaya and Kalinowski (1961) observed that increasing the carrier gas velocity increased the adsorption coefficient (Tables 6.4 and 6.5, Figures 6.19 and 6.20). Data in Table 6.6 (Koch and Grandy, 1957) also show a strong increase in the adsorption coefficient as the carrier gas velocity is increased. The same effect is apparent in Figure 3.2 taken from Khan, et al. (1976).

There are, on the other hand, a number of studies in which the carrier gas velocity was observed to have no effect on the adsorption coefficient. In a series of carefully controlled experiments, Lovell and Underhill (1979) examined the effect of a 30 fold change in carrier gas velocity on the adsorption coefficient of krypton. These measurements, which had an estimated error of about 3%, appeared to show that the adsorption coefficient, determined from moment analysis, was independent of the carrier gas velocity.

Rozhdestvenskaya, et al. (1975), also observed no effect of the carrier gas velocity on the adsorption coefficient in tests with superficial velocities ranging from 0.8 to 4 cm/sec. In addition, Siegwarth, et al. (1973), found the adsorption coefficient to be independent of the carrier gas velocity. Finally, the results of Kawazoe (1967) (Table 6.7) indicate that, if the adsorption coefficient is affected by the carrier gas velocity, the effect is not great.

It is recognized that the vast majority of adsorption sites are located internally, apart from the flow paths of the carrier gas, and therefore it would appear that the carrier gas velocity should have no effect on the adsorption coefficient. As Lovell and Underhill (1979) point out, this is almost but not quite true. A pulse injection in the case of a highly nonlinear adsorption isotherm would lead to a situation where the carrier gas velocity affects the measured adsorption coefficient, but then the results are essentially meaningless because there is no way to determine the concentration to which this adsorption coefficient corresponds.

In the experiments of Kenney and Eshaya (1960), Eshaya and Kalinowski (1961), and Wirsing, et al. (1970), step function inputs were used. Under this condition there seems to be no possible explanation for a carrier gas velocity effect on the adsorption coefficient. In other cases where pulse inputs were used, the noble gas isotherms are so nearly linear that the possibility that nonlinearity had any influence on these results can be discounted. Most of the reported effects that the carrier gas velocity has had on the adsorption coefficients appear to be experimental artifacts. Other researchers (as noted above) have not observed a velocity effect.

6.5 Conclusions

From the large amount of data presented in this chapter, four basic guidelines have emerged. These may be summarized as follows:

6.5.1 Use of Theoretical Breakthrough Curves

It is important to determine whether the theoretical equation adequately fits the experimental data. Table 6.1 lists conditions of mass transfer for which specific breakthrough curves are most appropriate.

6.5.2 Use of the van Deemter Equation

The van Deemter equation permits correlation of mass transfer data from a wide range of experimental conditions, including allowances for the effects of velocity, particle diameter, temperature, relative humidity, and pressure.

6.5.3 Calculation of the Decontamination Factor

The effect of mass transfer on the decontamination factor (DF) can be determined from Figures 6.16 and 6.17.

6.5.4 Effect of Carrier Gas Velocity on the Adsorption Coefficient

There are experimental data showing that the adsorption coefficient increases, decreases or remains constant as the carrier gas velocity is increased. From theoretical considerations, it appears that the adsorption coefficient should not be affected by velocity and that the contrary findings cited here are in error.

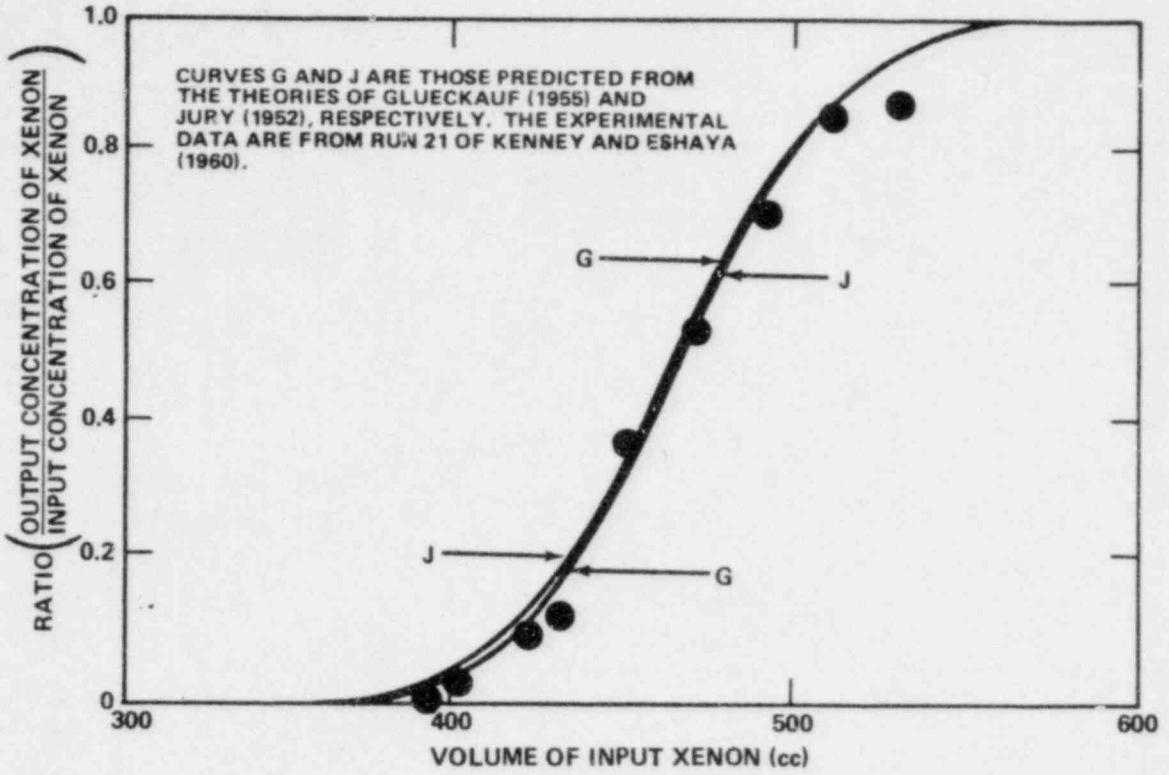

Figure 6.1 Comparison of experimental results with theoretical breakthrough curves.
Reference: Kenney and Eshaya (1960)

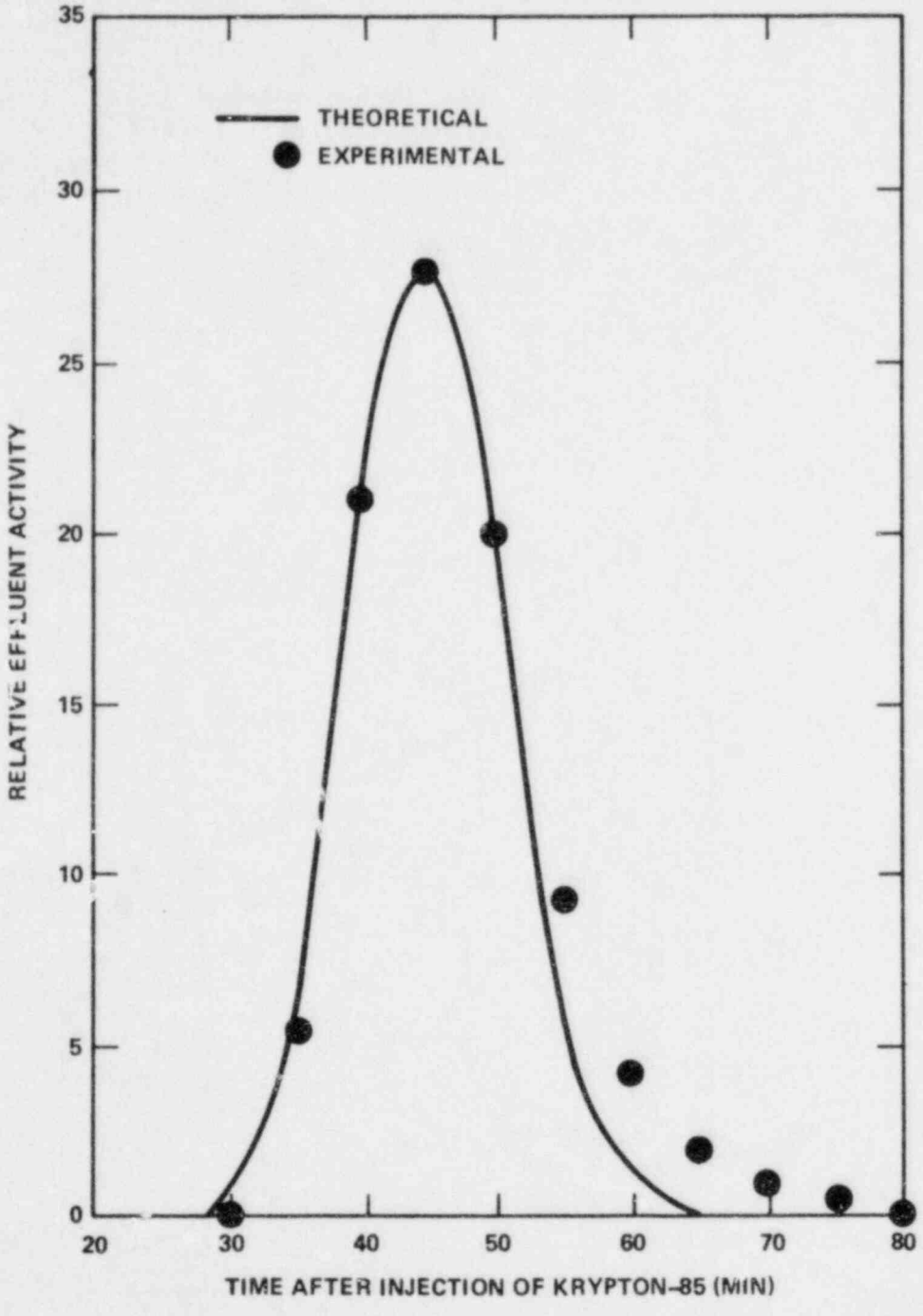

Figure 6.2 Fit of breakthrough data for krypton to the theoretical chamber equation.
Reference: Ackley et al (1960)

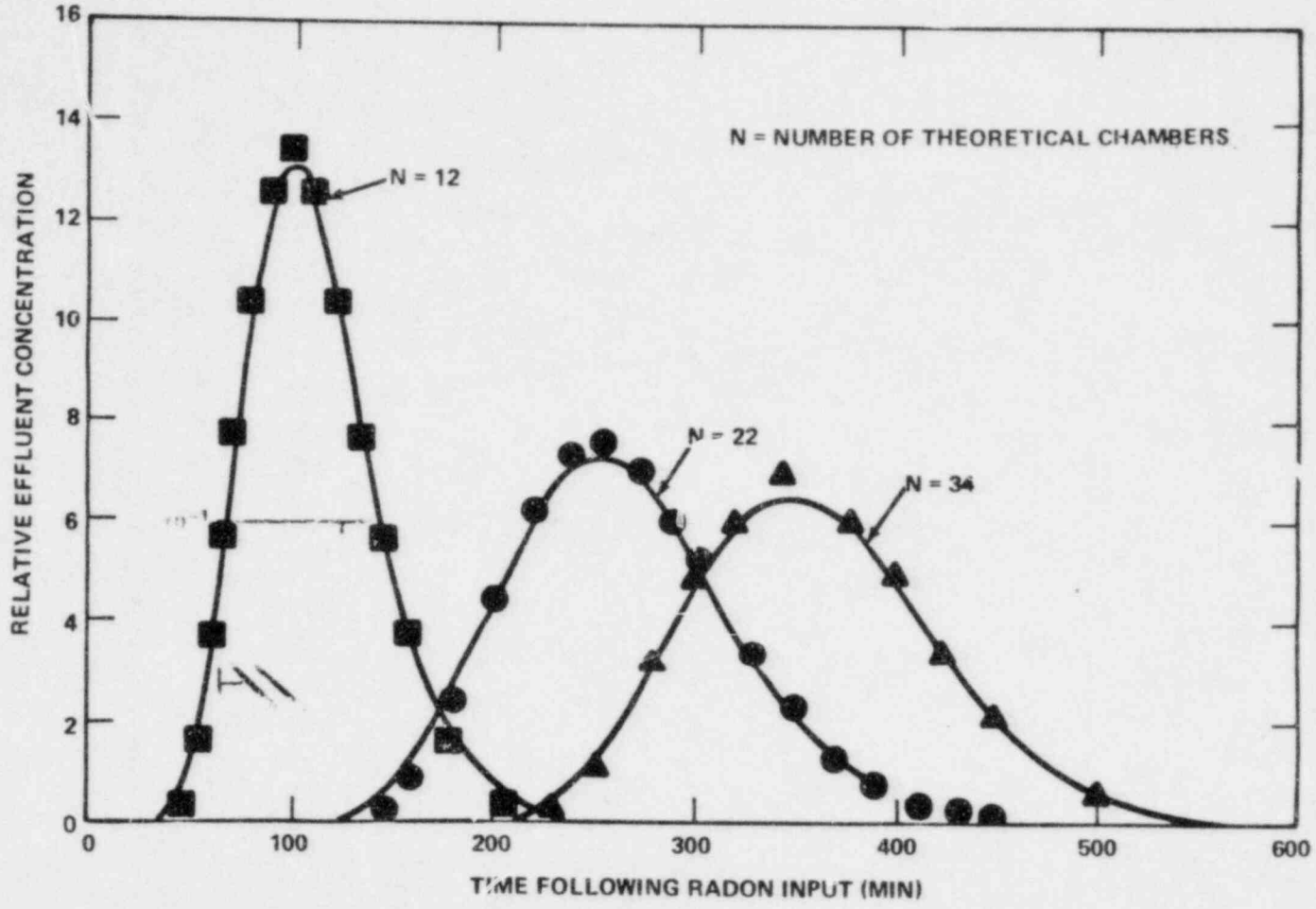

Figure 6.3 Application of the theoretical chamber equation to radon breakthrough data. Reference: Strong and Levins (1979).

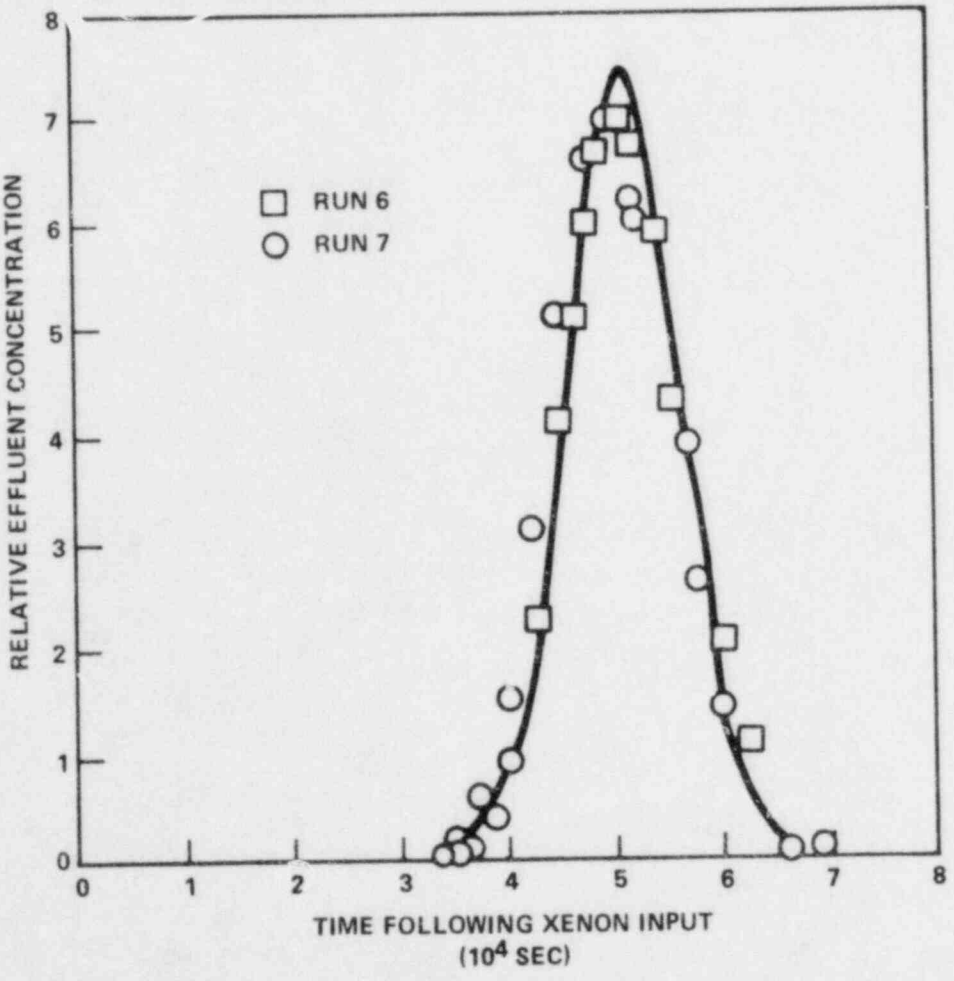

Figure 6.4 Fit of breakthrough data for xenon to a Gaussian curve.
Reference: Collard et al (1977)

METHOD #1

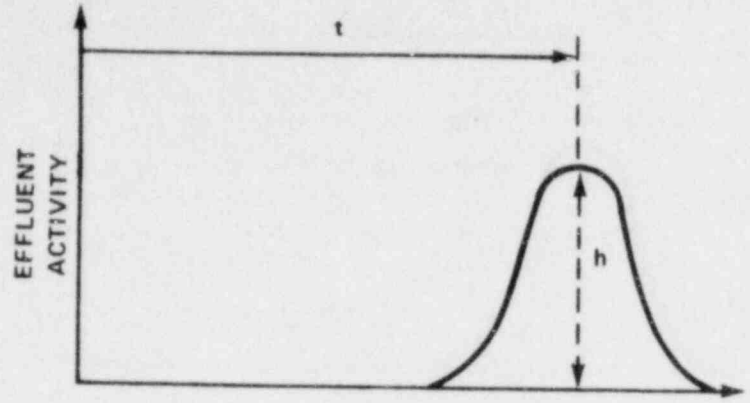

ACCORDING TO THIS METHOD: $N = 2\pi\left(\frac{ht}{A}\right)^2$

WHERE
A = AREA UNDER PEAK
h = HEIGHT OF PEAK
t = TIME AT WHICH EFFLUENT CONCENTRATION OF FISSION GAS REACHES A MAXIMUM

METHOD #2

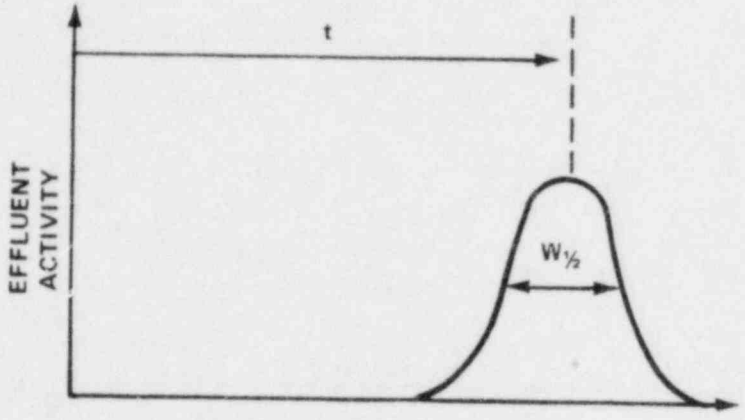

ACCORDING TO THIS METHOD: $N = 5.54\left(\frac{t}{W_{½}}\right)^2$

WHERE
$W_{½}$ = WIDTH OF PEAK AT HALF HEIGHT

METHOD #3

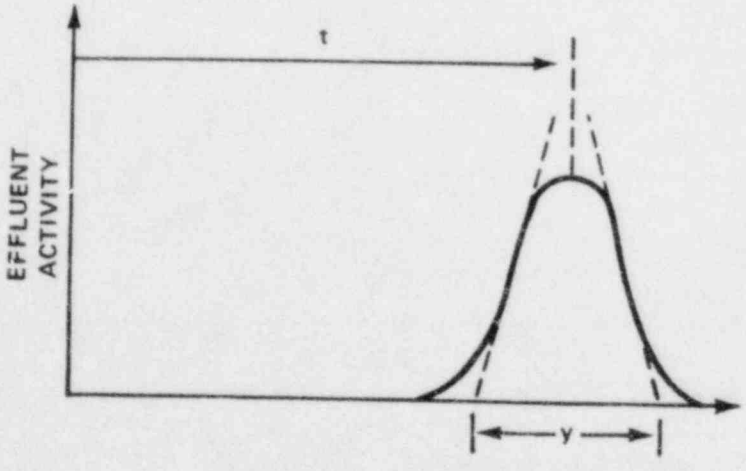

ACCORDING TO THIS METHOD: $N = 16\left(\frac{t}{y}\right)^2$

WHERE
y = WIDTH OF PEAK AT BASE AS DESCRIBED BY LINES DRAWN TO POINT OF INFLECTION (WHERE THE CURVE IS THE STRAIGHTEST)

Figure 6.5 Three methods of determining the number (N) of theoretical plates from Gaussian breakthrough curves.

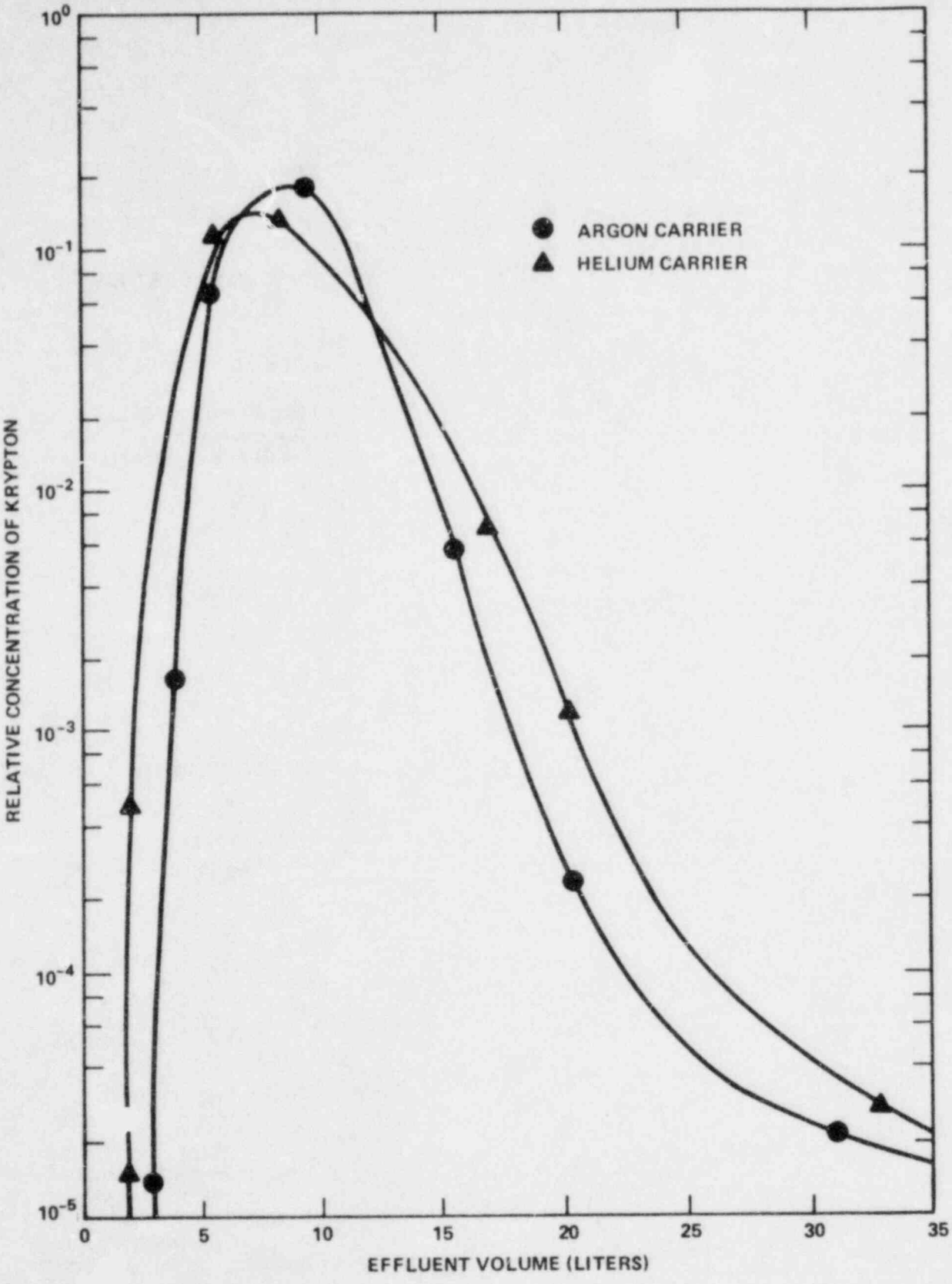

Figure 6.6 Breakthrough data for krypton at 100° F.

Reference: First et al (1971a)

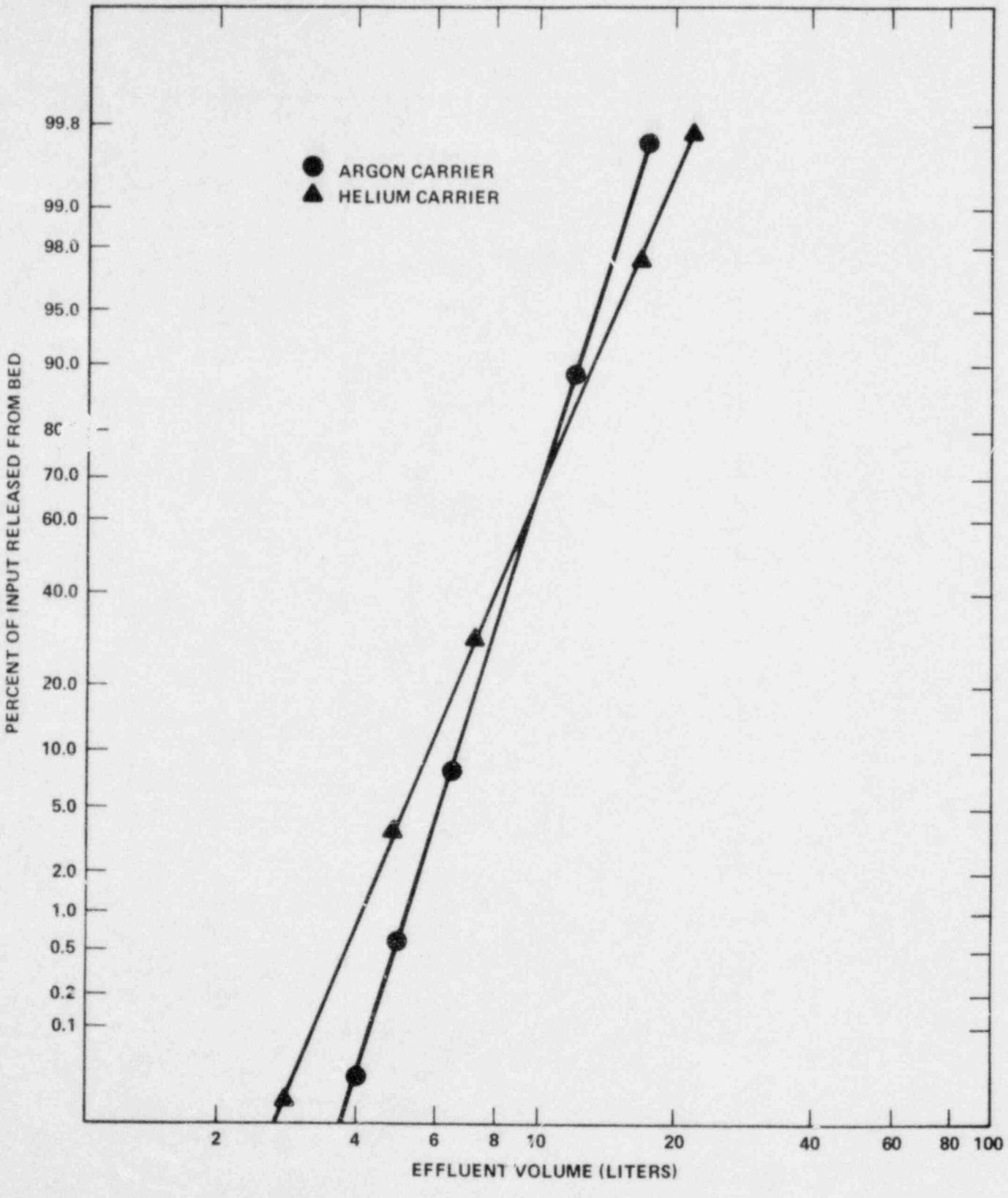

Figure 6.7 Krypton breakthrough data plotted on log-normal coordinates.
Reference: First et al (1971a)

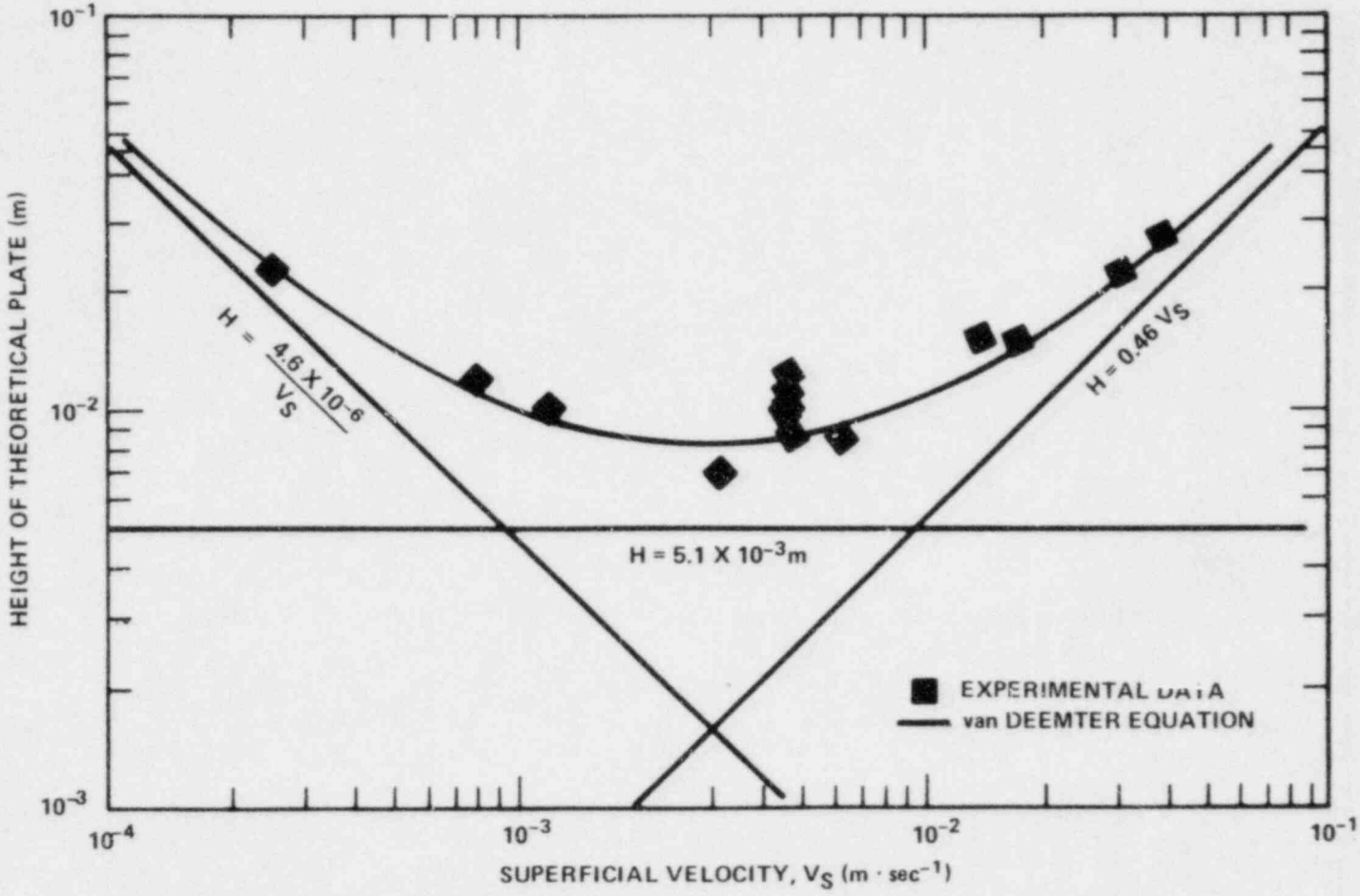

Figure 6.8 van Deemter plot of mass transfer of xenon in nitrogen.
Reference: Collard et al (1977).

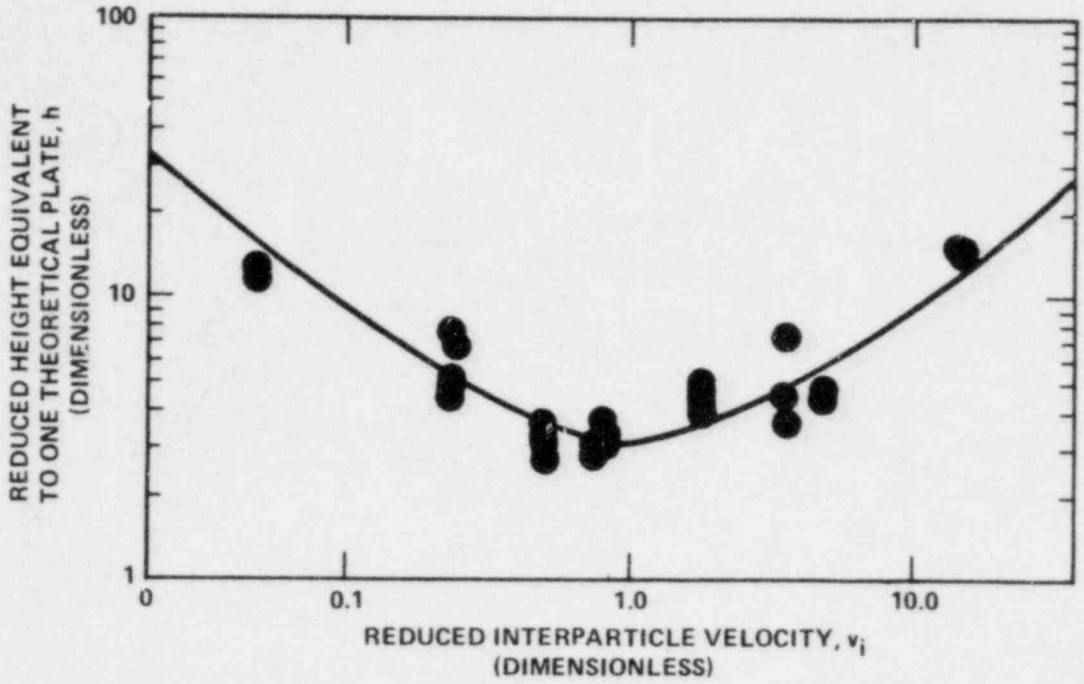

Figure 6.9 Effect of moisture on mass transfer of krypton.
Reference: Castellani (1975)

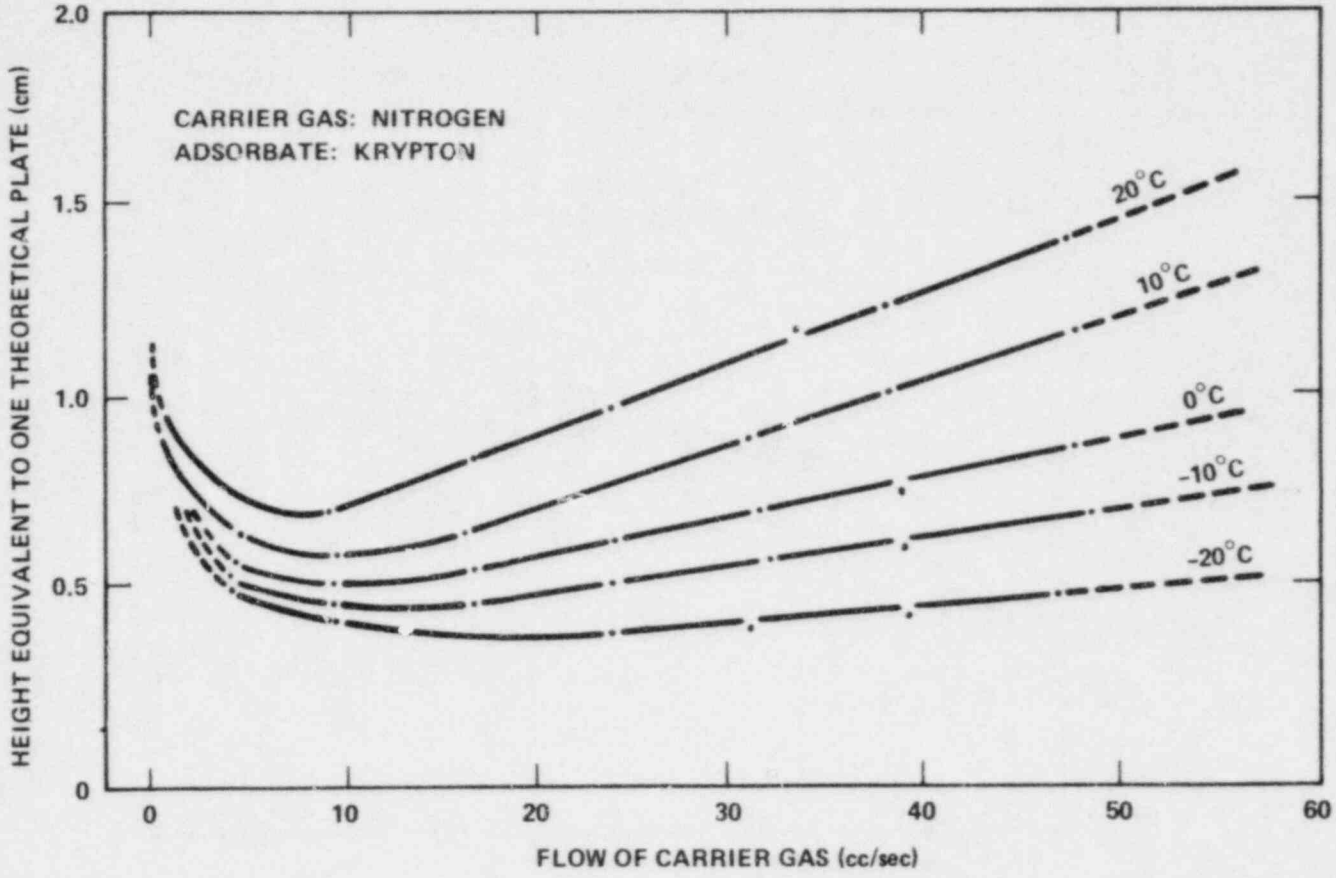

Figure 6.10 Effect of temperature on mass transfer of krypton.
Reference: Lepold (1965)

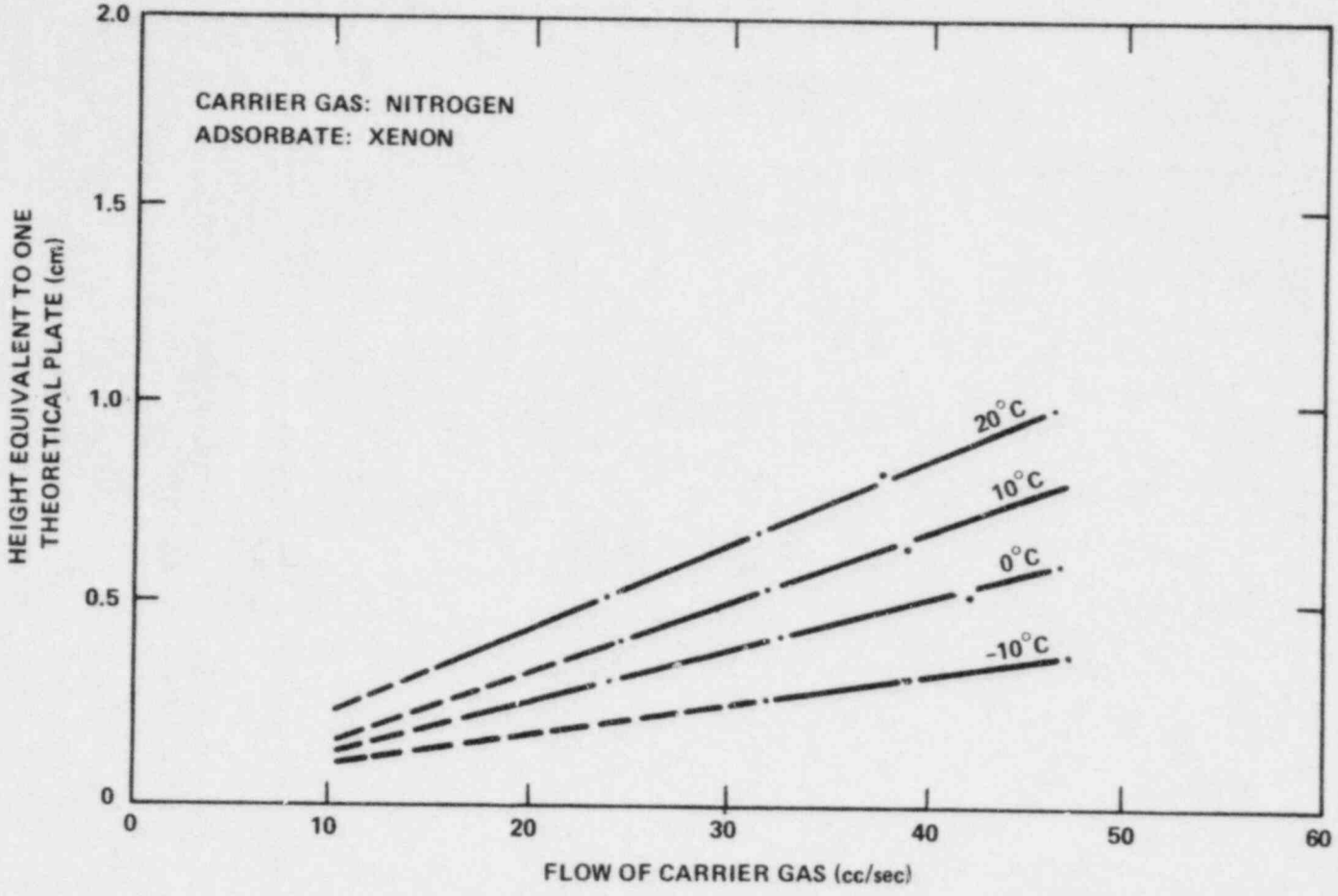

Figure 6.11 Effect of temperature on mass transfer of xenon.
Reference: Lepold (1965)

Figure 6.12 van Deemter plot corrected for temperature effects.
Reference: Curzio and Gentili (1972).

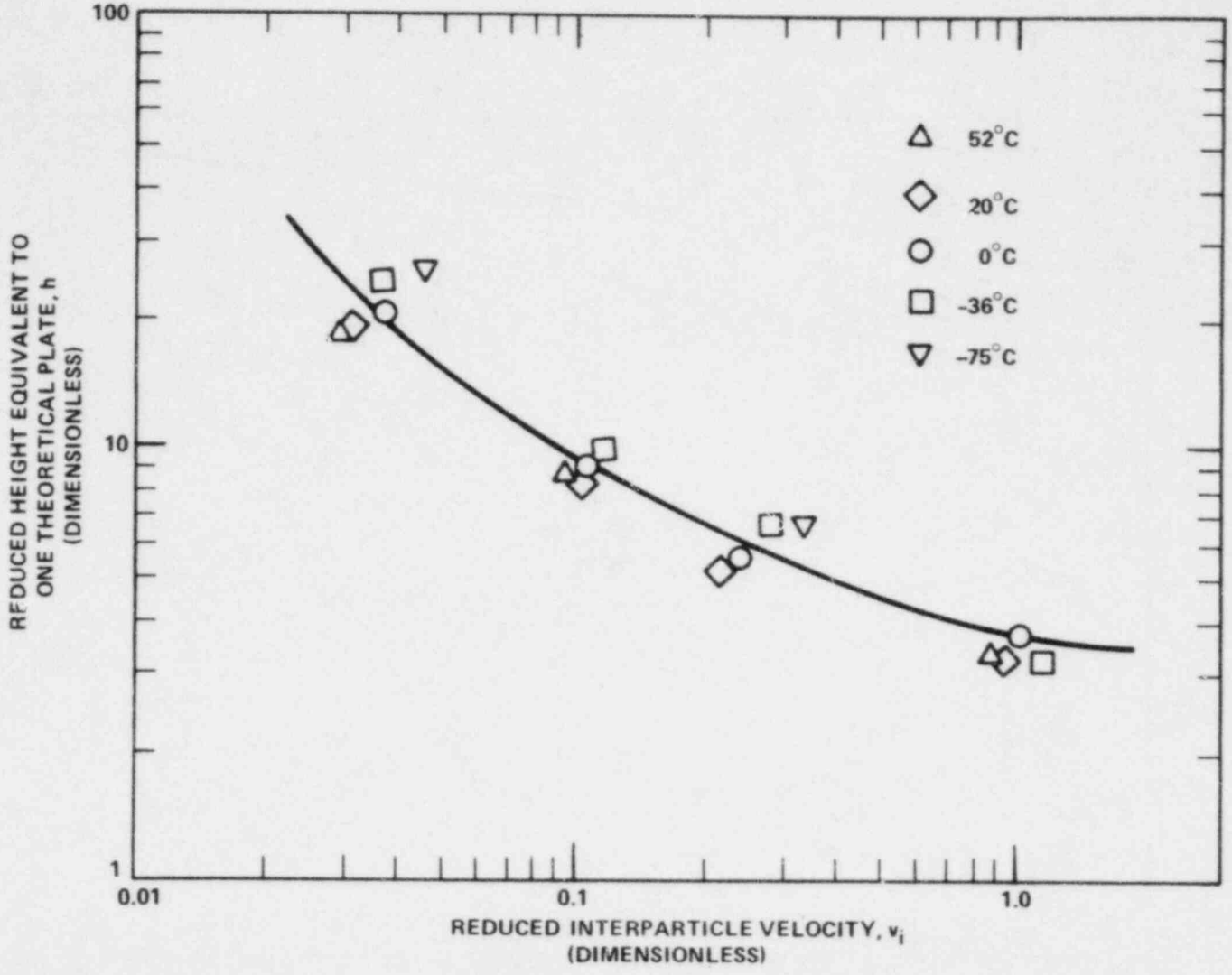

Figure 6.13 van Deemter plot uncorrected for temperature effects.

Reference: Curzio and Gentili (1972)

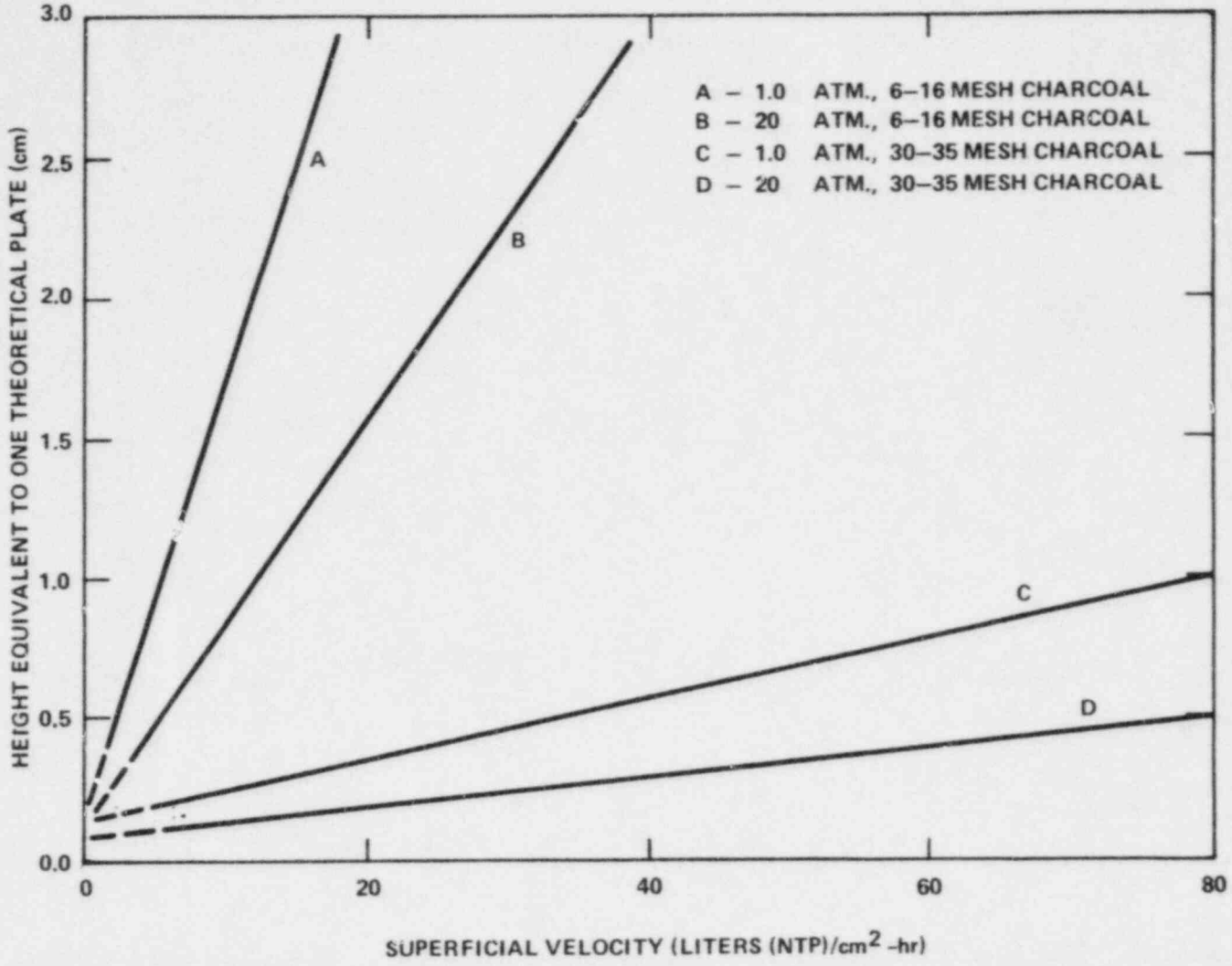

Figure 6.14 Effect of pressure, superficial velocity, and mesh size on height equivalent to one theoretical plate.
Reference: Ayers et al (1975)

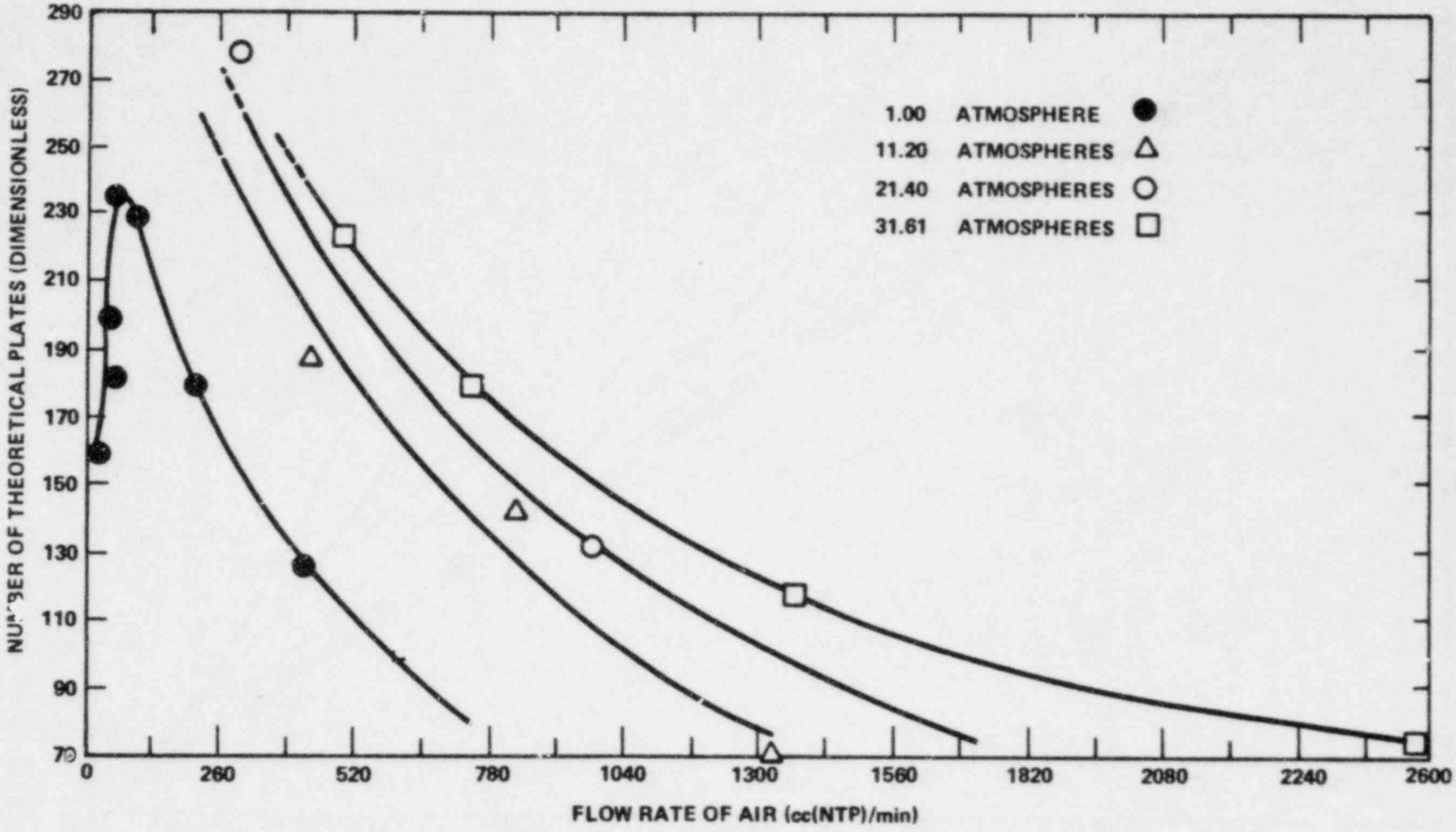

Figure 6.15 Effect of pressure on number of theoretical plates.
Reference: First et al (1974)

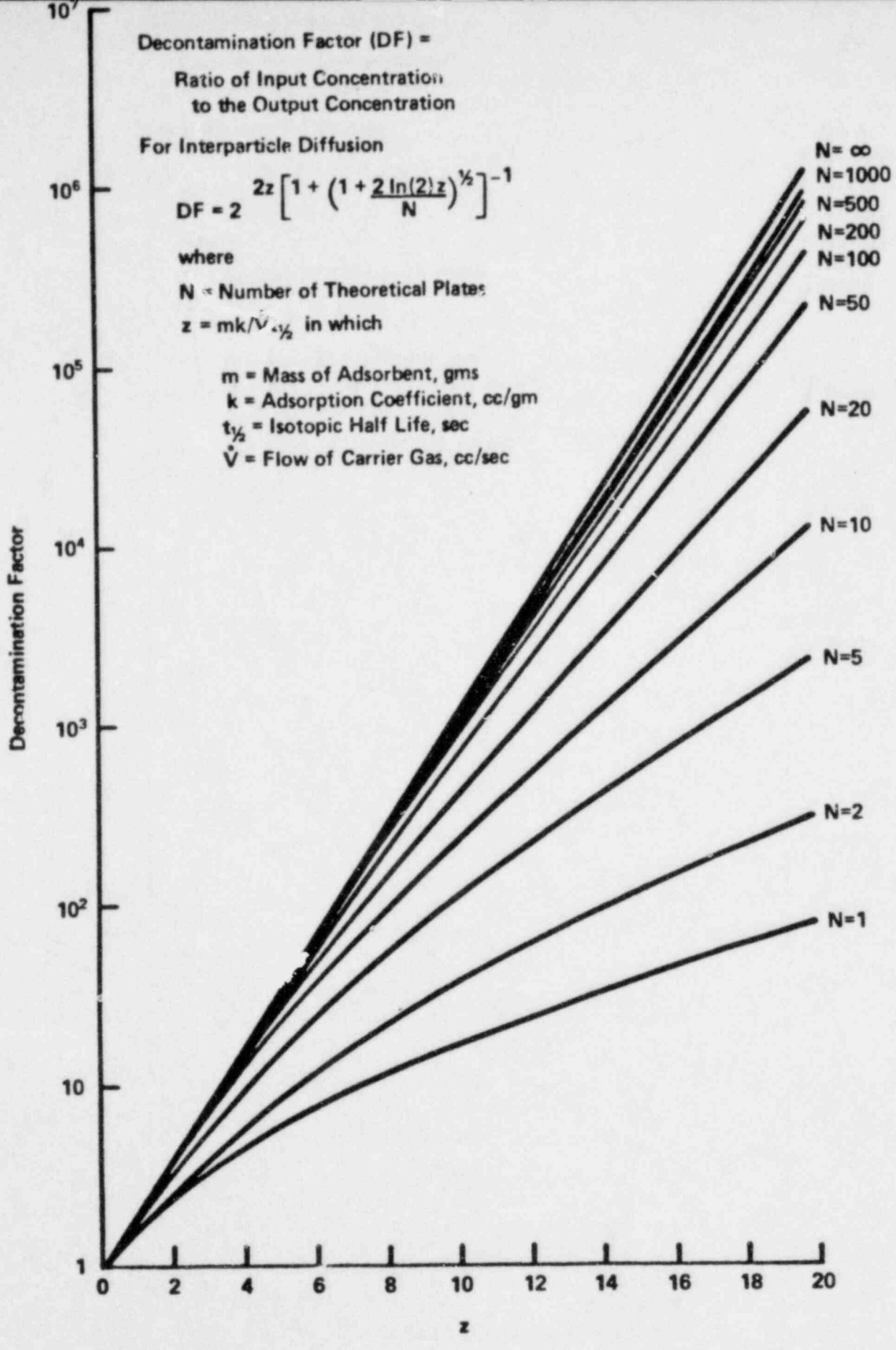

Figure 6.16 Effect of Interparticle Diffusion on the Decontamination Factor

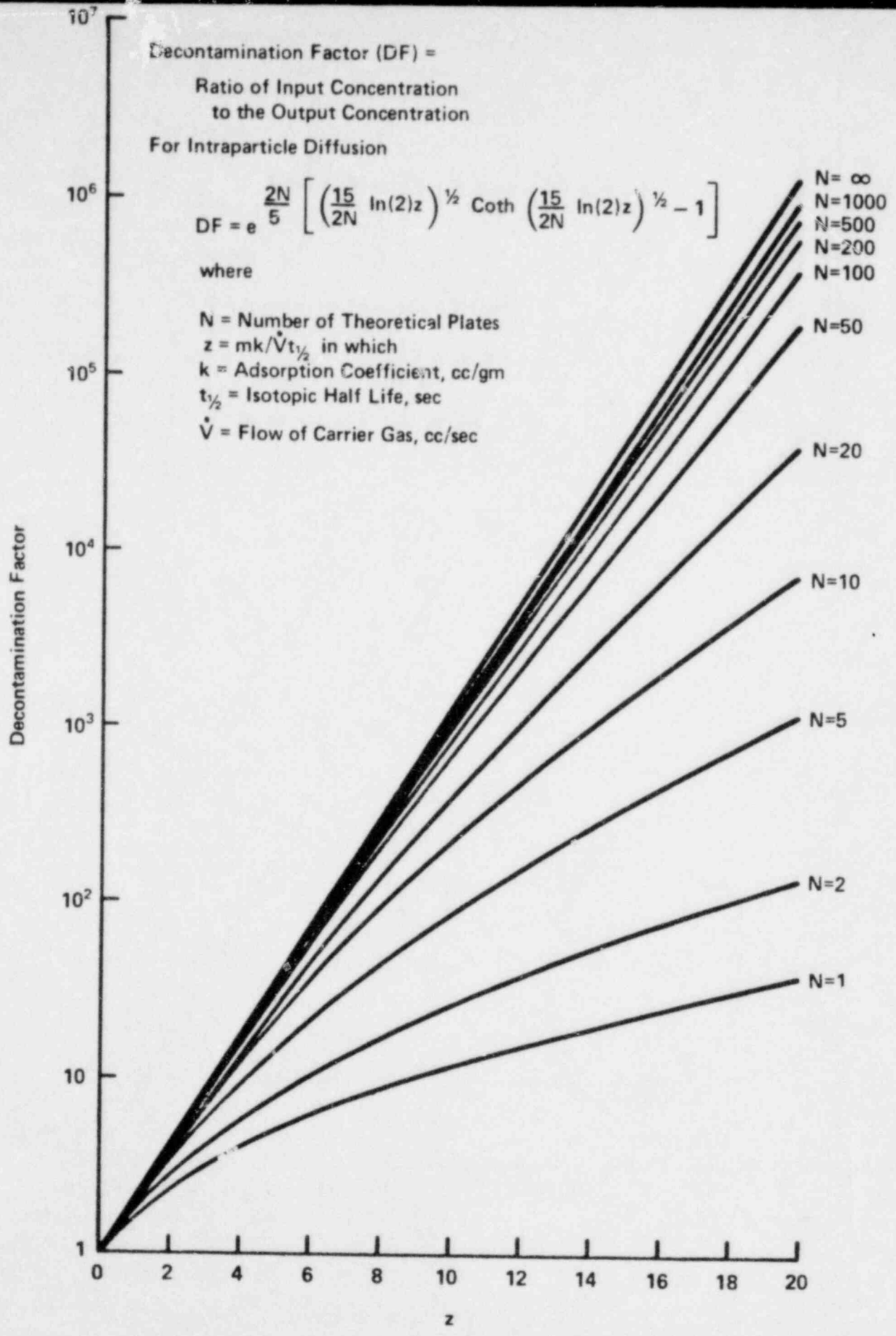

Figure 6.17 Effect of Intraparticle Diffusion on the Decontamination Factor

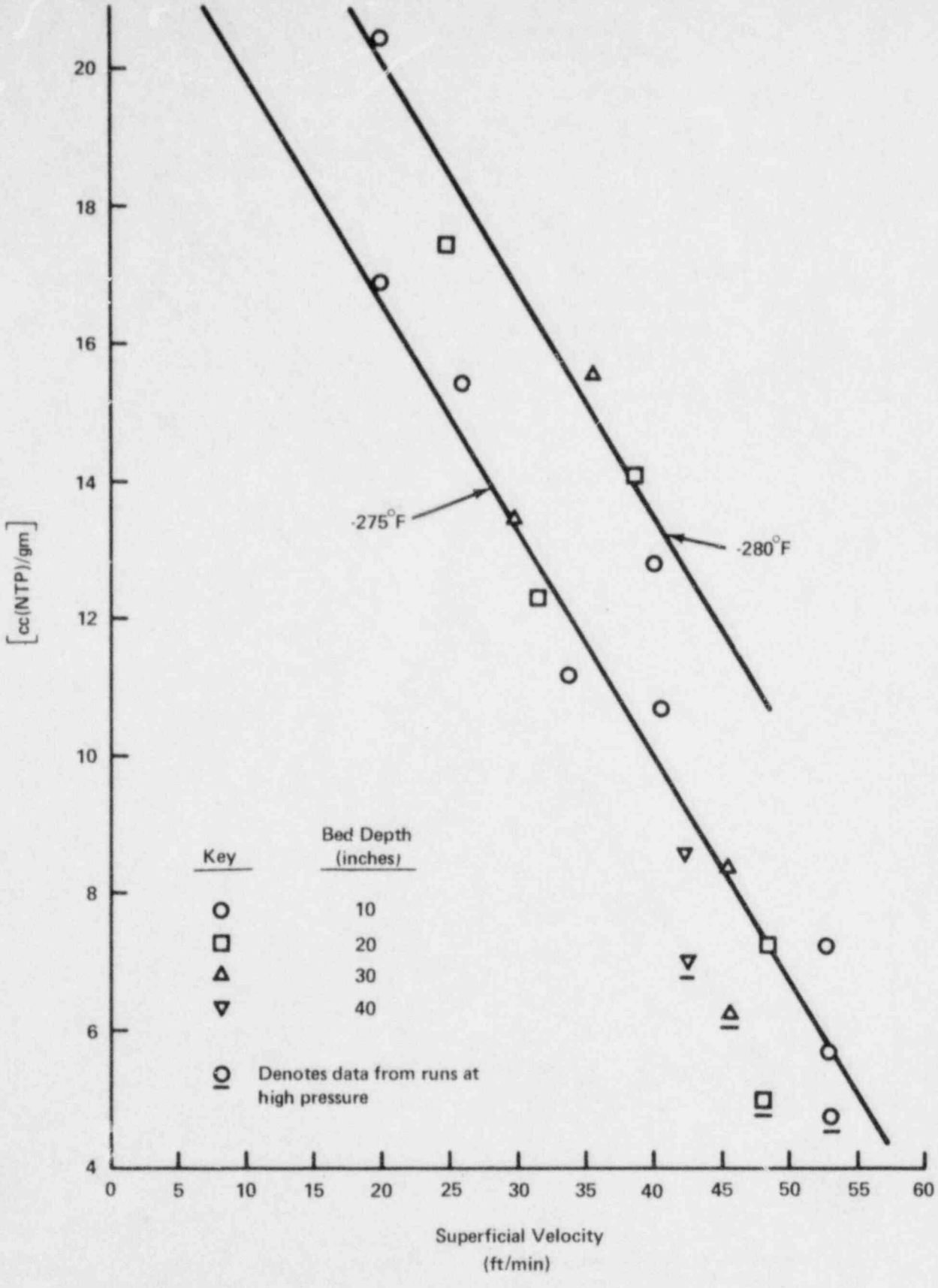

Figure 6.18 Effect of Carrier Gas Velocity on the Adsorption Coefficient
Reference: Parish (1979)*

* Parish, H. (1979): Personal Communication.

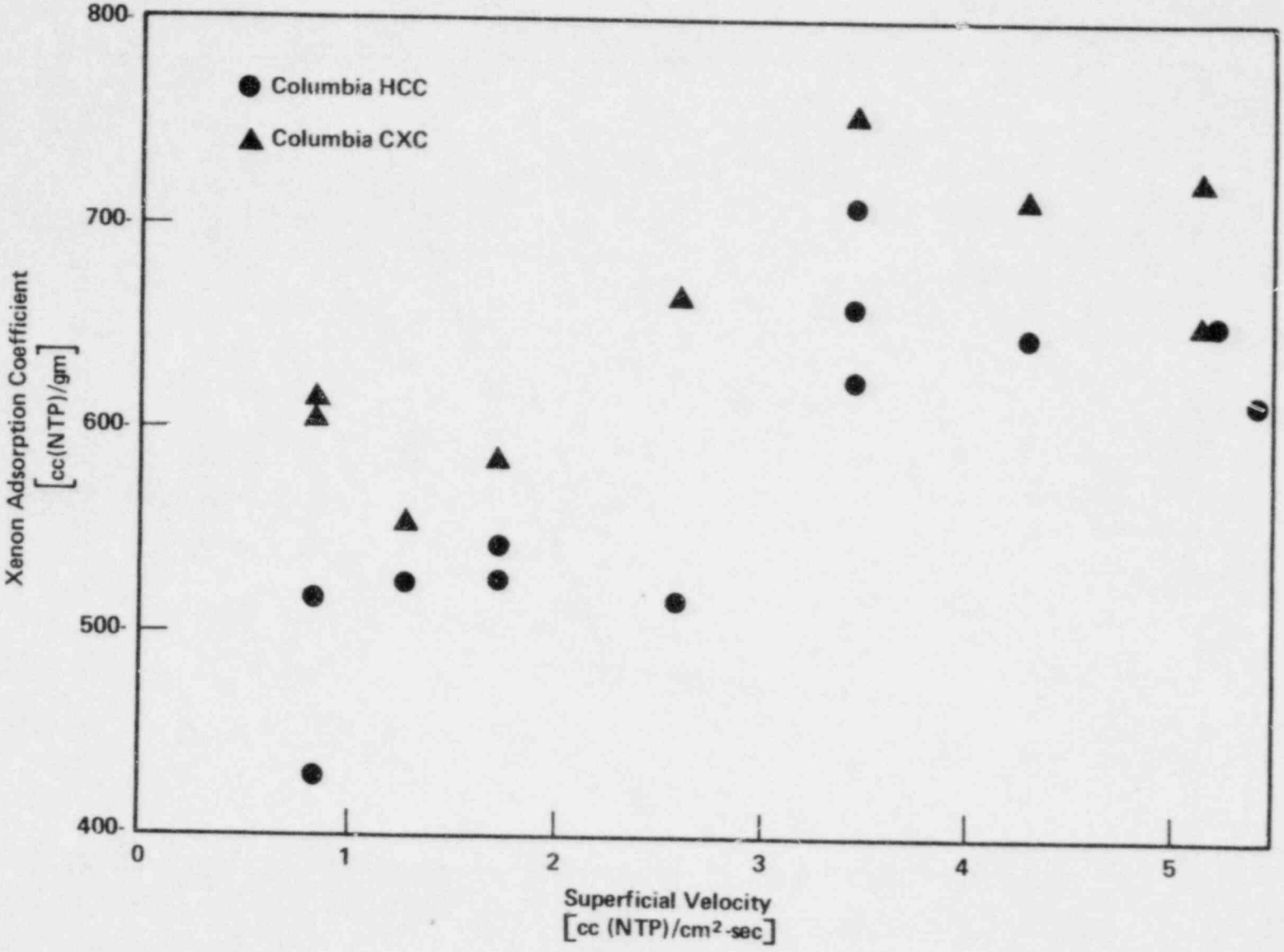

Figure 6.19 Effect of superficial velocity on the adsorption coefficient of xenon
Reference: Kenney and Eshaya (1960)

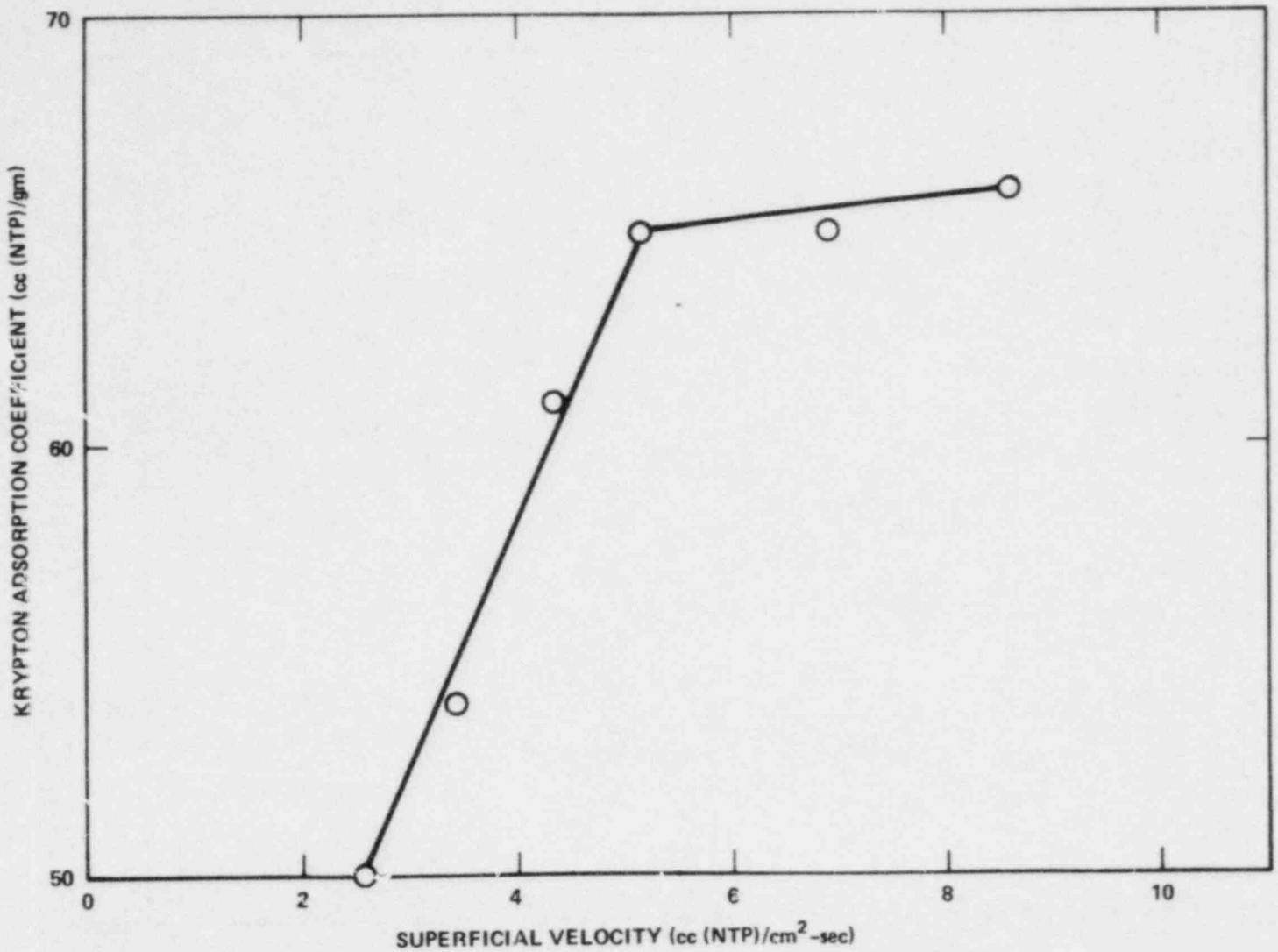

Figure 6.20 Effect of superficial velocity on adsorption coefficient for krypton.
Reference: Eshaya and Kalinowski (1961).

TABLE 6.1

Conditions of Mass Transfer for Which Specific Breakthrough Curves are Most Appropriate

Mechanism	Where Important	Related References	
		Pulse Input	Step Input
Interparticle Diffusion	Low Carrier Gas Velocities	Madey, et al. (1962)	Glueckauf (1955)
Diffusion Through Gas Film Around Adsorbent Particle	Seldom	Young (1958)	Hougen & Marshall (1947) Jury & Licht (1952)
Intraparticle Diffusion	High Carrier Gas Velocities	Rosen (1954)	Rosen (1954)

TABLE 6.2

Effect of Pressure on Mass Transfer of Krypton in Nitrogen

Absolute Pressure (Atm)	Temperature (^{o}C)	Superficial Velocity /cc(NTP)/cm^2. sec/	Mass Transfer Coefficient (sec^{-1})		
			Overall	Film	Intraparticle
123	20	0.0736	0.0188	0.16	0.0232
30.0	20	0.288	0.0676	0.64	0.0805
30.0	16	0.170	0.0595	0.48	0.0746
25.2	17	0.124	0.0679	0.60	0.0917
25.2	17	0.139	0.0699	0.62	0.0901
25.2	17	0.171	0.0791	0.65	0.102
25.2	17	0.213	0.0689	0.69	0.0834
10.7	20	0.822	0.155	1.8	0.171
10.7	20	0.778	0.153	1.8	0.177
1.22	20	7.11	1.02	20	1.11
1.22	20	7.11	0.97	20	1.05

Adsorbent: Activated Charcoal Type HGR-510

Reference: Kawazoe and Kawai (1972)

TABLE 6.3

Fractional Loss of Holdup Time for ^{133}Xe

Superficial Velocity, V_s /cc(NTP)/cm^2. sec/	Height Equivalent to One Theoretical Plate, H (cm)	Fractional Loss of Holdup Time, W, where $W = 1 - \left[\left(1 + \frac{\ln(2)\rho k H}{2t_{1/2}V_s}\right)\right]^{-1}$
10	5.1	0.00014
1	1.0	0.00027
0.1	1.0	0.0027
0.01	5.1	0.12

Assumptions

k, Adsorption Coefficient for Xenon, = 700 cc(NTP)/gm

ρ, Bulk Density of Adsorbent, = 0.5 gm/cc

$t_{1/2}$ = Half Life for ^{133}Xe, = 4.55×10^5 sec

References: Collard, et al. (1977) and Burnette, et al. (1962)

TABLE 6.4

Effect of Superficial Velocity on Adsorption of Xenon From Helium

Test Conditions	Superficial Velocity /cc(NTP)/cm^2-sec/	Adsorption Coefficient /cc(NTP)/gm/
Adsorbent: Columbia HCC Activated Charcoal	0.86	430
	0.86	518
	1.28	526
	1.72	528
	1.72	542
Xenon Concentration: 0.5 Volume %	2.59	518
	3.45	624
	3.45	660
	3.45	710
Temperature: 25°C	4.32	648
	5.21	654
	5.45	616
Adsorbent: Columbia CXC Activated Charcoal Other Conditions as given above	0.86	608
	0.86	616
	1.29	552
	1.72	584
	2.59	668
	3.45	754
	4.32	716
	5.18	726

Reference: Kenney and Eshaya (1960)

TABLE 6.5

Effect of Superficial Velocity on Adsorption of Krypton from Helium

Test Conditions	Superficial Velocity /cc(NTP)/cm^2-sec/	Adsorption Coefficient /cc(NTP)/gm/
Adsorbent: Columbia HCC 12x28 Mesh Krypton Concentration: 0.025 Volume % Temperature: 25°C	2.59	50
	3.45	54
	4.32	61
	5.18	65
	6.91	65
	8.64	66

Reference: Eshaya and Kalinowski (1961)

TABLE 6.6

Effect of Superficial Carrier Gas Velocity on Adsorption of Krypton from Nitrogen at Various Temperatures

Test Conditions	Temperature (°C)	Superficial Velocity /cc(NTP)/cm²-sec/	Adsorption Coefficient /cc(NTP)/gm/
Adsorbent: Fisher Brand Activated Charcoal, 40 x 50 Mesh Adsorbent: 25 gms.	-80	20	108
		41	112
		81	84
		152	252
	0	20	10
		41	12
		81	38
		152	88
	100	20	16
		41	16
		81	21
		152	44

Reference: Koch and Grandy (1957)

TABLE 6.7

Effect of Superficial Velocity on Adsorption of Krypton from Nitrogen

Test Conditions	Superficial Velocity /cc(NTP)/cm^2-sec/	Adsorption Coefficient /cc(NTP)/gm/
Adsorbent: Activated Carbon Type HGR-513 Temperature: 20°C	2.49	59.2
	4.69	55.4
	7.04	56.1
	9.39	57.3
	11.74	55.4
	13.76	54.8
	18.08	54.6
Adsorbent: Activated Carbon Type 2GS Temperature: 20°C	2.42	31.3
	4.65	31.7
	6.88	32.1
	9.20	32.8

Reference: Kawazoe (1967)

Chapter 7

SIGNIFICANCE AND APPLICABILITY OF DATA

One of the major objectives of this review has been to summarize clearly and concisely the published data on the adsorption of krypton and xenon on activated carbon. A secondary objective has been to determine our current ability to specify mean values and the ranges of probable errors for adsorption coefficients under specified conditions. Such information is essential for making accurate estimates of the performance of noble gas adsorption beds. These data can also provide guidance for upgrading the performance of existing beds and for assessing the adequacy of current design criteria as well as for specifying additional criteria that would result in improved performance. Only with the availability of such data is it possible to determine what efficiency of performance is reasonable to accept and what is possible through applications of the As Low As Reasonably Achievable (ALARA) criterion.

7.1 Variability of Adsorption Coefficients

The large body of data compiled in this report has permitted a statistical analysis to be made to determine the most likely values for the adsorption coefficients for krypton and xenon as well as the variability associated with the selection of a specific value. As may be noted, there was a wide range of possible values for these adsorption coefficients at any particular temperature. For example, at 25°C the adsorption coefficient for krypton in an air carrier was estimated to be $\leq$ 22 cc/gm for 5% of the charcoals tested; for 95% of the charcoals, the corresponding value was $\leq$ 72 cc/gm. Unfortunately, this could result in a possible error of a factor of more than

three if the charcoals represented by these two extremes were accidentally interchanged in an adsorption bed.

The estimated value of the adsorption coefficient for krypton from air at 25°C, as quoted by the U. S. Nuclear Regulatory Commission (Cardile and Bellamy, 1979), is 70 cc/gm. This value is significantly higher than the mean value of 40 cc/gm found here for beds operated under similar conditions. Although the NRC estimate is within the range of adsorption coefficients determined from this analysis to be realistic, the difference in the value observed here and that suggested by the NRC could mean that licensees who have adsorption beds designed on the basis of the NRC value may have facilities that are undersized. These data also show that significant upgrading of many fission gas adsorption beds could be accomplished by replacing lower quality charcoals with those having better characteristics. The quality of commercially available charcoals covers a wide range; licensees should be encouraged to specify, through their purchase orders, charcoals that are in the higher ranges with respect to their adsorption coefficients for krypton and xenon.

7.2 Significance of Mass Transfer

This review has shown that interparticle mass transfer can have significant effects on the performance of a charcoal adsorption bed, particularly in those cases where the velocity of the carrier gas is extremely low. At such velocities, molecular diffusion of krypton and xenon becomes competitive with transport of the carrier gas by convection. These two mechanisms, operating in concert, reduce the efficiency of the adsorption bed.

This problem can be eliminated by keeping the diameter of a bed sufficiently small to raise the convection velocity of the carrier gas above the regime where interparticale particle diffusion can be important. The actual velocity at which such effects become important is a function of temperature, carrier gas, the adsorption coefficient of the bed, and the decay constant of the radionuclide, under consideration. In general, a flow rate greater than 0.1 cm/sec is recommended. This is a matter that the NRC should consider including in its design specifications for adsorption systems for krypton and xenon in commercial nuclear power plants.

7.3 Significance of Pressure and Moisture

This review of the data shows that knowledge of the effects of pressure is sufficiently complete to permit reasonably good estimates to be made of the change in the adsorption coefficient brought about by variations in this parameter. One of the major results of this analyses has been to show that the commonly held assumption, that the adsorption coefficients for krypton and xenon increase directly with the absolute pressure, is not valid. This review has similarly disproved the assumption that the adsorption coefficient increases directly with the surface area of the adsorbent. On the other hand, this review did confirm that for most adsorption systems the assumption of linear adsorption isotherms is justified.

Unfortunately, data on the effects of moisture on adsorption coefficients are less complete than those for pressure. As this review has shown, there is only a limited amount of data on the effects of moisture at temperatures other than ambient. In addition, there are essentially

no data on the combined effects of moisture and pressure. Both of these are areas in need of additional research.

7.4 Commentary

Using the data in this report, there are a number of additional correlations that could be made. For example, a comparison could be made between the data developed by research personnel in the U. S. and the U.S.S.R. to determine if there are appreciable differences in their observations. This would be particularly interesting since adsorption phenomena have been a focal point of U.S.S.R. technology for several decades. Another evaluation that could be made would be to examine the data published over the past three decades (the time span for which data are available) to determine if there have been any improvements in the performance of activated charcoals. If improvements have been observed, the next step would be to try to determine what has been responsible for the changes noted and what steps can be taken to further improve the performance of charcoals selected for the adsorption of radioactive noble gases.

Such analyses, and the continuing publication of additional data on the various parameters affecting the performance of fission gas adsorption beds, should assist in updating and improving the data presented in this report. Regardless of such additions, however, one conclusion is clear. There are wide variations in the adsorption coefficients of different charcoals. Although nominal values can be used for purposes of system design, it is imperative that those responsible for evaluating such systems recognize that the only positive method of predicting bed

behavior is through direct measurements of the adsorptive capacity of the adsorbent as installed. This is particularly true in light of the fact that there is no scaleup factor for applying laboratory data to full scale plant design.

In the design of noble gas retention systems, the goal should be to maintain an acceptable holdup time for the specific radionuclides being released. This review has shown that non-critical acceptance of adsorption coefficients obtained from the published literature can lead to considerable error both in the design and the expected performance of such systems. Through the data provided here, people responsible for such systems have been provided with a range of acceptable values for adsorption coefficients under a variety of operating conditions. This should enable them to estimate in advance what type of performance should be possible as well as reasonable to expect. This, in turn, should lead to the design of adsorption systems that will provide not only better, but also more reliable, performance. Knowledge of the degree of variability of charcoal adsorbents for the retention of krypton and xenon can also assist regulatory agencies, such as the NRC, in establishing more meaningful and realistic testing requirements to assure the adequate performance of such systems.

REFERENCES

Ackley, R. D., Adams, R. E., and Browning, W. E., Jr., (1960): The Disposal of Radioactive Fission Gases by Adsorption, 6th AEC Air Cleaning Conference, USAEC Report TID-7593: 199-216.

Ackley, R. D. and Browning, W. E., Jr. (1961): Equilibrium Adsorption of Krypton and Xenon on Activated Charcoal and Linde Molecular Sieves. U. S. AEC Report ORNL-CF-61-2-32.

Adams, R. E. and Browning, W. E., Jr. (1958): Fission Gas Holdup Tests on HRT Charcoal Beds, U. S. AEC Report ORNL-CF-58-4-14.

Amphlett, C. B. and Greenfield, B. F. (1958): Krypton and Xenon Adsorption Isotherms on Charcoal Irradiated with 1 MeV Electrons, AERE C/R 2632.

Antoine, Ch. (1888): Thermodynamique: Tensions des rapeurs: Nouvelle relation entre les tensions et les temperatures, Comptes Rendus Hebdomadaives des Seances de Academie des Sciences, 107: 681-684.

Aristarkhov, N. N. Efimov, I. A., Krasnoyarov, N. V. and Shoreshkov, V. S. (1975): Adsorption Procedures for the Removal of Xenon from the Cover Gas of the Primary Coolant of the Reactor BR-5. Original Publication - 1975, German Translation Available from Kernforschungszentrum Karlsruhe as KFK-tr-488 (1976).

Ayers, J. W., Goldin, A. S. and Underhill, D. W. (1975): Pressure-Swing Sorption Concentration of Krypton-85 for Permanent Storage, U. S. AEC Report CONF-740807:203-227.

Barilli, L., Bruzzi, L. and Shorrock, J. C. (1969): Fission Product Removal from the Cover Gas of a Vented Fuel FBR, U. S. AEC Report CONF-691104-5.

Browning, W. E., Jr. and Bolta, C. C. (1959): Measurement and Analysis of the Holdup of Gas Mixtures by Charcoal Adsorption Beds, U. S. AEC Report ORNL-2116.

Brunauer, S. and Emmett, P. H. (1937): The Use of Low Temperature van der Waals Adsorption Isotherms in Determining the Surface Areas of Various Adsorbents. J. Am. Chem. Soc. 59:2682-9.

Burnette, R. D., Graham, W. W. III and Morse, D. C. (1962): The Removal of Radioactive Krypton and Xenon from a Flowing Helium Stream by Fixed Bed Adsorption, U. S. AEC Report TID-7622: 218-35.

Cardile, F. P. and Bellamy, R. R. (1979): Calculation of Releases of Radioactive Materials in Gaseous and Liquid Effluents from Boiling Water Reactors (BWR-Gale Code), U. S. Nuclear Regulatory Commission, NUREG-0016, Revision 1.

Castellani, F. F., Curzio, G. G. and Gentili, A. F. (1975): Effects of Moisture on Krypton Adsorption Characteristics of Charcoal Beds, Kerntechnik 17: 486.

---

*Available from the NRC/GPO Sales Program, U.S. Nuclear Regulatory Commission, Washington, DC 20555, and the National Technical Information Service, Springfield, VA 22161.

REFERENCES

Collard, G., Put, M. Broothaerts, J. and Goossens, W. R. A. (1977): The Delay of Xenon on Charcoal Beds, U. S. ERDA Report CONF-760822: 947-56.

Collins, D. A., Taylor, R. and Taylor, R. L. (1967): The Adsorption of Krypton and Xenon from Argon by Activated Charcoal, AERE Report TRG-1578 (W).

Cooper, M. H., Simmons, C. R. and Taylor, G. R. (1975): Adsorption of Krypton from Helium by Low Temperature Charcoal, U. S. AEC Report, CONF-740807: 151-64.

Curzio, G. G. and Gentili, A. F. (1972): Noble Gas Adsorption Characteristics of Charcoal Beds: van Deemter's Coefficients Evaluation, Anal. Chem. 44: 1544-5.

de Bruijn, H. Gruetter, A., Roemberg, E., Shorrock, J. C., Werner, L. and Wood, F. C. (1964): Removal of Fission-Product Noble Gases from the Helium of a High-Temperature Gas-Cooled Reactor Using Charcoal at Low Temperature, Trans. Inst. Chem. Eng. (London) 42: T365-T386.

Eshaya, A. M. and Kalinowski, W. L. (1961): Adsorption of Krypton and of Mixed Xenon and Krypton on Activated Charcoal, U. S. AEC Report BNL-724 (T-258).

First, M. W., Underhill, D. W., Hall, R. R., Grubner, O., Reist, P. C., Baldwin, T. W. and Moeller, D. W. (1971a): Semiannual Progress Report, Harvard Air Cleaning Laboratory, U. S. AEC Report NYO-841-24.

First, M. W., Underhill, D. W., Tadmor, J., Hall, R. R., Ratney, R. S., Baldwin, T. W. and Moeller, D. W. (1971b): Semiannual Progress Report, Harvard Air Cleaning Laboratory, U. S. AEC Report NYO-841-25.

First, M. W., Goldin, A. S., Underhill, D. W., Ayers, J. W. and Moeller, D. W. (1974): Semiannual Progress Report, Harvard Air Cleaning Laboratory, U. S. AEC Report COO-3049-4.

Foerster, K. (1971): Delaying Radioactive Fission Product Inert Gases in Cover Gas and Offgas Streams of Reactors by Means of Activated Charcoal Delay Lines, Kerntechnik 13: 214-9.

Glueckauf, E. (1955): Theory of Chromatography, Part 10, Formulae for Diffusion into Spheres and Their Application to Chromatography, Trans. Faraday Soc., 51: 1540-55.

Goldin, A. S. and Trindade, H. A. (1973): Adsorption of Fission Noble Gases on Activated Charcoal, U. S. AEC Report COO-3019-8: 16-33.

Homfray, I. F. (1910): Absorption of Gases by Charcoal, Z. physik, Chem. 74: 129-201.

REFERENCES

Hotchkiss, R. C. (1976): CFR Blanket Gas Composition Control; Sorption of Nitrogen, Xenon, Krypton and Argon on Active Carbon and Molecular Sieves, R/M/N888.

Hougen, O. A., and Marshall, W. R., Jr. (1947): Adsorption from a fluid Stream Flowing Through a Stationary Granular Bed. Chem. Eng. Prog. 43: 7197-208.

Jury, S. H., and Licht, W. (1952): Drying of Gases. Adsorption Wave in Desiccant Beds, Chem. Eng. Prog. 48: 102-9.

Kabele, T. J., McElroy, J. L., Badgett, E. O. and Bohringer, A. P. (1973): FFTF Fission Gas Delay Beds: Engineering Scale Test Report, U. S. AEC Report HEDL 73-26.

Kabele, T. J. and Bohringer, A. P. (1975): Engineering Scale Tests of an FFTF Fission Gas Delay Bed, U. S. AEC Report CONF-740807: 166-76.

Kanazawa, T., Soya, M., Tanabe, H., An, B., Yuasa, Y., Ohta, M., Watanabe, A., Nagao, H., Tani, A. and Miharada, H. (1977): Development of the Cryogenic Selective Adsorption-Desorption Process on Removal of Radioactive Noble Gases, U. S. ERDA Report, CONF-760822: 964-1001.

Kawazoe, K. (1967): On Intraparticle Diffusion Rate in Adsorption, Chemical Engineering (Japan) 31: 354-8.

Kawazoe, K. and Kawai, T. (1972): Investigation of Effective Diffusivities and Equilibra of Trace Component in Adsorption at Elevated Pressures, Chemical Engineering (Japan) 36: 71-8.

Kenney, W. F. and Eshaya, A. M. (1960): Adsorption of Xenon on Activated Charcoal, U. S. AEC Report BNL-689 (T-235).

Khan, A. A., Deshingkar, D. S., Ramarathinam, K. and Kishore, A. G. (1976): Evaluation of Activated Charcoal for Dynamic Adsorption of Krypton and Xenon, Bhabha Atomic Research Centre (Bombay, India) Report, BARA-839.

Kitani, S., Uno, S., Takada, J., Takada, H., and Segawa, T. (1968): Recovery of Krypton by Adsorption Process, Japan Atomic Energy Research Institute Report (JAERI) 1167.

Koch, R. C. and Grandy, G. L. (1957): Retention Efficiencies of Charcoal Traps for Fission Gases, U. S. AEC Report NSEC-7.

Kovach, J. L. (1972): Dynamic Adsorption Coefficient and its Application for Krypton-Xenon Delay Bed Design, Nuclear Consulting Services (Columbus, Ohio) Report NUCON 019.

Kovach, J. L. and Etheridge, E. L. (1973): Heat and Mass Transfer of Krypton-Xenon Adsorption on Activated Carbon, U. S. AEC Report CONF-720823: 71-85.

REFERENCES

Lee, K. B. and Madey, R. (1971): The Transmission of Xenon-133 Through Activated Charcoal Adsorber Beds, Nucl. Sci. Eng. 43: 27-31.

Lepold, M. F. (1965): Systematic Study of Gas Chromatographic Separation of Xenon and Krypton as Well as Determination of Nuclear Data of Kr-90, Gesellschaft Fuer Kernforschung m.b.H., Karlsruhe KFK-365.

Littlefield, P. S., Miller, S. R. and DerHagopian, H. (1975): Vermont Yankee Advanced Off-Gas System (AOG), U. S. AEC Report CONF-740807: 99-124.

Lovell, R. and Underhill, D. W. (1979): Experimental Determination of Fission Gas Adsorption Coefficients, U. S. ERDA Report CONF-780819: 893-900.

Madey, R. (1961): A Physical Theory of Adsorption of a Radioactive Gas, Trans. Am. Nuclear Soc. 4: 354-5.

Madey, R., Fiore, R. A., Pflumm, E. and Stephenson, T. E. (1962): Transmission of a Pulse of Gas Through An Adsorber Bed, Trans, Am. Nuclear Soc. 5: 465-6.

Nakhutin, I. E., Ochkin, D. V. and Linde, Yu. V. (1969): Dynamic Adsorption of Noble Gases, Russian J. Phys. Chem 43: 1012-4.

Nakhutin, I. E., Ochkin, D. V., Tretyak, S. A. and Dekalova, A. N. (1976): Investigation of Krypton and Xenon Adsorption in Samples of Commercial Charcoals at Low Partial Pressures, At. Energ. (USSR), 4: 295-298.

Peters, K., and Weil, K. (1930): Adsorption Experiments with Heavy Noble Gases, Z. physik. Chem. A148: 1-26.

Ratney, R. S. and Underhill, D. W. (1972): The Effect of High Pressure and Low Temperature on the Adsorption of Xenon and Krypton from Helium and Argon Streams, U. S. AEC Report COO-3019-3: 22-33.

Razga, J. (1975): Adsorption of Krypton and Xenon on Solid Materials, Jaderna energie 21: 455-6.

Robinson, G. Y., Jr. (1961): Design and Test of a Gas Adsorption System for the N. S. Savannah, Cryogenic Engineering Conference.

Roemberg, E. (1964): The Effect of Moisture on the Adsorption of Krypton on Charcoal, Dragon Project Report 276. AEE Winfrith, Dorchester, Dorset, England.

REFERENCES

Rosen, J. B. (1954): General Numerical Solution for Solid Diffusion in Fixed Beds, Ind. Eng. Chem. 46: 1590-4.

Rozhdestvenskaya, A. G., Cherepov, B. R., Keier, B. R., Chechetkin, Yu. V. and Kizin, V. D. (1975): Effect of Ammonia on the Adsorption of Krypton and xenon on SKT-M Carbon, II. Determination of the Equilibrium Adsorption Coefficients of the Inert Gases Under Dynamic Conditions, J. Phys. Chem. (USSR) 49: 1500-1502.

Schroeter, H., Juentgen, M., Zuendorf, D., and Knoblauch, K. (1974): Process for Retarding Flowing Radioactive Noble Gases, U. S. Patent 3,803,802.

Schumann, F. (1973): Purification of Krypton by Charcoal, Isotopenpraxis 9: 23-7.

Siegwarth, D. P., Neulander, C. K., Pao, R. T. and Siegler, M. (1973): Measurement of Dynamic Adsorption Coefficients for Noble Gases on Activated Carbon, U. S. AEC Report CONF-720823: 28-47.

Strong, K. P. and Levins, D. M. (1979): Dynamic Adsorption of Radon on Activated Carbon, U. S. ERDA Report CONF-780819: 627-39.

Thiele, E. W. (1939): Relation Between Catalytic Activity and Size of Particle, Ind. Eng. Chem. 31: 916-20.

Trofimov, A. M. and Pankov, A. M. (1965): Influence of the Macrocomponent on the Distribution of ^{85}Kr and ^{133}Xe Between the Gas Phase and Solid Carbon Sorbent, Soviet Radiochemistry 7: 293-8.

Trofimov, A. M. and Pankov, A. M. (1972a): Chromatographic Separation of Radioactive Noble Gases on Carbon Sorbents, I. Investigation of the Influence of the Experimental Parameters of the Chromatographic Process, Soviet Radiochemistry 14: 424-30.

Trofimov, A. M. and Pankov, A. M. (1972b): Chromatographic Separation of Radioactive Noble Gases on Carbon Sorbents, II. Investigation of the Mechanism of the Blurring of the Chromatographic Peaks of ^{85}Kr and ^{133}Xe, Soviet Radiochemistry 14: 431-6.

Underhill, D. W. (1967): Dynamic Adsorption of Fission Product Noble Gases on Activated Charcoal, U. S. AEC Report NYO-841-8.

Underhill, D. W. (1969): A Mechanistic Analysis of Fission Gas Holdup Beds Nuclear Applications 6: 544-8.

Underhill, D. W. (1970): An Experimental Analysis of Fission-Gas Holdup Beds, Nuclear Applications and Technology 8: 255-60.

REFERENCES

Underhill, D. W. (1972): Effect of Rupture in a Pressurized Noble Gas Adsorption Bed, Nuclear Safety 13: 478-81.

Underhill, D. W., Yusa, H., and Grubner, O., (1971): Design of Fission Gas Holdup Systems, U. S. AEC Report CONF-700816: 216-23.

Underhill, D. W., Goldin, A. S. and Trindade, H. A. (1973): Adsorption of Argon on Activated Charcoal, U. S. AEC Report COO-3019-4: 2.1-2.6.

van Deemter, J. J., Zuiderweg, F. J. and Klinkenberg, A. (1956): Longitudinal Diffusion and Resistance to Mass Transfer as Causes of Nonideality in Chromatography, Chem. Eng. Sci. 5: 271-89.

Wirsing, E., Jr., Hatch, L. P. and Dodge, B. F. (1970): Low Temperature Adsorption of Krypton on Solid Adsorbents, U. S. AEC Report BNL-50254 (T-586).

Yakshin, E. K., Cherepov, A. G., Chechetkin, Yu. V., Keier, B. R. and Chukhlov, G. Z. (1973): Efficiency of the Decontamination System for Radioactive Gas Waste at the VK-50 Atomic Power Station, Atomic Energy (USSR) 34: 285-6.

Yoder, R. E. and Imbarro, R. L. (1965): Krypton-85 Adsorption on Activated Charcoal, Harvard University Air Cleaning Laboratory Progress Report.

Young, J. F. (1958): A Derivation of the Equation for Elution Chromatography Assuming Linear Rate Constants in "Gas Chromatography," Edited by V. J. Coates, et al., Academic Press, NY, NY.

Yuasa, Y., Ohta, M., Watanabe, A., Tani, A. and Takashima, N. (1975): Selective Adsorption - Desorption Method for the Enrichment of Krypton, U. S. AEC Report CONF-740807, 1: 177-202.

Zeldowitsch, Ya. (1934): Theory of the Freundlich Adsorption Isotherm, Acta Physicochim, URSS 1: 961-74.

NRC FORM 335 (7-77)

U.S. NUCLEAR REGULATORY COMMISSION

BIBLIOGRAPHIC DATA SHEET

1. REPORT NUMBER *(Assigned by DDC)*
NUREG-0678

4. TITLE AND SUBTITLE *(Add Volume No., if appropriate)*
The Effects of Temperature, Moisture, Concentration, Pressure and Mass Transfer on the Adsorption of Krypton and Xenon on Activated Carbon

2. *(Leave blank)*

3. RECIPIENT'S ACCESSION NO.

7. AUTHOR(S)
Dwight W. Underhill, Sc.D. and Dade W. Moeller, Ph.D.

5. DATE REPORT COMPLETED
MONTH: July | YEAR: 1980

9. PERFORMING ORGANIZATION NAME AND MAILING ADDRESS *(Include Zip Code)*
Advisory Committee on Reactor Safeguards
U.S. Nuclear Regulatory Commission
Washington, DC 20555

DATE REPORT ISSUED
MONTH: August | YEAR: 1980

6. *(Leave blank)*

8. *(Leave blank)*

12. SPONSORING ORGANIZATION NAME AND MAILING ADDRESS *(Include Zip Code)*
Same as 9, above.

10. PROJECT/TASK/WORK UNIT NO.

11. CONTRACT NO.

13. TYPE OF REPORT

PERIOD COVERED *(Inclusive dates)*

15. SUPPLEMENTARY NOTES

14. *(Leave blank)*

16. ABSTRACT *(200 words or less)*

This report is a critical review of the published literature on the adsorption of radioactive krypton and xenon on activated charcoal. The report includes a tabulation and evaluation of the adsorption coefficients for these two gases as related to temperature, pressure, moisture, mass transfer effects, and the nature of the carrier gas. Wherever possible, the resulting data have been used to develop simple correlations for quantitatively evaluating the effects of these parameters on noble gas adsorption. Important conclusions of the study include the observations that (a) individual charcoals have a wide range of adsorption coefficients and therefore the performance of a given bed is heavily dependent on the quality of the charcoal it contains; (b) because of the detrimental effects of mass transfer on noble gas adsorption, consideration should be given to including this factor in developing technical specifications for adsorption beds; and (c) additional research is needed on the determination of the interrelationship of moisture and temperature and their effects on adsorption bed performance.

17. KEY WORDS AND DOCUMENT ANALYSIS

17a. DESCRIPTORS

17b. IDENTIFIERS/OPEN-ENDED TERMS

18. AVAILABILITY STATEMENT
Public availability

19. SECURITY CLASS *(This report)*
Unclassified

21. NO. OF PAGES

20. SECURITY CLASS *(This page)*

22. PRICE
$

NRC FORM 335 (7-77)